

Examining the Neuromuscular and Mechanical Characteristics of the Abdominal
Musculature and Connective Tissues: Implications for Stiffening the Lumbar Spine

by

Stephen Hadley Morgan Brown

A thesis
presented to the University of Waterloo
in fulfillment of the
thesis requirement for the degree of
Doctor of Philosophy
in
Kinesiology

Waterloo, Ontario, Canada, 2008

©Stephen H.M. Brown 2008

I hereby declare that I am the sole author of this thesis. This is a true copy of the thesis, including any required final revisions, as accepted by my examiners.

I understand that my thesis may be made electronically available to the public.

Stephen H. M. Brown

Abstract

Research has uncovered an essential role of proper abdominal muscle function in ensuring the health and integrity of the lumbar spine. The anatomical arrangement of the abdominal musculature (rectus abdominis, external oblique, internal oblique, transverse abdominis) and intervening connective tissues is unique in the human body. Despite the hypothesized importance and uniqueness of the abdominal muscles, very little research has been directed to understanding their role from a neuro-mechanical standpoint. Thus, this thesis was designed to study the neuro-activation and mechanical characteristics of the abdominal musculature and connective tissues, with a specific focus on torso stiffening mechanisms. Several experiments were performed and unified around this theme. The first study explored the fundamental relationship between EMG muscle activation recordings and the moments generated by the trunk musculature. This study was novel in that investigation of the abdominal musculature was augmented with consideration of antagonist muscle co-activation. The main finding was that the EMG-moment relationships were quite similar in both the abdominal and extensor muscle groups; however, the form of this relationship differed from that often reported in the literature. Specifically, consideration of antagonist muscle moments linearized the EMG-moment relationship of the agonist muscle groups. Once this activation-moment relationship had been established, the next line of questioning explored the association between torso muscle activation, driven through the abdominals, and torso stiffness. Two studies addressed this issue: the first examined the intrinsic resistance of the torso to bending in the flexion, extension, and lateral bend directions, while varying the levels of torso muscle activation; the second examined the response of the trunk to perturbations while varying the levels of torso muscle activation under the presence of

limited reflexes. The first of these two studies demonstrated a rise in trunk stiffness as muscle activation increased over the lower 40% of range of motion. At greater ranges of motion in flexion and lateral bend the trunk appeared to become less stiff as the musculature contracted to higher levels. The latter study revealed substantial spinal displacements in response to trunk perturbations, indicating that in the absence of reflex activity, the stiffness produced by muscular contraction may be inadequate to stiffen the torso to prevent damage to spinal tissues. The fourth study was designed to enable in-vivo observation of abdominal muscle and connective tissue deformation using ultrasound imaging. During relatively simple abdominal contractions, the oblique aponeurosis demonstrated surprising deformation patterns that often exhibited the characteristic of a negative Poisson's ratio. This was hypothesized to be facilitated by the composite laminate arrangement of the abdominal wall, whereby the loose connective tissues separating layers of collagen fibres may allow for separation of adjacent layers, giving the appearance of structural volume expansion. Further, a lateral displacement of the rectus abdominis muscle was noted in a majority of contractions, highlighting the dominance of the laterally oriented forces generated by the oblique muscles. The final study questioned, at a basic level, the nature of the anatomical arrangement of the abdominal muscle-connective tissue network. Examining the contraction of the rat abdominal wall uncovered the transfer of muscularly generated force and stiffness through the connective tissues binding the layered muscles. This suggests a functionality of the abdominal wall as a composite laminate structure, allowing substantial multi-directional stiffness to be generated and transmitted around the torso, thereby enhancing the ability to effectively stabilize the spine.

Acknowledgements

First, I would like to thank my advisor Dr Stuart McGill. Your time was always greatly appreciated, as was your encouragement and lessons to not shy away from taking chances and to always shoot for big things.

Thank-you to my committee, Drs Jack Callaghan, Clark Dickerson, and John Medley, as well as my external examiner Dr Cheryl Hubley-Kozey, for taking the time and effort to read my work, make helpful suggestions, and provide advice whenever I asked. Also, to Dr Jim Potvin, thanks for getting me started in all of this work and for always being available to talk and share ideas.

Thanks to Janice Moreside and Sam Howarth, who helped me with parts of my thesis collections, to Danielle Greaves for guiding me with the use of ultrasound, Wendell Prime and Jeff Rice for technical support, and especially to Dawn McCutcheon for providing a tonne of time and effort to teach and assist me with the animals.

I appreciate all of the fun that I've had during my time at Waterloo, making a lot of new friends, and appreciate also all of the support from my friends and family (Mom, Dad, and Eric) back home.

Finally, and most importantly, I want to thank Diane Gregory for ensuring that I always enjoyed my time and work at Waterloo, for helping me with ALL aspects of this thesis project, and most of all for being my best friend.

Table of Contents

Author's Declaration	ii
Abstract	iii
Acknowledgements	v
List of Tables	ix
List of Figures	x
Chapter 1: General Introduction	1
1.1 Muscular Contribution to Joint Stiffness	4
Chapter 2: General EMG Methodology	9
2.1 Instrumentation	10
2.2 General EMG Processing	10
2.3 Maximum Voluntary Isometric Contractions	11
Chapter 3: Co-activation Alters the Linear Versus Non-linear Impression of the EMG-Moment Relationship of Trunk Muscles	12
Chapter Synopsis	13
3.1 Introduction	14
3.2 Methods	15
3.2.1 <i>Participants</i>	15
3.2.2 <i>Task</i>	16
3.2.3 <i>Instrumentation and Processing</i>	17
3.3 Results	21
3.3.1 <i>Effect of Antagonist Muscle Activity</i>	21
3.3.2 <i>Amount of Antagonist Muscle Activity Present</i>	25
3.4 Discussion	28
Chapter 4: How the Inherent Stiffness of the in-vivo Human Trunk Varies with Changing Magnitudes of Muscular Activation	30
Chapter Synopsis	31
4.1 Introduction	33
4.2 Methods	35
4.2.1 <i>Participants</i>	35
4.2.2 <i>Data Collection</i>	35
4.2.3 <i>Instrumentation</i>	37
4.2.4 <i>Moment-Angle Curves</i>	38
4.2.5 <i>Statistical Analysis</i>	39
4.3 Results	39
4.3.1 <i>EMG</i>	39
4.3.2 <i>Stiffness Curves</i>	42
4.3.3 <i>Moment-Angle Characteristics</i>	47
4.4 Discussion	49

Chapter 5: The Intrinsic Stiffness of the in-vivo Human Trunk in Response to Quick Releases: Implications for Reflexive Requirements	55
Chapter Synopsis	56
5.1 Introduction	57
5.2 Methods	59
5.2.1 <i>Participants</i>	59
5.2.2 <i>Data Collection</i>	59
5.2.3 <i>Instrumentation</i>	61
5.2.4 <i>Second-Order Linear Model of the Trunk</i>	62
5.2.5 <i>EMG Onset and Offset Latencies</i>	63
5.2.6 <i>Statistical Analysis</i>	64
5.3 Results	65
5.3.1 <i>Stiffness and Damping</i>	65
5.3.2 <i>Applied Moment and EMG Pre-Perturbation Activation</i>	68
5.3.3 <i>EMG Latency Probabilities</i>	71
5.4 Discussion	72
Chapter 6: An Ultrasound Investigation into the Morphology of the Human Abdominal Wall Uncovers Complex Deformation Patterns During Contraction	77
Chapter Synopsis	78
6.1 Introduction	79
6.2 Methods	81
6.2.1 <i>Participants</i>	81
6.2.2 <i>Data Collection</i>	81
6.2.3 <i>Procedures</i>	82
6.2.4 <i>Ultrasound Image Analysis</i>	85
6.2.5 <i>Reliability</i>	87
6.2.6 <i>Muscle Force Estimates</i>	88
6.2.7 <i>Statistical Analysis</i>	89
6.3 Results	89
6.3.1 <i>Muscle Force Production</i>	89
6.3.2 <i>Reliability of Ultrasound Image Digitization</i>	90
6.3.3 <i>Rectus Abdominis Tendon and Muscle</i>	91
6.3.4 <i>Oblique Aponeurosis</i>	92
6.4 Discussion	93
Chapter 7: Transmission of Muscularly Generated Force and Stiffness between Layers of the Rat Abominal Wall	100
Chapter Synopsis	101
7.1 Introduction	102
7.2 Methods	104
7.2.1 <i>Pilot Work</i>	104
7.2.2 <i>Experimental Procedures</i>	104

7.3 Results	108
7.3.1 <i>Muscle Measurements</i>	108
7.3.2 <i>The Effect of Cutting the Aponeurosis</i>	109
7.3.3 <i>The Effect of Time</i>	111
7.4 Discussion	112
Chapter 8: Summary	117
8.1 Closing	121
Appendix	122
References	126

List of Tables

Table 3.1: Best-fit coefficients and root-mean-square differences for the linear and best non-linear fits between EMG moments and externally determined moments alone.	22
Table 3.2: Best-fit coefficients and root-mean-square differences for the linear and best non-linear fits between EMG moments and combined antagonist and externally determined moments.	22
Table 4.1: Best-fit coefficients and root-mean-square error characterizing the moment-angle curves from an exponential curve fit.	46
Table 5.1: Mean percent root-mean-square error between the model predicted and experimentally recorded trunk rotational displacements.	65

List of Figures

Figure 1.1: Theoretical example of the stiffening and stabilizing contribution of muscles supporting a hinge joint.	5
Figure 1.2: Diagram of a transverse view of the abdominal wall.	6
Figure 1.3: Organizational flow chart of the thesis studies.	8
Figure 2.1: Diagram of EMG electrode locations.	11
Figure 3.1: Participant positioning for the four conditions of Study 1.	17
Figure 3.2: Scatterplots displaying the EMG-moment relationships of the Flexor Moment 50% flexed condition.	23
Figure 3.3: Scatterplot displaying the EMG-moment relationship of the Extensor Moment Upright condition.	24
Figure 3.4: Co-activation index for each of the four conditions.	26
Figure 4.1: Experimental set-up of Study 2.	36
Figure 4.2: EMG pre-activation levels for each applied moment direction.	41
Figure 4.3: Scatterplot of moment-angle data points and curve fit for the light brace flexion condition.	43
Figure 4.4: Rotational stiffness curves for each of the three applied moment directions, at each torso muscle activation level.	44
Figure 4.5: Average moments required to initiate bend in each direction for each torso muscle activation level.	47
Figure 4.6: Average peak moment at end range of motion in each direction for each torso muscle activation level.	48
Figure 4.7: Average maximum trunk displacement in each direction for each torso muscle activation level.	49
Figure 4.8: Diagram of pressurized cylinder theory for the abdominal cavity.	52
Figure 5.1: Experimental set-up of Study 3.	61

Figure 5.2: Example of the model predicted and experimentally recorded trunk rotational displacement for a heavy flexor moment trial.	66
Figure 5.3: Average rotational stiffness calculated for each torso muscle activation level in flexion and lateral bend directions.	67
Figure 5.4: Average rotational damping calculated for each torso muscle activation level in flexion and lateral bend directions.	68
Figure 5.5: Pre-perturbation muscle activation levels.	70
Figure 5.6: Example EMG traces displaying both a muscle turning on and a muscle turning off in response to the perturbation.	72
Figure 6.1: Participant posture in which ultrasound images were obtained.	82
Figure 6.2: Diagram of the locations and orientations of the ultrasound probe.	84
Figure 6.3: Example of an ultrasound image displaying the oblique aponeurosis in the relaxed and contracted states.	86
Figure 6.4: Example of an ultrasound image displaying the rectus abdominis transverse tendon in the relaxed and contracted states.	87
Figure 6.5: Average modeled force generated by each abdominal muscle during contractions of different magnitudes.	90
Figure 6.6: Relationship between the ratio of summed oblique muscle force to rectus abdominis muscle force, and the lateral displacement of the rectus abdominis muscle.	92
Figure 7.1: Experimental set-up of Study 5 (rat study).	106
Figure 7.2: Picture of the rat abdominal wall in the intact state and with the aponeurosis of the transverse abdominis cut.	108
Figure 7.3: Average force recorded from the abdominal wall in the intact and cut states.	110
Figure 7.4: Average stiffness recorded from the abdominal wall in the intact and cut states.	110
Figure 7.5: Percent drops in abdominal wall force and stiffness in the cut aponeurosis and elapsed time states.	111

Figure A.1: Example time histories of the EMG signals from two abdominal muscles that maintain relatively constant activation over the course of the flexion ROM (as per Chapter 4)	124
Figure A.2: Example time histories of the EMG signals from two abdominal muscles that display a reduced activation over the course of the flexion ROM (as per Chapter 4)	124
Figure A.3: Example time histories of the EMG signals from two abdominal muscles that display opposite trends, relating to their lengthening and shortening, over the course of the right-side lateral bend ROM (as per Chapter 4)	125

Chapter 1:

General Introduction

The study of joint stability and spine stability in particular has received a great deal of attention over the past 20 years. The concept of spine stability was first introduced by Lucas and Bresler (1961), who demonstrated that the human thoraco-lumbar spine, in the absence of muscular attachments, buckles and becomes damaged under compressive loads of less than 20 N. In everyday life, the human spine supports compressive loads into the many thousands of Newtons. This knowledge has led a number of research groups to investigate the mechanisms that make this possible. Bergmark (1989) was the first to formally propose a method of examining the stabilizing contributions of individual muscles about individual spinal joints. Subsequent work by a number of groups, led by Panjabi, McGill, Cholewicki, Stokes and Gardner-Morse have shown definitively that muscles co-activate around a joint to provide the stability necessary to allow the joint to support loads far beyond those possible in the absence of muscular activity. McGill, in particular, has used the analogy of muscles acting as “guy wires” about the spine to provide support and stability through the entire lumbar column.

The human spine, being comprised of a number of vertebral bodies organized in a column formation, makes this structure well suited for stability analyses based on the theory of Euler column buckling. This theory states that a column will be stable if the total summed potential energy of the elements of the system is at a minimum. In this case, a rotational perturbation of a single joint within the column would result in a net storage of energy that would return the joint to its original equilibrium configuration. If the potential energy of the system was not at a minimum, then the net energy post-perturbation would function to further rotate the joint away from its original equilibrium configuration. The joint, in this case, would find a new equilibrium point without injury, or may buckle to the point of injury.

In either case, the system is considered to be unstable. For a system with multiple degrees of freedom (DoF), the potential energy at each DoF must be at a minimum. If a single DoF does not meet this criterion, the system can be considered to be at a saddle point and can initiate buckling about that single DoF.

The definition of stability described above can be considered a mechanical definition, dealing with energy changes within a system in response to a rotational perturbation. Other definitions are often described in the literature as well: a clinical definition dealing with, in a spine sense, an abnormally large range of motion, or a loss of stiffness, at single vertebral levels. Variations of this definition are widely used in surgical applications, as well as performance training and rehabilitation settings. Another definition of stability is found in postural research, relating stability to the maintenance of one's centre of mass (CoM) within its base of support. All of these definitions have one thing in common: the utility of stiffness in the preservation of a stable state. In the mechanical sense, system stiffness is essential to store energy upon deformation and subsequently return the system to its original equilibrium state. In the clinical sense, a stiffer joint will limit the displacement it will undergo given a certain load application. Finally, in the postural sense, a stiffer system is one in which the system CoM undergoes smaller displacements and is therefore less likely to fall outside its base of support.

While stiffness is essential in maintaining stability in any of these senses, a system that is too stiff will not be able to function in the appropriate manner. It has been shown that in the mechanical sense, a maximally stiff spine will create extremely high compressive forces acting on the spinal joints (Stokes and Gardner-Morse, 2001; Brown and Potvin, 2005). Further, an extremely stiff joint will limit its ROM, often preventing motions

necessary for normal function. These systems can often be considered extremely stable, but at the expense of limiting normal function and potentially creating other damaging load induced injury states.

1.1 Muscular Contribution to Joint Stiffness

A muscle fibre develops force and stiffness in proportion to the number of actin and myosin cross-bridge links formed at an instant in time. The number of links formed is dependent upon a number of factors, notably, activation level, fibre length and fibre velocity.

The force developed by the muscle fibres is transmitted through its tendon to bone. The stiffness of the muscle will be dependent upon the relative stiffness of each of its parts (eg. fibre, tendon) in series.

A muscle's contribution to the rotational stiffness about a joint will be dependent upon the muscle's force and stiffness characteristics as well as its geometric orientation. Briefly, the potential energy stored in a muscle can be quantified as:

$$V = F\Delta l + \frac{1}{2}k\Delta l^2 \quad (1.1)$$

where V is the potential energy stored in the muscle (Nm), F is the instantaneous muscle force (N), Δl is the change in muscle length upon rotational perturbation (m), and k is the instantaneous muscle stiffness (N/m).

The second derivative of this potential energy function with respect to a rotational perturbation ($d^2V/d\theta^2$) represents the muscular contribution to the rotational stiffness about the joint. Figure 1.1 displays a visual example of a muscle acting about a joint. Upon an applied rotational perturbation (θ) a muscle will shorten or lengthen and its instantaneous force will change corresponding to its stiffness in line with Hooke's law ($\Delta F = k*\Delta l$). In the

Figure (1.1), Muscle A shortens and exhibits a corresponding drop in force, while Muscle B lengthens and exhibits a corresponding increase in force. The initial orientation of the muscle will dictate the change in its moment arm upon perturbation. If the change in muscle moment post-perturbation is such that it opposes the direction of the perturbation, the muscle can be considered stabilizing about the joint in question.

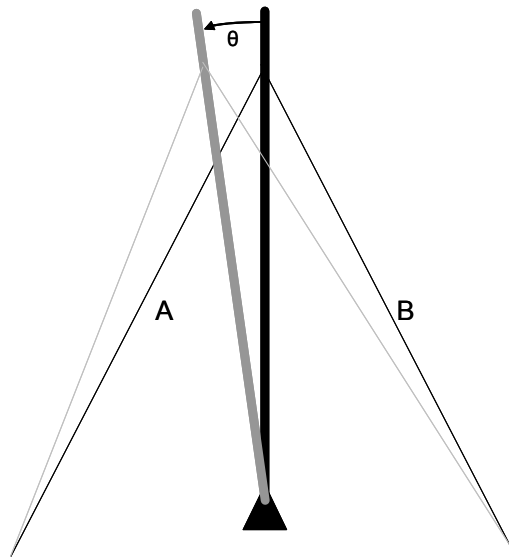


Figure 1.1. A simplified example of two muscles (A and B) acting about a hinge joint. Upon rotational perturbation (θ) muscle A shortens and consequently its force decreases while muscle B lengthens and consequently its force increases. The net change in the torque produced by each muscle will determine its stiffening and stabilizing contribution.

Stiffening mechanisms of the muscles and passive tissues surrounding the lumbar spine are not well understood. In particular, little is known about the stiffening and stabilizing function of the abdominal musculature, especially in light of its unique anatomical arrangements. The abdominal musculature consist of four muscle groups; rectus abdominis, external oblique, internal oblique, and transverse abdominis. The two oblique muscles and the transverse abdominis overlies one another and are separated by layers of connective tissue;

they originate from the pelvis, thoraco-lumbar dorsal fascia and the lower ribs and insert primarily into the abdominal fascia connecting with the rectus abdominis (Figure 1.2).

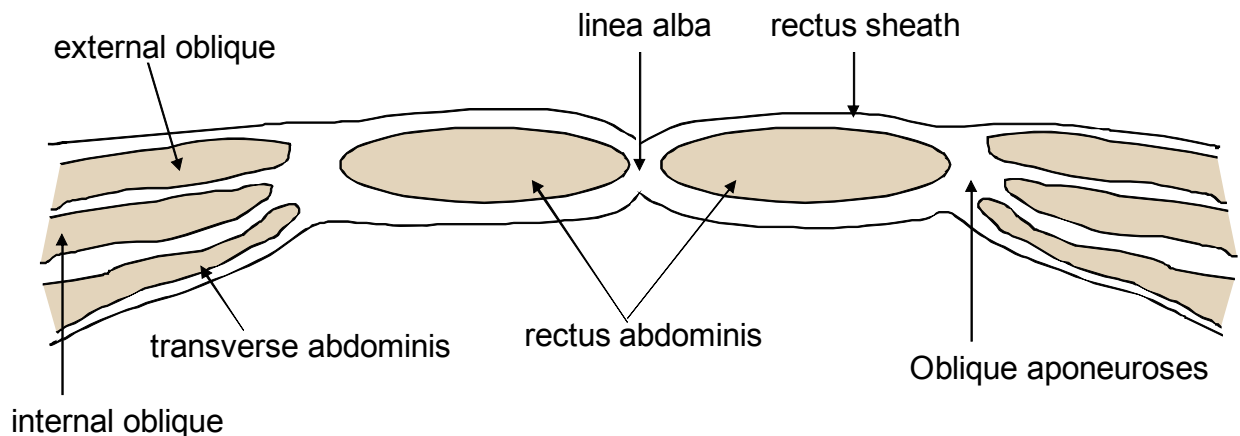


Figure 1.2 Top gross view of the three oblique abdominal muscles (external oblique, internal oblique, transversus abdominis), terminating to their aponeuroses and inserting into the abdominal fascia surrounding the rectus abdominis (rectus sheath).

In general, muscle is thought to primarily transfer its generated force from muscle fibres, through the myo-tendon junction to tendon attached to bone. Muscle aponeuroses function similar to tendons, with the exception that they do not attach the muscle fibre to bone, but rather to other muscular or connective tissue structures. Thus they are often referred to as “internal tendons”; meaning internal to the muscle itself. Each of the abdominal wall muscles attaches at the anterior of the torso through an aponeurosis that ultimately leads to the formation of the rectus sheath (Figure 1.2). Detailed investigations of the morphology of the oblique aponeuroses have uncovered a bi-layered arrangement stemming from each muscle. Specifically, the aponeurosis of each of the external oblique, internal oblique and transversus abdominis can be anatomically separated into two layers, one arising from the superficial fascial layer of the muscle and the other from the deep fascial

layer of the muscle (Askar, 1977; Rizk, 1980). Thus, both the superficial and deep layers of the rectus sheath are formed of three fascial layers (superficial: two from external and one from internal oblique; deep: one from internal oblique and two from transverse abdominis). The functional and/or mechanical purpose of this highly unique structural arrangement is unknown.

The interaction between each of these muscles during contraction is poorly understood and needs to be further studied in order to obtain a better understanding of their function in maintaining the spine in a stable state. Further, despite a distinct emphasis in the literature on the importance of the abdominal muscles in ensuring a stable spine (eg. Gardner-Morse & Stokes, 1998; Krajcarski et al., 1999; Chiang & Potvin, 2001; Hubley-Kozey & Vezina, 2002; O'Sullivan et al., 2002; van Dieen et al., 2003; Essendrop & Schibye, 2004; Shirazi-Adl et al., 2005; Watanabe et al., 2007), little direct mechanical evidence has been provided to explain exactly how these muscles function to achieve such stability or stiffness. Finally, in a study published in the early stages of my PhD progress (Brown et al., 2006), we uncovered experimental evidence that demonstrated that unbalanced abdominal muscle activation patterns could lead to a reduction in the stability margin of safety of the spine. While theories and hypotheses could be generated to explain this phenomenon (eg. Brown & McGill, 2005), no definitive mechanical evidence could be provided. It became clear that further experimental testing of the mechanics of abdominal muscle contraction, and subsequent connective tissue deformation and force and stiffness transfer to the skeleton, was needed. This thesis was borne out of that need.

The purpose of this thesis is therefore to examine, in more scientific detail, the ability of the abdominal musculature to provide stiffness to the joints of the lumbar spine. The

investigations are divided into four themes, each examining different aspects of potential stiffening effects: 1) the nature of the trunk muscle activation(EMG)-moment relationship; 2) the effect of differing magnitudes of abdominal muscle activation on trunk stiffness and damping characteristics; 3) anatomical arrangement and deformation of the abdominal oblique muscle group and connective tissues during contraction; 4) the ability of the fascial connections between the abdominal oblique and transverse abdominis muscles to transfer muscularly generated force and stiffness. Five studies were conducted to answer questions relating to each of these topics (two studies addressed theme two). An organizational chart displaying the progression and relationship between the studies is provided (Figure 1.3).

Examining the anatomical and mechanical characteristics of the abdominal musculature: implications for stiffening the lumbar spine

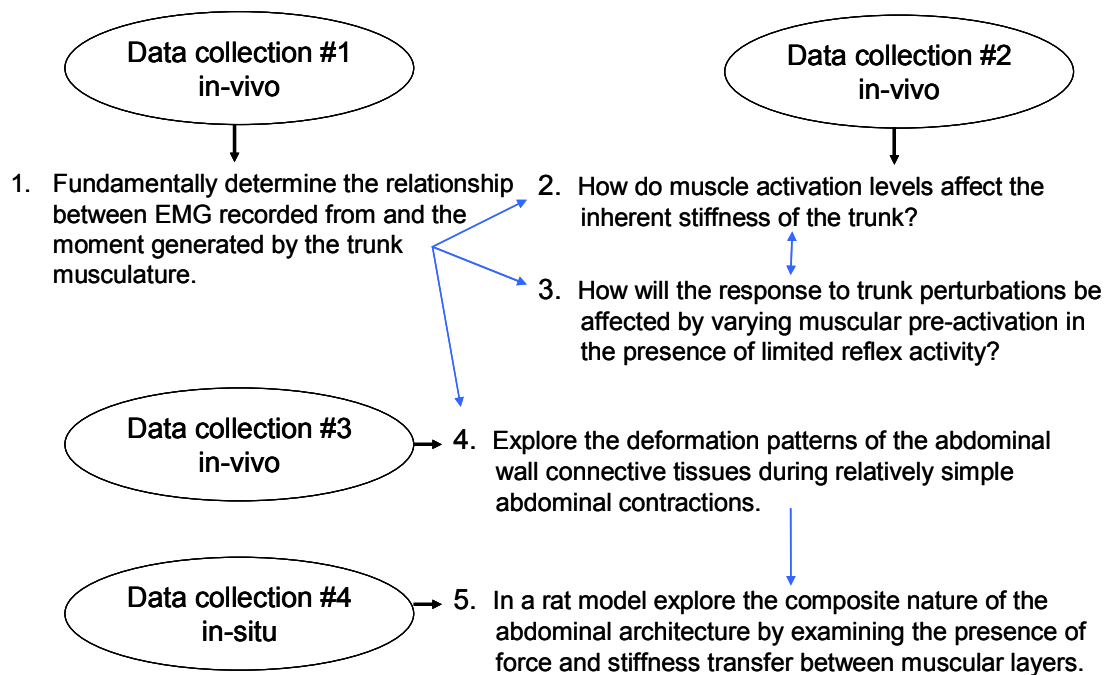


Figure 1.3. Organizational flow through the five studies encompassed within the four thesis themes.

Chapter 2:

General EMG Methodology

Studies one, two, three and four (Chapters 3 through 6) utilized similar electromyography (EMG) collection equipment and techniques. These will therefore be presented here to avoid repetition later in the document.

2.1 Instrumentation

Fourteen channels of EMG were collected from the following muscles bilaterally (Figure 2.1): rectus abdominis (RA; 2cm lateral to the midline at the approximate level of the umbilicus), external oblique (EO; approximately 14cm lateral to the midline oriented infero-medially at 45 degrees), internal oblique (IO; approximately 2cm medial and inferior to ASIS oriented horizontally), latissimus dorsi (LD; approximately 15cm lateral to midline at T9 level oriented supero-laterally), and three levels of the erector spinae (T9, L3 and L5; 5cm, 3cm, and 1cm lateral to midline, respectively). Blue Sensor bi-polar Ag-AgCl electrodes (Ambu A/S, Denmark, intra-electrode distance of 2.5 cm) were placed over the muscle belly of each muscle in line with the direction of fibres. Signals were amplified (± 2.5 V; AMT-8, Bortec, Calgary, Canada; bandwidth 10-1000 Hz, CMRR = 115 db at 60 Hz, input impedance = 10 G Ω). EMG signals were sampled at 2048 Hz.

2.2 General EMG Processing

First, the raw DC bias was removed, followed by low-pass filtering at 500 Hz, rectifying, low-pass filtering at 2.5 Hz (both Butterworth 2nd order), and normalizing to the maximum processed voltage obtained in maximum voluntary isometric contractions (MVCs).

2.3 Maximum Voluntary Isometric Contractions

The abdominal MVCs were obtained in one of two contractions: 1) a modified sit-up position in which participants isometrically attempted to produce trunk flexion, side bend and twist motions against resistance; 2) a reverse curl-up in which individuals lied supine with their hips and knees flexed to 90 degrees while isometrically attempting to pull their thighs towards their chest, and in each of the right and left twist directions against resistance. The trunk extensor (erector spinae) MVCs were obtained with the participants' torso balanced off of the end of a bench to which their legs were tightly secured. In this position the participants attempted isometric trunk extension against manually applied resistance. The LD MVCs were conducted using a standard standing isometric lat pull-down against resistance.

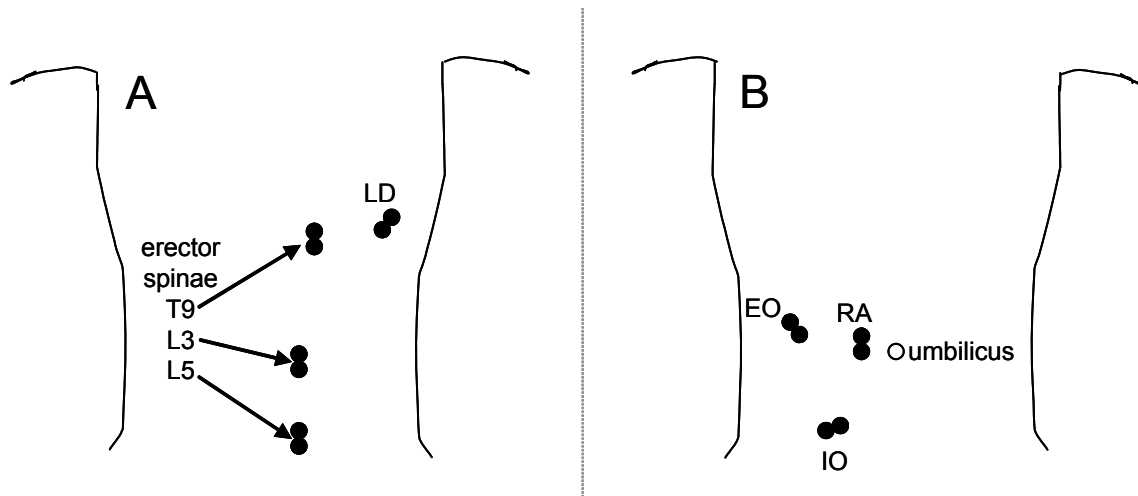


Figure 2.1. Location of the EMG electrodes, shown on the right side of the body, from a posterior (A) and anterior (B) view. Electrodes were placed bilaterally on both the right and left sides of the body in studies 1, 2 and 3 (Chapters 3, 4, 5).

Chapter 3:

Co-activation Alters the Linear Versus Non-linear Impression of the EMG-Moment Relationship of Trunk Muscles

Chapter Synopsis

The use of electromyographic signals in the modeling of muscle forces and joint loads requires an assumption of the relationship between EMG and muscle force. This relationship has been studied for the trunk musculature and been shown to be predominantly non-linear, with more EMG producing proportionally less moment output at higher levels of activation. Agonist-antagonist muscle co-activation is often substantial during trunk exertions, yet has not been adequately accounted for in determining such relationships. The purpose of this study was to revisit the EMG-moment relationship of the trunk, recognizing the additional moment requirements necessitated due to antagonist muscle activity. Eight participants generated a series of isometric ramped trunk flexor and extensor moment contractions. EMG was recorded from 14 torso muscles, and the externally resisted moment was measured. Agonist muscle moments (either flexor or extensor) were estimated from an anatomically detailed biomechanical model of the spine and fit to: the externally calculated moment alone; the externally calculated moment combined with the antagonist muscle moment. When antagonist activity was ignored the EMG-moment relationship was found to be non-linear, similar to previous work. However, when accounting for the additional muscle moment generated by the antagonist muscle groups, the relationships became, in three of the four conditions, more linear. Therefore it was concluded that antagonist muscle co-activation must be included when determining the EMG-moment relationship of trunk muscles and that previous impressions of non-linear EMG-force relationships should be revisited.

3.1 Introduction

Examinations of issues in spine and torso mechanics are often assisted by the use of electromyographic techniques; thus assumptions must be made regarding the relationship between EMG activation magnitudes and muscular force output. Much of the research concerning EMG-force/moment relationships in the spine literature has focused on that of the extensor musculature. The form of the relationship has been most often identified as non-linear (eg. Stokes et al., 1987; Thelen et al., 1994; Potvin et al., 1996; Sparto et al., 1998; Staudenmann et al., 2007) although some have determined it to be linear (eg. Seroussi et al., 1987; Dolan & Adams, 1993). Despite the increasing attention paid to the importance of well coordinated abdominal muscle contraction in ensuring optimal spine health (eg. van Dieen et al., 2003; Cholewicki et al., 2005; Urquhart et al., 2005; Lee et al., 2006), a very limited amount of work has been done investigating the EMG-moment relationships of the abdominal muscles, yet it too has identified a distinct non-linear form (Stokes et al., 1989, rectus abdominis; Thelen et al., 1994, rectus abdominis and external oblique), with a decline in the rise of the moment as EMG increases.

There is a fundamental importance in developing our understanding of the relationship between the electrical signals that we obtain from surface EMG recordings, and the true contractile force generated and transferred to the skeleton by the muscle or muscle group in question. Thus, a great deal of previous research has been dedicated to this elemental line of study, mostly focused on muscles of the limbs. Again, discrepancies have been uncovered regarding the degree of linearity that exists in this relationship for different muscles, and hypotheses have been proposed suggesting that factors such as motor unit recruitment and firing rate modulation, motor unit distribution within a muscle, and muscle

fibre composition all may affect the EMG-moment relationship (Lawrence & DeLuca, 1983; Woods & Bigland-Ritchie, 1983).

An additional factor, however, that has often lacked adequate consideration in determining the nature of the EMG-moment relationship, is the additional moment which must be overcome due to antagonist muscle co-activation. Co-activation of muscles acting both agonist and antagonist to a dominant moment is highly prevalent during trunk exertions (Lee et al., 2007; Ross et al., 1993; Thelen et al., 1995; van Dieen et al., 2003). Therefore, it is hypothesized that this activation may alter the perceived EMG-moment relationship of trunk muscles, as the moment produced by agonist muscle groups will be continuously underestimated as a function of the comparative amount of antagonist co-activation. The purpose of this paper was thus two-fold: 1) examine in more detail the EMG-moment relationship of the abdominal musculature; 2) re-examine the EMG-moment relationship of the extensor musculature with and without accounting for the additional resistive moment that must be overcome due to antagonist muscle co-activation.

3.2 Methods

3.2.1 Participants

Eight healthy males (mean/SD: age = 24.9/4.7 years; height = 1.79/0.03 m; mass = 82.0/9.1 kg), with no history of back problems, volunteered from the University population. Each read and signed a consent form approved by the University Office of Research Ethics.

3.2.2 Task

Participants sat with knees supported and pelvis secured in an apparatus designed to foster a neutral spine position (Vera-Garcia et al., 2006). A harness was secured across the chest and attached with a cable to a wall. A force transducer was mounted in-series with the cable (Figure 3.1).

Participants were instructed to produce controlled isometric (no trunk motion) ramped moment contractions from rest to maximum and back to rest in each of four positions: 1) Extensor moment with torso upright (Extensor Upright); 2) Extensor moment with torso flexed about the hips to 50% of maximum range of motion (Extensor 50); 3) Flexor moment with torso upright (Flexor Upright); 4) Flexor moment with torso flexed about the hips to 50% of maximum (Flexor 50). Three trials of each moment contraction were performed in a randomized order.

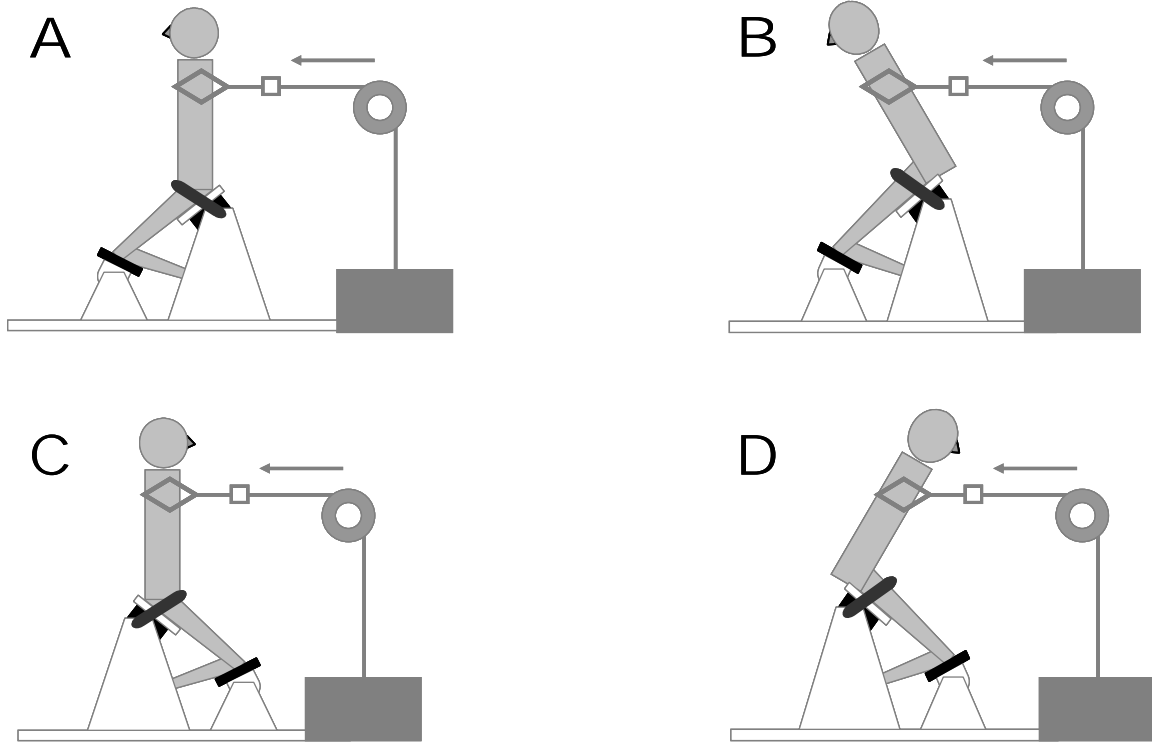


Figure 3.1. Participant positioning for each of the Flexor Upright (A), Flexor 50 (B), Extensor Upright (C), and Extensor 50 (D) conditions.

3.2.3 Instrumentation and Processing

EMG was recorded and analyzed as reported in Chapter 2.

An active marker system (Optotrak, Northern Digital Inc., Waterloo, Canada) was used to monitor the position of the upper body throughout each of the contractions. Markers were placed on the following locations on the right side of the body: 1) head (zygomatic process); 2) shoulder (greater tubercle of humerus); 3) elbow (lateral epicondyle); 4) wrist (ulnar styloid); 5) hand (3rd metacarpal-phalangeal joint). Fins, each with two co-linear markers, were placed at the spinal levels of C7, T12 as well as the sacrum. These fins were used to determine the relative flexion angle of the lumbar spine as well as the projection into the body to determine the approximate locations of the C7/T12 and L4/L5 joint centres.

Finally, two markers were placed on the cable attached to the upper body to determine the line of pull of the generated force. Marker data were sampled at 64 Hz.

A two-dimensional top down linked-segment model was used to determine the L4/L5 moment produced by the weight of the upper body (anthropometrics from Winter, 2005). This was summed with the moment determined from the product of the force applied to the cable and its moment arm to the L4/L5 joint to obtain the net external L4/L5 moment.

The normalized EMG signals were entered along with the lumbar flexion angle into an anatomically detailed model of the lumbar spine (McGill & Norman, 1986; Cholewicki & McGill, 1996). A Distribution-Moment approach was utilized to determine individual muscle forces based on normalized activation, instantaneous muscle length, cross-sectional area, and an assumed muscle stress of 35 N/cm². The net moment produced by each of the extensor and abdominal muscle groups were determined:

$$\begin{aligned}
 M_{extensor} &= \sum_{m=1}^{78} r_{m\ extensor} \times F_{m\ extensor} \\
 M_{flexor} &= \sum_{m=1}^{10} r_{m\ flexor} \times F_{m\ flexor}
 \end{aligned}
 \tag{3.1}$$

where: $M_{extensor}$, M_{flexor} = moment produced by the extensor musculature (78 muscle fascicles representing the lumbar and thoracic longissimus and iliocostalis, multifidus, latissimus dorsi and quadratus lumborum muscle groups) and flexor musculature (10 muscle fascicles representing the rectus abdominis, external oblique and internal oblique muscle groups), about the L4/L5 joint, respectively

$r_{m\ extensor}$, $r_{m\ flexor}$ = extensor and flexor muscle moment arms, about the L4/L5 joint, respectively

$F_{m\ extensor}, F_{m\ flexor}$ = individual muscle fascicle forces in each of the extensor and flexor muscle groups.

The total resistive moment required to be overcome by the agonist muscle group was determined as either: a) the externally calculated moment alone; b) the summation of the externally calculated moment and the antagonist muscle moment:

$$\begin{aligned} a) M_{resistive} &= M_{external} \\ b) M_{resistive} &= M_{external} + M_{antagonist} \end{aligned} \quad (3.2)$$

where: $M_{resistive}$ = moment that must be produced by the agonist muscle group

$M_{external}$ = moment measured externally

$M_{antagonist}$ = moment produced by the antagonist muscle group (flexor muscles in the extensor moment trials and extensor muscles in the flexor moment trials).

All moment data were visually windowed over the period from the start of external moment generation until the end of external moment generation. For further analysis, subsequent windows were made of the force increasing and force decreasing portions of the contraction, which will be referred to as concentric and eccentric portions of the contraction (assuming compliant tendinous attachments allowing the musculature to shorten and lengthen in the absence of gross spine movement).

In each of these cases, data from all trials of each condition were pooled, and the linearity between the agonist muscle moment and the resistive moment was tested with the following equation (Potvin et al., 1996):

$$M_{agonistN} = \frac{e^{(-M_{agonistL} * \delta * 0.001)} - 1}{e^{(-0.1 * \delta)} - 1} \quad (3.3)$$

where: $M_{agonistN}$ = agonist muscle moment non-linearly normalized to 100% maximum

$M_{agonist L}$ = agonist muscle moment linearly normalized to 100% maximum

δ = constant to define exponential curvature (a loop was run ranging from -50 to 50; total of 101 iterations)

The root mean square difference was calculated between each of the linearly and non-linearly normalized muscle moments ($\delta = -50$ to 50 ; total 101) and the resistive moment (both with and without accounting for the antagonist moment). For each of the four conditions (Extensor Upright; Extensor 50; Flexor Upright; Flexor 50) the minimum RMS difference indicated the curvature resulting in the best fit between the muscle and resistive moments:

$$RMSdifference = \sqrt{\frac{1}{T} \sum_{t=1}^T (M_{agonistN_t} - M_{resistive_t})^2} \quad (3.4)$$

T = total number of time instances analyzed across all trials and participants per condition.

Finally, an index of trunk muscle co-activation was calculated as the percent ratio of antagonist moment to agonist moment at each instant throughout the contraction:

$$Co - activation = \frac{AntagonistMoment}{AgonistMoment} * 100 \quad (3.5)$$

3.3 Results

3.3.1 Effect of Antagonist Muscle Activity

When determining the linearity in the EMG-moment relationship without consideration of antagonist muscle activity, relationships ranged from nearly linear (Extensor Upright) to varying degrees of the non-linear form reported previously in the literature, with a declining increase in moment as EMG increased across its spectrum from zero to 100% of maximum (Extensor 50, Flexor Upright, Flexor 50) (Table 3.1).

Accounting for the additional resistive moment generated by the antagonist muscle groups altered the EMG-moment relationship in all cases, making it more linear in each of the Extensor 50, Flexor Upright and Flexor 50 conditions (Figure 3.2; Table 3.2). The relationship became slightly more non-linear in the Extensor Upright condition; however, the non-linearity was opposite to that found previously in the experimental literature, with a rise in the increasing moment as EMG increased across its spectrum (Figure 3.3; Table 3.2). This same slight non-linear form was also detected in each of the Flexor Upright and Flexor 50 conditions.

Table 3.1. Best-fit coefficients (determined for equation 3.1) and root-mean square difference (% MVC) for both the linear and best non-linear fits, between EMG moments and the externally determined moments alone (in the absence of antagonist muscle moments).

	Full ramp			
	Extensor Upright	Extensor 50%	Flexor Upright	Flexor 50%
coefficient	1	6	9	14
RMS	10.32	13.09	13.06	13.50
RMS linear	10.39	14.16	14.88	16.97

Table 3.2. Best-fit coefficients (determined for equation 3.3) and root-mean square difference (% MVC) for both the linear and best non-linear fits, between EMG moments and resistive moments (calculated as the sum of the antagonist muscle moment and externally determined moment).

	Full ramp			
	Extensor Upright	Extensor 50%	Flexor Upright	Flexor 50%
coefficient	-3	2	-3	-1
RMS	9.15	10.92	12.90	12.34
RMS linear	9.49	11.05	13.06	12.38

	Concentric			
	Extensor Upright	Extensor 50%	Flexor Upright	Flexor 50%
coefficient	-2	2	-3	-2
RMS	8.52	11.38	13.83	10.61
RMS linear	8.78	11.48	14.13	10.72

	Eccentric			
	Extensor Upright	Extensor 50%	Flexor Upright	Flexor 50%
coefficient	-2	3	4	2
RMS	7.52	7.40	9.55	8.64
RMS linear	7.65	7.68	9.98	8.75

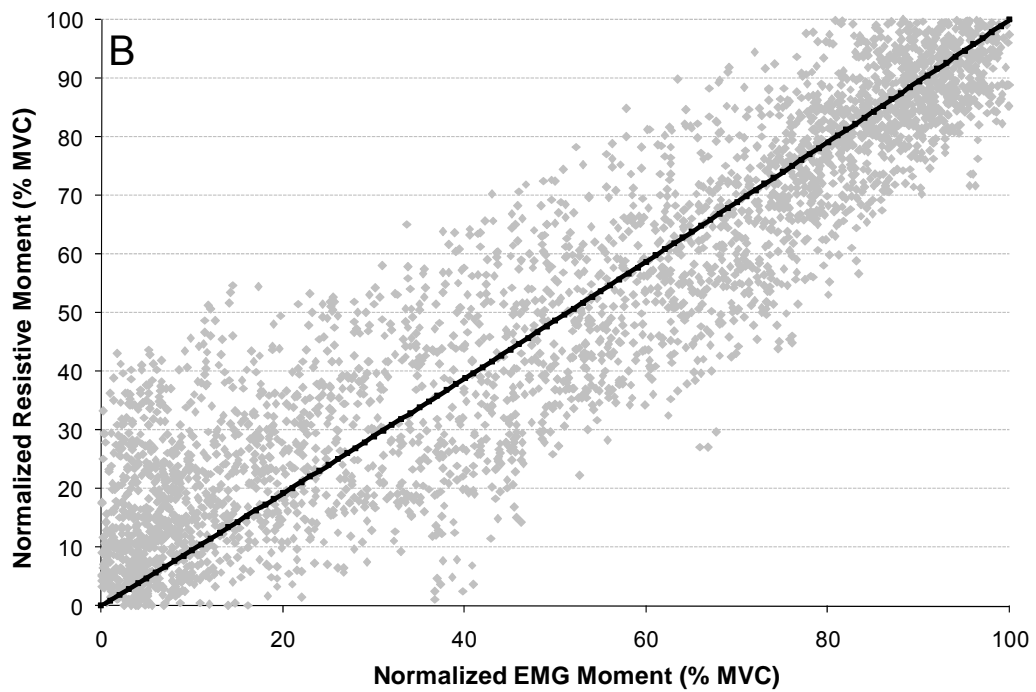
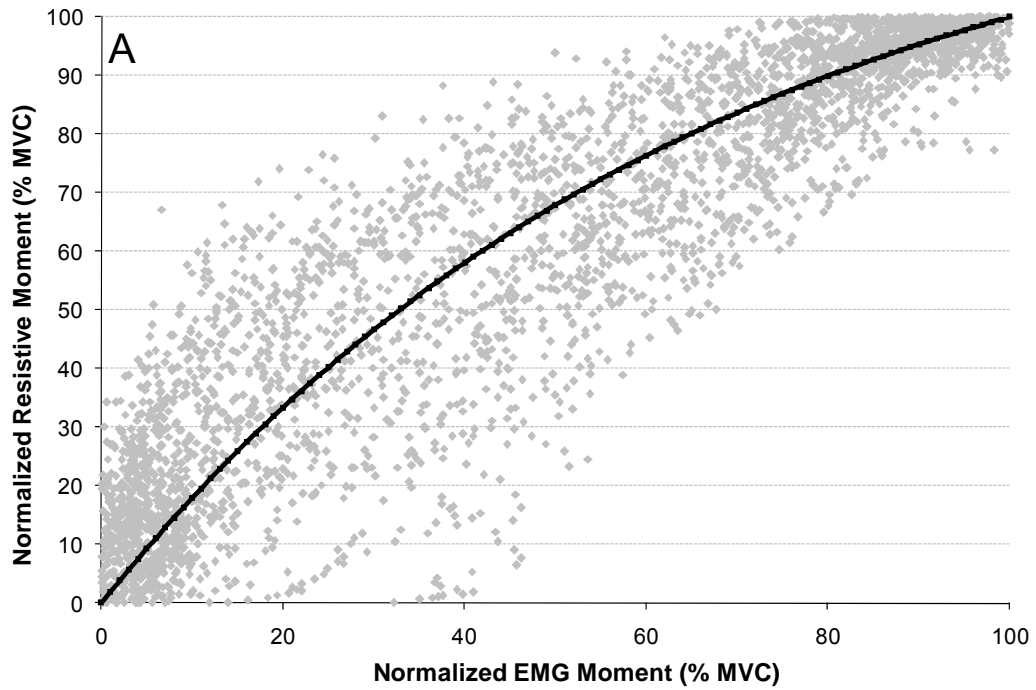


Figure 3.2. Scatterplots (all participants and trials) for the Flexor Moment 50% condition displaying the Agonist EMG Moment normalized to 100% of maximum versus the Resistive Moment normalized to 100% of maximum. A: Resistive Moment is the externally calculated moment alone; B: Resistive Moment is the combined externally applied moment and antagonist muscle moment.

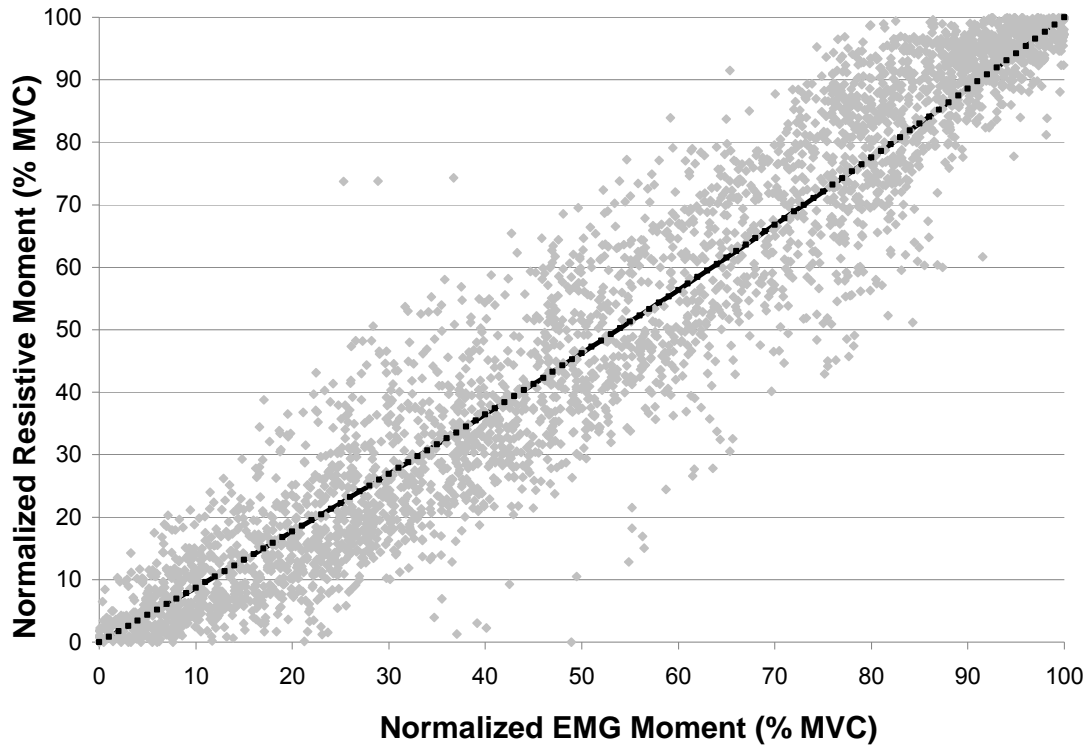


Figure 3.3. Scatterplot (all participants and trials) for the Extensor Upright condition displaying the Agonist EMG Moment normalized to 100% of maximum versus the Resistive Moment (accounting for the antagonist muscle moment) normalized to 100% of maximum. Note that the slight non-linearity in the curve fit is opposite to that normally cited in the experimental literature.

Further analysis determined that the majority of the change in linearity occurred in the concentric (force increasing) portion of the contraction (Table 3.2); the eccentric portion (force decreasing) of the contraction still displayed a slightly rising increase in moment per unit increase in EMG in all conditions except Extensor Upright.

3.3.2 Amount of Antagonist Muscle Activity Present

A relatively high level of antagonist muscle activity was present in all of the conditions examined in this study (Figure 3.4). The greatest amount of antagonist activity occurred in the Flexor 50 condition (co-activation ratio ranging from 50 to 298%), and the least in the Extensor 50 condition (co-activation ratio ranging from 19 to 27%). The points in the figures represent the average (across all participants) co-activation ratio normalized from zero to 100 percent of the dominant EMG moment.

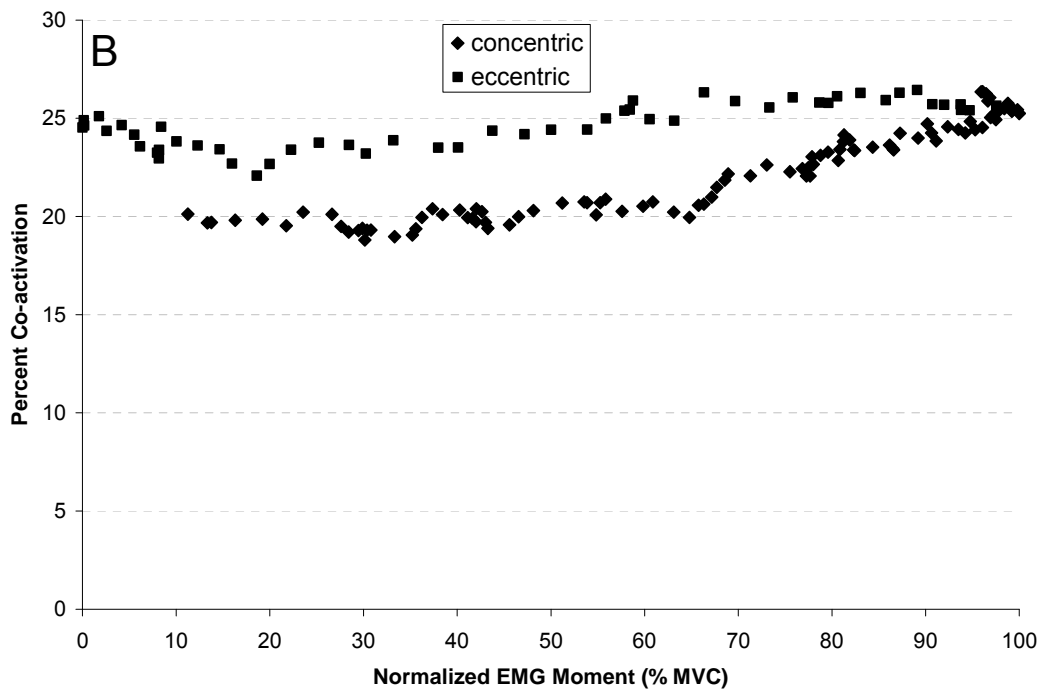
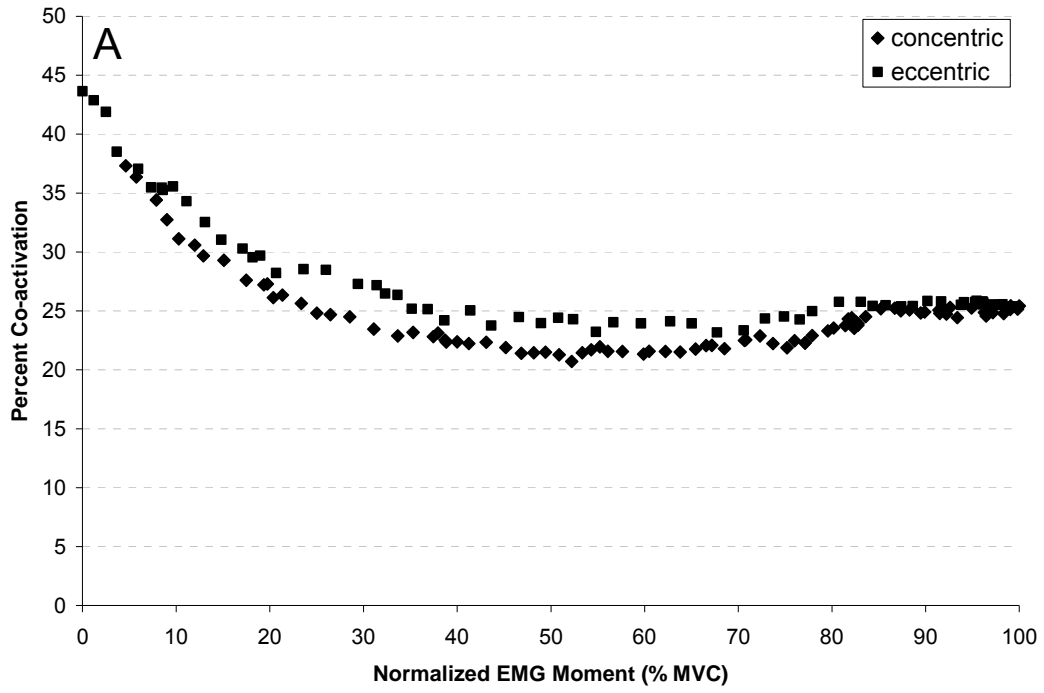


Figure 3.4. Continued next page.

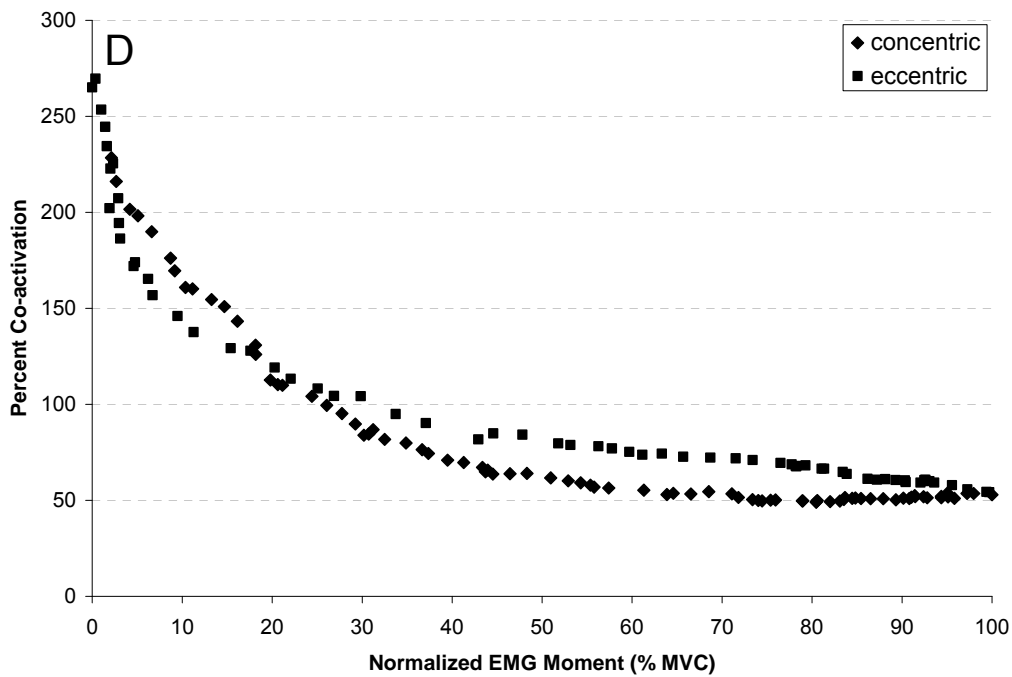
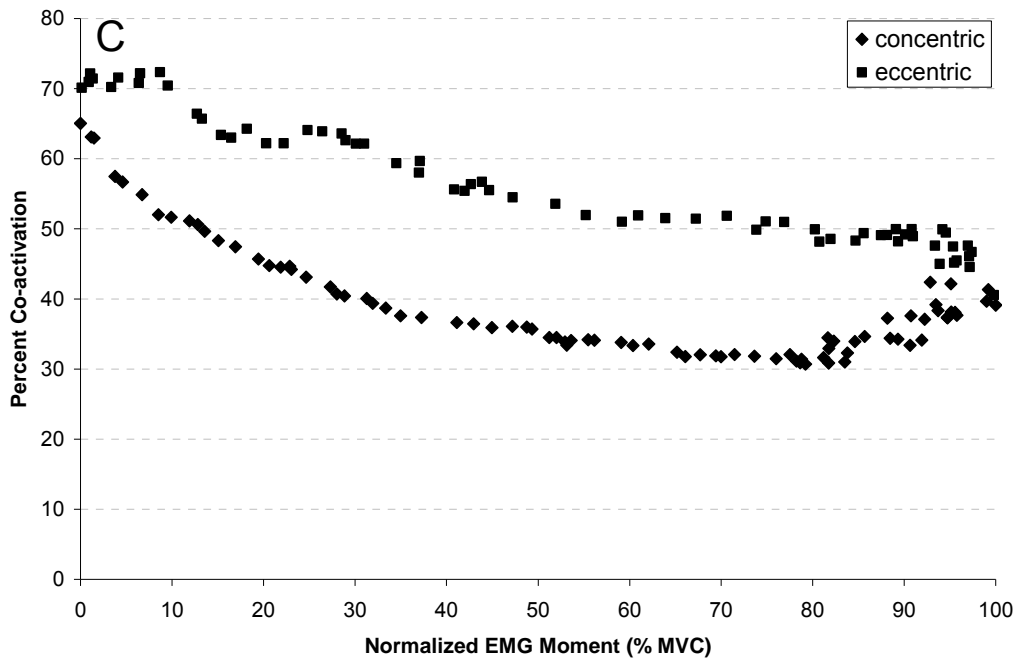


Figure 3.4. Average co-activation index (percent ratio of antagonist to agonist muscle moment) normalized with respect to the dominant EMG moment across all participants for each condition: A) Extensor Upright; B) Extensor 50%; C) Flexor Upright; D) Flexor 50%. Relationship is shown for each of the concentric and eccentric portions of the ramped contraction.

3.4 Discussion

The primary result of this study was that accounting for antagonist muscle activity influences the relationship between trunk EMG and its generated moment. Specifically, antagonist muscle activity creates an additional resistive moment that has to be overcome by the agonist muscle groups; ignoring this gives the impression of a non-linear relationship between the agonist EMG and the externally generated moment. The true nature of the trunk EMG-moment relationship was found to be more linear than has often been previously reported (Figure 3.1), and in fact may display a slight opposite non-linearity (Table 3.2; Figure 3.2) to that normally cited in the experimental literature, with an increase in the rise in moment as EMG increases through its range of activation. This opposite non-linearity has been predicted theoretically using motor unit based models of EMG (Milner-Brown & Stein, 1975; Fuglevand et al., 1993).

The amount of co-activation that occurred in the isometric flexor and extensor moment tasks studied here was quite high (Figure 3.4). Generating the flexor moments, in particular, produced a substantial amount of activation from the trunk extensor musculature. This is not at all surprising in the Flexor 50 condition, where activation of the extensor musculature was required simply to balance the flexor moment created by the mass of the upper body. In the other three conditions, however, the co-activation served very little or no direct purpose in balancing externally produced moments, and therefore acted primarily to provide a level of stiffness and stability sufficient to prevent the spine from buckling under load. The average level of co-activation, as calculated in this study, never dropped below 18%. This supports previous findings and hypotheses stating that some level of antagonist co-activation is constantly required to maintain the integrity of the spinal column

(Cholewicki & McGill, 1996; Brown & Potvin, 2005). Therefore, it is not surprising that consideration of this consequent additional moment is necessary to properly model the moment generated by the agonist muscle group of interest.

The participants in the current study were limited to eight healthy males. The goodness of fit of the experimental data, combined with the intended purpose of the study to demonstrate the necessity of considering antagonist muscle activation in determining EMG based estimates of spinal force/moment, indicates that this number of participants has been sufficient to accomplish this goal. Consideration of antagonist activity has been clearly shown to be essential for at least the eight participants studied here; this makes sense both biologically and mechanically, and alone should indicate that this is a consideration that should not be overlooked in these types of analyses.

Finally, the additional purpose of this paper was to test the EMG-moment relationship of the abdominal musculature. Negligible differences were found between trunk extensor and abdominal flexor muscles in terms of the form of the EMG-moment relationship. Thus, the surface EMG signals obtained from these muscles can be treated similarly in the data processing stage; however, the scaling magnitude between the EMG estimated moment and actual moment will be highly dependent upon model assumptions, anatomical fidelity, and measurement accuracy, and must be additionally considered in order to model the net muscle force and moment outputs, and corresponding joint forces and measures of stability and/or stiffness. The current findings will improve the modeling and estimation of these joint parameters, which is essential to further the understanding of the muscular relationship to spine injury, rehabilitation, and performance.

Chapter 4:

How the Inherent Stiffness of the in-vivo Human Trunk Varies with Changing Magnitudes of Muscular Activation

Chapter Synopsis

The abdominal muscles provide stiffness to the torso in a manner that is not well understood. Their unique anatomical arrangement may modify their stiffening ability with respect to the more commonly studied long strap-like muscles of the limbs. The purpose of this study was to examine stiffness inherent to the trunk, as modified by different torso, and in particular, abdominal muscle activation levels. Nine healthy male participants were secured in a “frictionless” apparatus and subjected to applied bending moments about either the flexion/extension or lateral bend axis. Abdominal muscle activation levels were modified through biofeedback from the right external oblique muscle. Moment-angle curves were generated and characterized by an exponential function for each of flexion, extension, and right-side lateral bend, at each of four abdominal muscle activation target level conditions. Stiffness measured in extension increased in a linear fashion throughout the range of motion and increased with each successive rise in abdominal activation. Stiffness in flexion and lateral bend increased in an exponential fashion over the range of motion. In flexion and lateral bend, stiffness increased with each successive rise in abdominal activation from zero to approximately 40% and 60% of the range of motion, respectively. After these points, stiffness at the highest levels of activation displayed a phenomenon whereby the torso stiffness dropped below that characterized at lower levels of activation. Increasing torso muscle co-activation leads to a rise in trunk stiffness over postures most commonly adopted by individuals through daily activities (neutral to approximately 40% of maximum range of motion). However, towards the end range of motion in both flexion and lateral bend, individuals became less stiff at the maximum abdominal muscle co-activation levels. The

source and mechanism of this apparent yielding are not fully understood; future work will be directed toward elucidating the cause.

4.1 Introduction

The torso musculature is quite unique in its anatomical arrangement. In particular, the abdominal wall muscles (external and internal obliques, transverse abdominis) overlay each other in a sheet-like formation and act through attachments to the abdominal and thoraco-lumbo-dorsal fascias to create a hydraulically pressurized abdomen. These abdominal muscles, when activated, create a stiffened wall to provide stability and structural integrity to the spinal column (Farfan, 1973; Tesh et al., 1987; Cholewicki et al., 1999).

Muscle mechanics theory tells us that muscle tissue, while creating force, also provides stiffness about a joint that is at least partially dependent on the inherent spring-like stiffness of the muscle itself. Its stiffness is a combination of active components, namely myosin cross-bridge attachments, the numbers of which are dependent upon activation level and type of contraction, and passive components, namely the connective tissue network running throughout the muscle and tendon complex (Ford et al., 1981; Rack & Westbury, 1984; Lieber et al., 1992; Gajdosik, 2001). Moreover, muscle reflexes further modulate stiffness about a joint by reacting to a perturbation to either increase contraction to counteract motion, or to decrease contraction so as to not accentuate the motion (Nichols and Houk, 1976; Hoffer and Andreassen, 1981; Franklin and Granata, 2007). Most of what we know about muscle stiffness and its effect on surrounding joints has been obtained from studies of the long strap-like muscles of the limbs. The abdominal wall muscles, however, may not be expected to stiffen the joints of the spine in an entirely similar manner given their distinctive architecture. In fact their ability to stiffen may be enhanced through a hydraulic mechanism, modifying intra-abdominal pressure and transferring hoop stresses around the torso (Farfan, 1973; Cresswell & Thorstensson, 1989; McGill & Norman, 1993).

A number of studies have dealt with determining the effect of altering trunk muscle activation levels on trunk stiffness and/or stability by utilizing rapid perturbation paradigms (eg. Krajcarski et al., 1999; Chiang and Potvin, 2001; Gardner-Morse and Stokes, 2001; Andersen et al., 2004; Moorhouse and Granata, 2005). In this way, these studies have captured the combined stiffness of all active, passive, and reflexive components acting within the spinal system. The consensus reached from this body of work has been that increasing muscle activation through an increased challenge imparted to the system leads to a stiffer system. More recently, Vera-Garcia et al. (2006) demonstrated that consciously increasing trunk muscle co-activation through abdominal brace techniques improved trunk stiffness in preparation for a sudden load. However, other studies have shown that attempting to consciously alter trunk muscle co-activation might constitute a non-optimal motor scheme and result in a drop in stability for more demanding situations (Brown et al., 2006).

Previous work has attempted to isolate and determine the passive, or inherent, stiffness of the in-vivo trunk in each of the three anatomical planes of motion (McGill et al., 1994) and after time-varying alterations (Beach et al., 2005; Parkinson et al., 2004). To date, no study has attempted to quantify the trunk stiffness inherent, in the absence of reflexive mechanisms, at varying levels of trunk muscle activation. This may elucidate the role of torso muscle activation on the hydraulic stiffening mechanisms discussed above. Therefore, the purpose of this study was to examine trunk stiffness related to torso, and in particular abdominal, muscle activation levels, while minimizing the effect of muscle reflexes. Further, the goal was to determine the effect of increasing muscle stiffness on global trunk stiffness in each of the flexion, extension, and lateral bend directions.

4.2 Methods

4.2.1 Participants

Nine healthy male individuals volunteered from the University population (mean/SD: age 23.9/2.8 years; height 1.81/0.05 m; mass 79.0/7.1 kg). All signed consent forms approved by the University Office of Research Ethics.

4.2.2 Data Collection

Participants were secured at the hips, knees and ankles on a solid lower body platform. Each participant's upper body was secured to a cradle with a plexi-glass bottom surface, about their upper arms, torso and shoulders. The upper body cradle was free to glide overtop of a similar plexi-glass surface with precision nylon balls between the two structures (Figure 4.1). This jig minimizes measurable friction and allows trunk movement about either the flexion-extension or lateral bend axis, depending upon how the participant is secured. Participants lay on their right side for the flexion-extension trials, and on their back for the lateral bend trials. Their torsos were supported in each position to ensure that participants adopted and maintained a non-deviated spine posture throughout the testing. Participants were then instructed to maintain one of four torso activation patterns: relaxed (minimal activation); activate biofeedback site to approximately 5 % maximum voluntary contraction (MVC) (light brace); activate biofeedback site to approximately 10 % MVC (moderate brace); activate biofeedback site to approximately 15 % MVC (heavy brace). Participants were instructed to tighten their abdominal muscles isometrically in order to achieve the desired brace levels.

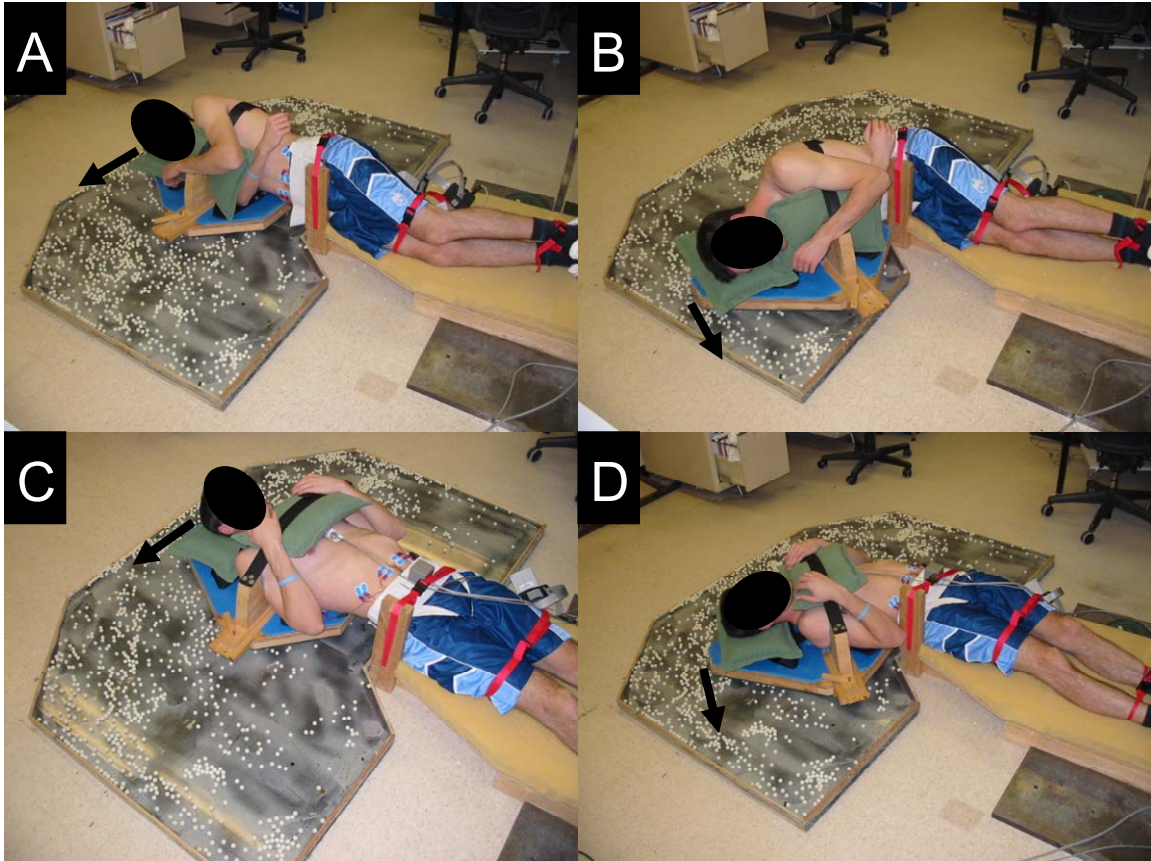


Figure 4.1. Experimental set-up in the neutral position (A: flexion/extension; C: lateral bend) and at end ROM (B: flexion; D: lateral bend). Arrows indicate the direction of the applied force (perpendicular to the upper body cradle).

Once each participant had achieved his target activation pattern during each trial, the experimenter pulled a cable such that the upper body rotated in the desired direction. For flexion trials, the participant was pulled into flexion; for extension trials, the participant was pulled into extension; for lateral bend trials, the participant was pulled into right-side lateral bend. Participants were pulled at a relatively slow velocity (mean(SD) (degrees/s) = 5.0(2.9) flexion; 3.9(2.5) extension; 6.1(3.4) lateral bend), until a point was reached at which the experimenter could no longer effectively rotate the participant about the lumbar spine. The

direction of pull of the cable with respect to the upper body cradle always remained constant; perpendicular to the upper body cradle.

Once the motion began, participants were no longer able to utilize the visual biofeedback to maintain their activation level; they instead were instructed to maintain the “feel” of the abdominal brace level throughout the movement. However, EMG was recorded throughout the trials and examined post-hoc to ensure that EMG remained near the targeted levels. Three trials of each activation condition were conducted in a randomly assigned order for each participant.

4.2.3 Instrumentation

EMG was recorded and analyzed as reported in Chapter 2.

An EMG biofeedback device (MyoTrac, Thought Technology Ltd., Montreal, Canada) was placed in line with the right EO electrode site to allow participants to visually monitor muscle activity at this level.

Three-Dimensional trunk motion was recorded using an electromagnetic tracking system (Isotrak, Polhemus, Colchester, VT, USA) with the source secured over the sacrum and the sensor over T12 for the flexion/extension trials, and the source over the lower abdomen at a level slightly below the ASIS and the sensor over the xiphoid process for the lateral bend trials. The trunk motion data was sampled digitally at 32 Hz and dual-pass filtered (effective 4th order 3 Hz low-pass Butterworth).

The moments applied to the torso were recorded by the product of the force applied perpendicular to the distal end of the upper body cradle and the moment arm from the location of the applied force to the L4/L5 joint. Force was recorded with a force transducer

(Transducer Techniques Inc., Temecula, CA, USA) and digitally sampled at 2048 Hz. Force signals were dual-pass filtered (effective 4th order 3 Hz low-pass Butterworth). Both the linear enveloped EMG and force signals were downsampled to 32 Hz to match the trunk motion data.

4.2.4 Moment-Angle Curves

The applied moment and corresponding trunk angle were windowed for each trial and normalized in time to ensure equal trial length across all trials and participants. Trunk angles were normalized as a percentage of the maximum range of motion (ROM) that participants were able to obtain in trials conducted from an upright standing position.

Data were combined across trials and subjects for each muscle activation/brace level for each of the flexion, extension, and lateral bend directions. Exponential curve fits of the following form were performed for each brace level/direction combination:

$$M = \lambda e^{\delta\phi} \quad (4.1)$$

where: $M = \text{applied moment (Nm)}$

$\lambda, \delta = \text{curve fitting coefficients}$

$\phi = \text{trunk angle as a percent of the standing max ROM}$

This equation was differentiated once with respect to ϕ to obtain a measure of trunk angular stiffness:

$$K = \lambda\delta e^{\delta\phi} \quad (4.2)$$

where: $K = \text{angular stiffness (Nm/\%ROM)}$

Additionally, the applied moment required to initiate trunk motion, the peak applied moment, and the maximum trunk angular displacement were all recorded for each trial. The normalized EMG activation averaged over each of the 250 ms prior to the initiation of the applied moment, as well as the 250 ms prior to the end of movement, was quantified and averaged across the right and left side muscles. For a comparison in activation levels between each of the two 250ms periods, right and left side muscles were kept separate for the lateral bend condition.

4.3.4 Statistical Analysis

Each of the dependent variables was averaged within each subject for each condition.

Repeated Measures 1-way (four muscle activation levels) ANOVAs were conducted for each of the following dependent variables: the applied moment required to initiate trunk motion; the peak applied moment; and the maximum trunk angular displacement. The effect of time on muscle activation levels, and possible interactions with brace levels, were evaluated using a Repeated Measures 2-way (brace level and EMG pre versus final 250ms of movement) ANOVA. Tukey's HSD tests were run in cases where a significant effect ($p < 0.05$) was determined by the ANOVA.

4.4 Results

4.4.1 EMG

Average muscle activation levels, quantified prior to the initiation of movement, increased between each of the relaxed, light, moderate, and heavy abdominal brace levels for every muscle except the RA between the relaxed and light brace levels in the flexion

condition and the ES-L5 between the moderate and heavy brace levels in the extension condition (Figure 4.2). Statistically significant ($p < 0.05$) differences between levels are indicated in Figure 4.2.

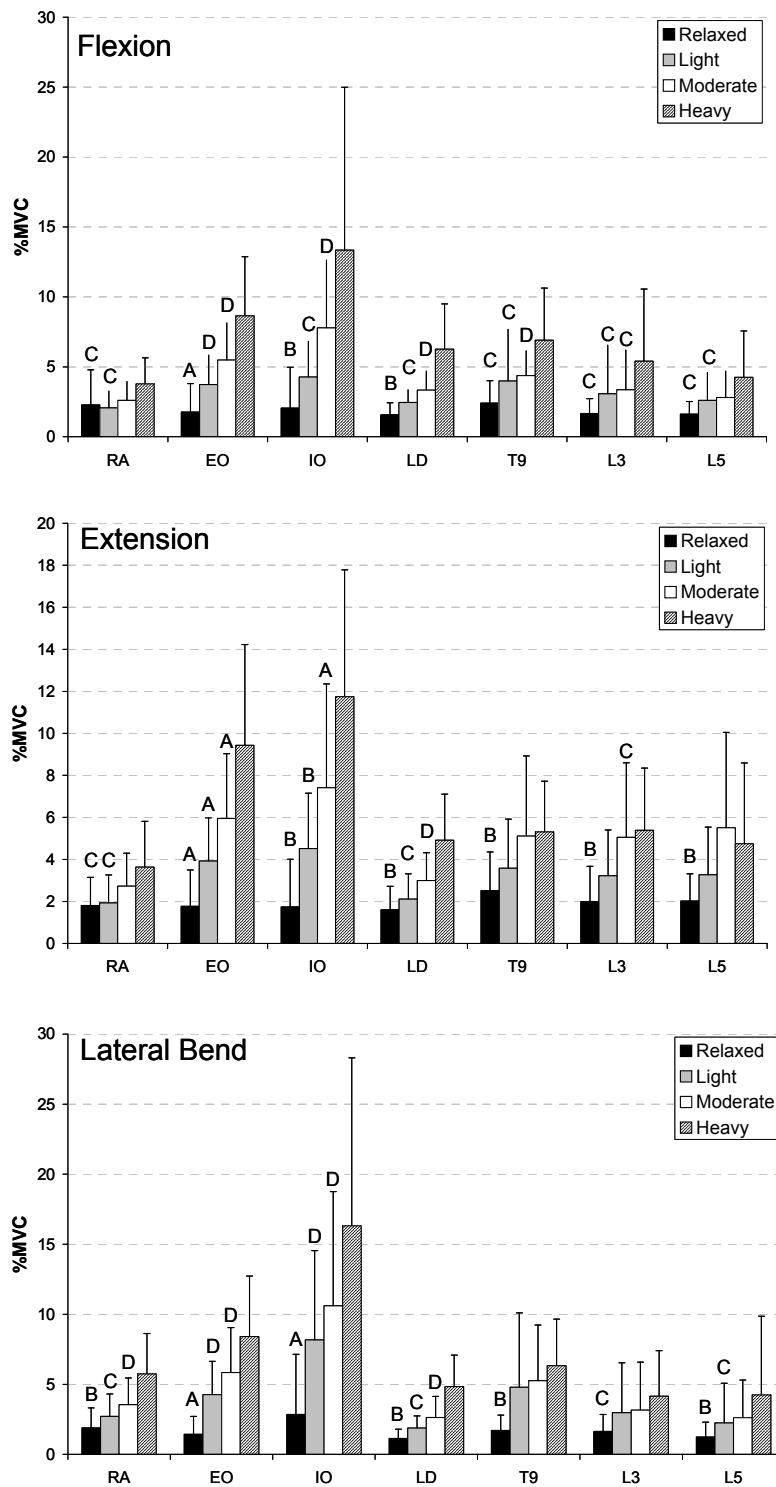


Figure 4.2. EMG averages (across all trials and bilaterally across right and left sides) and standard deviations for the 250 ms prior to the initiation of the applied moment for each brace level in each of the flexion, extension and lateral bend conditions. Significance ($p < 0.05$) is as follows: A = different from all other levels; B = different from the moderate and heavy levels; C = different from the heavy level; D = different from the relaxed and heavy levels.

A number of statistically significant differences, consistent across all brace levels, were found for average muscle activation levels prior to versus at the end of movement. Those that increased activation from initiation to the end of the movement were: in extension ES-L5 (3.9 to 6.0 %MVC); in lateral bend right RA (4.3 to 7.2 %MVC), right EO (6.2 to 10.4 %MVC), right ES-T9 (3.7 to 5.3 %MVC) and left ES-T9 (5.3 to 7.7 %MVC). Those that decreased activation from initiation to the end of the movement were: in flexion ES-L5 (2.8 to 1.8 %MVC); in lateral bend left ES-T5 (2.1 to 1.2 %MVC). The more interesting muscles were those that showed an interaction between time and brace level (in flexion LD and EO; in extension LD; in lateral bend both right and left LD). The LD in flexion and both LDs in lateral bend increased activation towards the end of movement in all brace conditions, with greater differences between the two time periods for each successive increase in brace level. In extension the LD showed a lower activation level at the end of movement in the relaxed condition but a higher level at the end of movement in each of the three brace conditions. The EO in the flexion trials was the only muscle to display a decrease in activation level at the end of movement that was greater with each successive magnitude of brace level. Despite these documented changes in activation level, a very similar pattern of increased torso muscle activation between each of the abdominal brace levels existed for all muscles over the last 250ms of movement as did prior to the initiation of movement.

4.4.2 Stiffness Curves

The light brace flexion moment-angle data, combined across all trials, is displayed as an example in Figure 4.3. Least squares best fit stiffness curves are shown, encompassing zero to 100 % of the maximum standing ROM, for each of the flexion, extension, and lateral

bend directions (Figure 4.4). Stiffness increased exponentially at each muscle activation level in both flexion and lateral bend. In flexion, from zero to approximately 40% ROM, stiffness increased with each level of abdominal brace; in lateral bend, this trend existed from zero to approximately 60% ROM. At the end ROM in flexion, individuals were stiffest when employing a light muscle activation level, followed by relaxed, with heavy and moderate activation levels displaying the lowest stiffness levels. In lateral bend, at the end ROM, individuals were stiffest when employing a moderate level of activation, followed by the light and heavy levels, with relaxed displaying the lowest stiffness levels. Best-fit coefficients are displayed in Table 4.1.

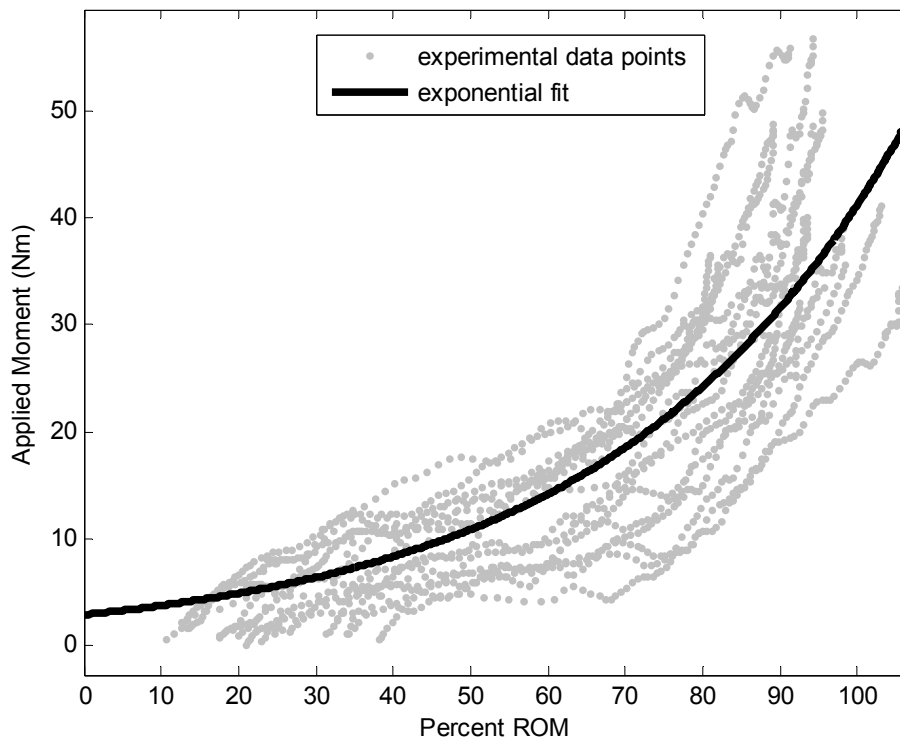


Figure 4.3. Scatterplot of moment-angle data points for all trials and participants within the light brace flexion condition. Thick line indicates exponential line of best fit.

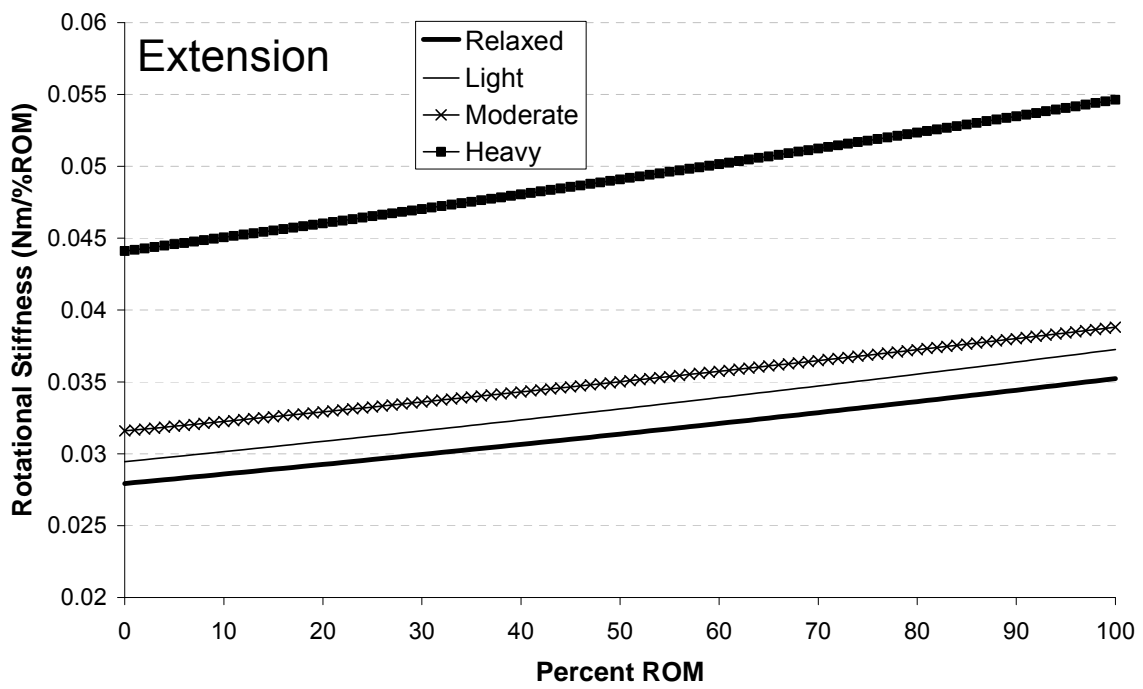
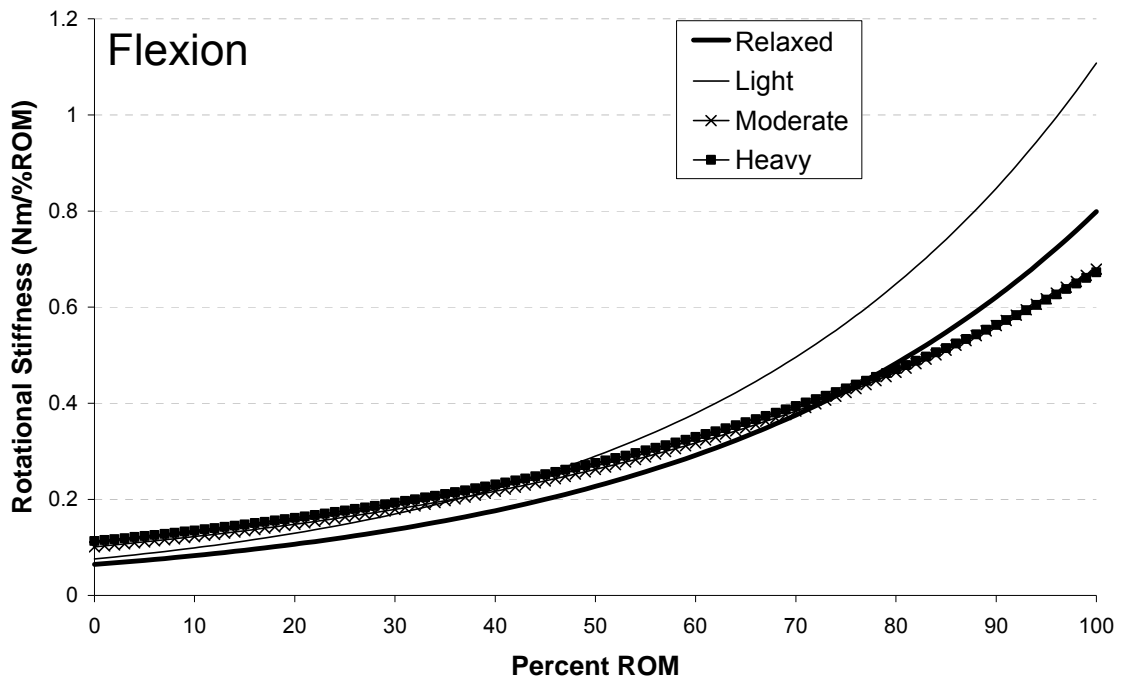


Figure 4.4. Continued on next page.

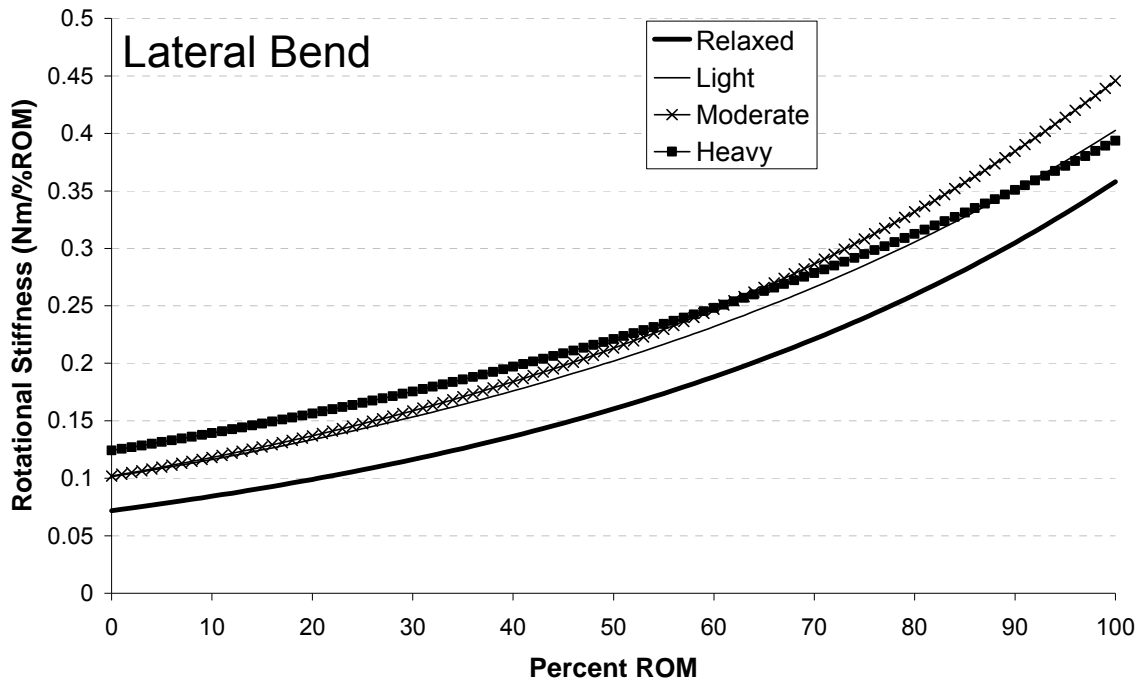


Figure 4.4. Stiffness (Nm/%ROM) determined from the first derivative of the moment-angle curve fits ($K = \lambda \delta e^{\delta \phi}$) across the ROM in each of the flexion, extension and lateral bend directions.

Stiffness in extension showed an increasing linear trend with increasing ROM for each of the muscle activation levels. Stiffness increased with each successive increase in trunk muscle activation.

Table 4.1. Best fit coefficients and root-mean-square (RMS) error (Nm) for equation 1 ($M = \lambda e^{\delta\phi}$) for the relaxed and each of the three different brace levels in each of flexion, extension, and lateral bend.

	flexion				extension				lateral bend			
	relaxed	light	moderate	heavy	relaxed	light	moderate	heavy	relaxed	light	moderate	heavy
λ	2.565	2.831	5.531	6.354	12.030	12.520	15.350	20.580	4.474	7.353	6.913	10.760
δ	0.0252	0.0268	0.0190	0.0178	0.00232	0.00235	0.00206	0.00214	0.0161	0.0138	0.0148	0.0115
RMS	5.17	7.31	9.21	10.23	8.04	7.11	8.31	11.77	8.55	10.82	9.86	13.24

4.2.3 Moment-Angle Characteristics

A higher applied moment was required to initiate movement in the heavy brace as compared to the relaxed condition in each of the flexion ($p=0.028$), extension ($p=0.025$), and lateral bend ($p=0.025$) directions (Figure 4.5). Additionally, the peak applied moments (corresponding to the point at which the experimenter could no longer rotate the participant) were significantly higher in extension ($p=0.004$) in the heavy brace as compared to the light condition, and in lateral bend ($p=0.043$) in the heavy brace as compared to the relaxed brace condition (Figure 4.6). Finally, the maximum trunk angular displacement was significantly greater in the relaxed as compared to the heavy brace condition in the flexion direction ($p=0.0245$) (Figure 4.7).

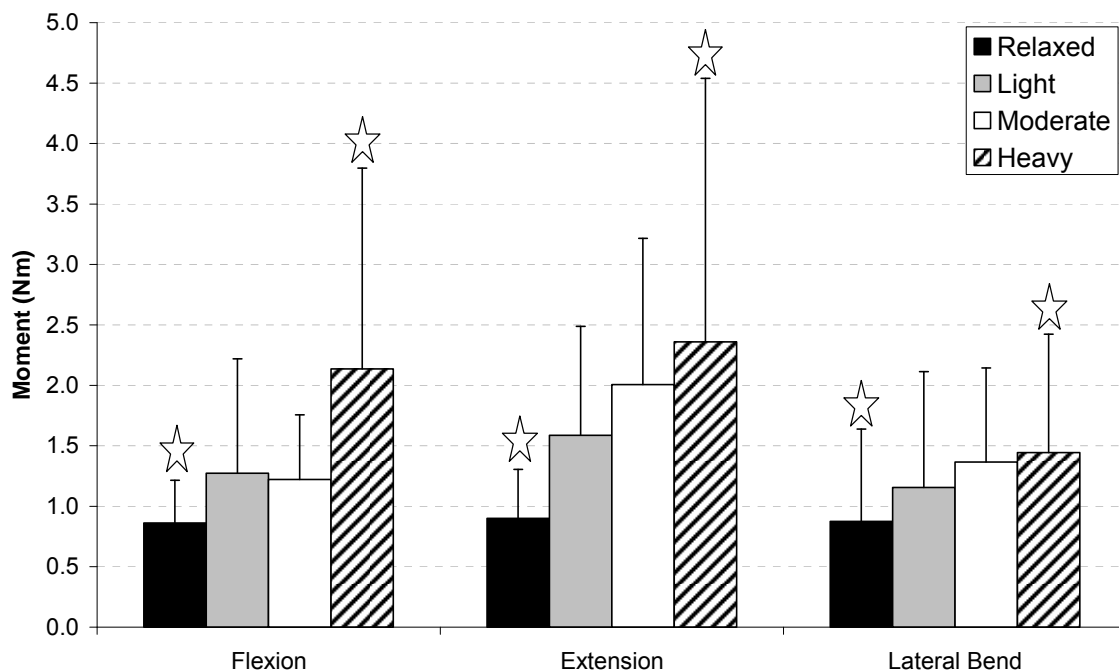


Figure 4.5. Average (SD) moment required to initiate bend about each axis in each of the relaxed and light, moderate and heavy brace conditions. Conditions, within each bend direction, which are significantly different ($p < 0.05$) from one another are indicated with stars.

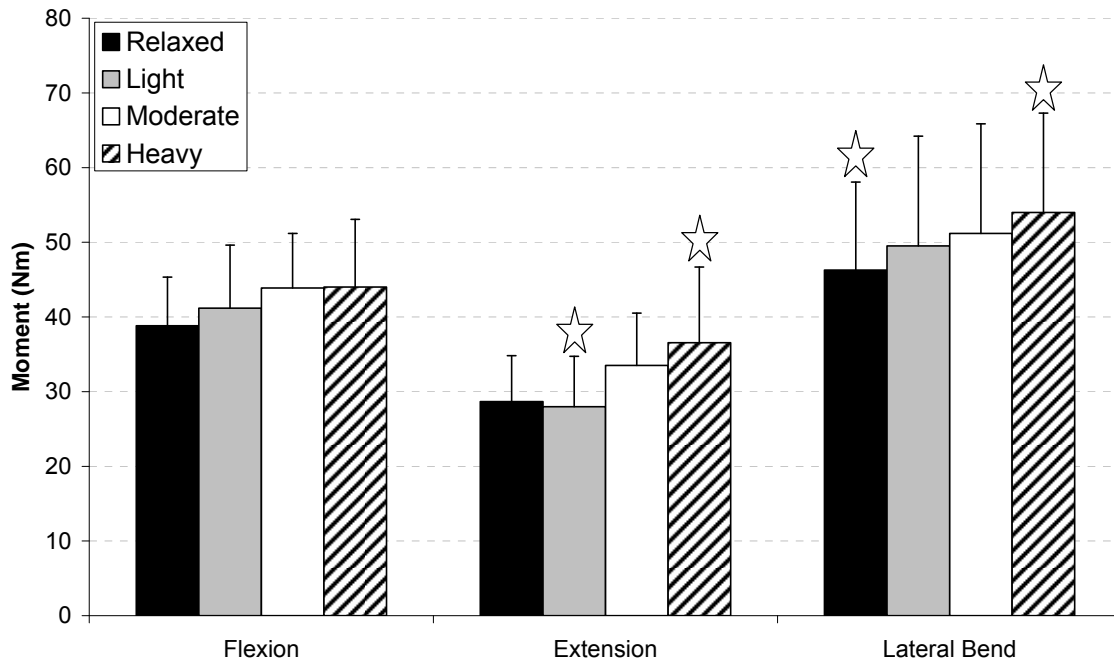


Figure 4.6. Average (SD) peak moment, corresponding to the end ROM, about each axis in each of the relaxed and light, moderate and heavy brace conditions. Conditions, within each bend direction, which are significantly different ($p < 0.05$) from one another are indicated with stars.

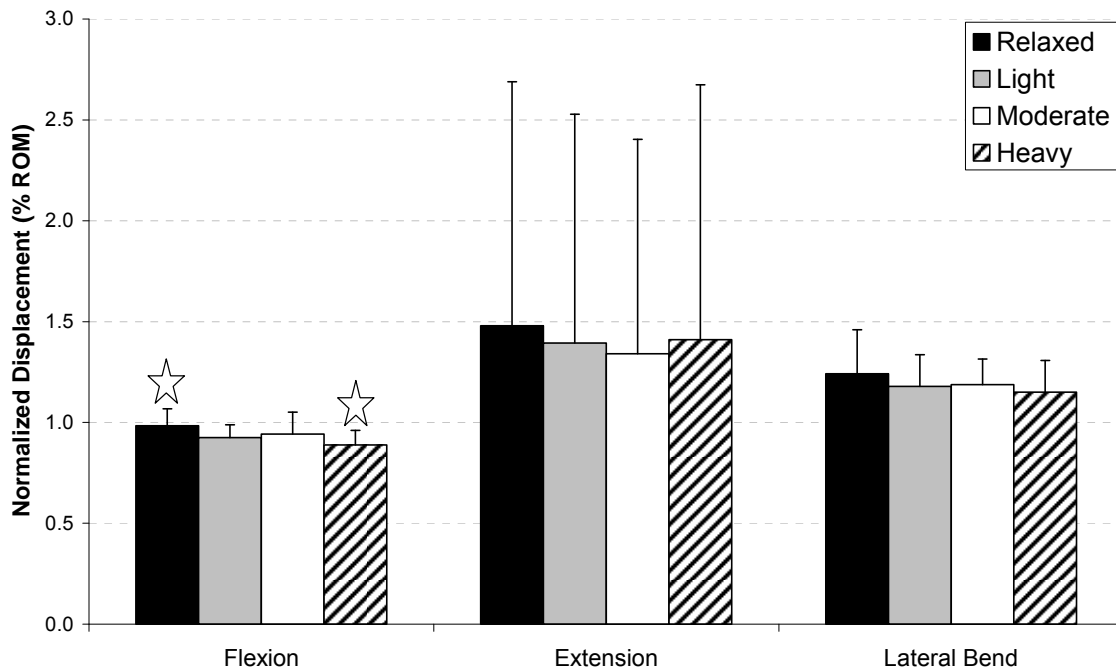


Figure 4.7. Average (SD) maximum trunk displacement, normalized to the maximum attained in standing ROM tests, about each axis for each of the relaxed and light, moderate and heavy brace conditions. Conditions, within each bend direction, which are significantly different ($p < 0.05$) from one another are indicated with stars.

4.4 Discussion

The primary purpose of this study was to determine the amount of torso stiffness inherent to the trunk musculature, and in particular the abdominal musculature, at different levels of activation. It was found that stiffness increased with each successive increase in muscle activation level across the entire ROM in a linear fashion in extension, and in a non-linear fashion with stiffness increasing at a greater rate at higher angles of rotation, through the low to mid ROM (neutral to approximately 40% of maximum) in each of flexion and lateral bend (Figure 4.4).

Muscle activation levels were manipulated through the use of abdominal bracing techniques. In this technique, individuals focus on isometrically tightening, or increasing activation levels, of the abdominal wall musculature. The isometric nature of this task induces opposing muscle groups, primarily the trunk extensors, to concomitantly increase activation (Figure 4.2). In addition, contraction of the abdominal wall stiffens posterior components of the spine via interaction with the lumbo-dorsal fascia (Tesh et al., 1987), and creates associated increases in intra-abdominal pressure (Cholewicki et al., 1999; Essendrop et al., 2002; Hodges et al., 2005). In the current study, varying levels of bracing were achieved through the use of visual biofeedback from the right external oblique muscle site. Therefore, the largest increases in activation between each of the brace levels were seen in the external and internal oblique muscles. Highest activation levels reached approximately 16% in the internal oblique in the lateral bend conditions, and 12-13% in the internal oblique in the flexion and extension conditions. The greatest activation changes between adjacent brace levels tended to occur between the moderate and heavy braces, and the smallest between the light and moderate brace levels. For the majority of the participants, the heavy brace level represented the maximum isometric abdominal contraction that they could achieve in the test position. They therefore were able to somewhat remove focus from the biofeedback and tend focus to attaining maximal contraction in these trials.

It was initially hypothesized that for each direction of movement, stiffness would increase along with successive increases in muscle activation. This was confirmed throughout the extension ROM, and in the flexion and lateral bend directions for the first 40 to 60% of ROM. For reasons that are not fully understood, there appeared to be a “yielding” phenomenon occurring with higher levels of activation as end range of flexion and lateral

bend were approached. There are two possible explanations for this finding: 1) Activation of the abdominal wall muscles creates a balloon-like structure of the abdomen. Increasing activation raises the tension and creates a stiffer balloon. As bending occurs, the balloon eventually folds upon itself, thus yielding its increasing resistance to bend; the stiffer the original state of the balloon, the greater the load acting upon it and thus the greater the yielding effect. A diagrammatic explanation for this hypothesis is provided in Figure 4.8; 2) The light and moderate brace levels were much easier to attain for the participants, and it is therefore plausible that individuals had difficulty in controlling the more difficult brace levels during the mid to upper ranges of the ROM. Indeed, the activation levels of certain muscles changed over the course of the movement, displaying different magnitudes over the last 250ms of movement as compared to the period prior to the initiation of movement. These changes were, however, counter to what one might expect to create the apparent “yielding” effect seen here; the muscles either changed consistently across the different brace levels or showed greater increases in activation at the higher levels of abdominal bracing. Still, it has been shown previously that increasing activation in isolated muscles can create an imbalance in torso stiffness (Brown & McGill, 2005; Brown et al., 2006). This idea is consistent with work showing that consciously increasing activation in the torso musculature can potentially degrade postural control (Reeves et al., 2006) and elevate motor control difficulty, thereby compromising torso stiffness in more challenging situations (Brown et al., 2006).

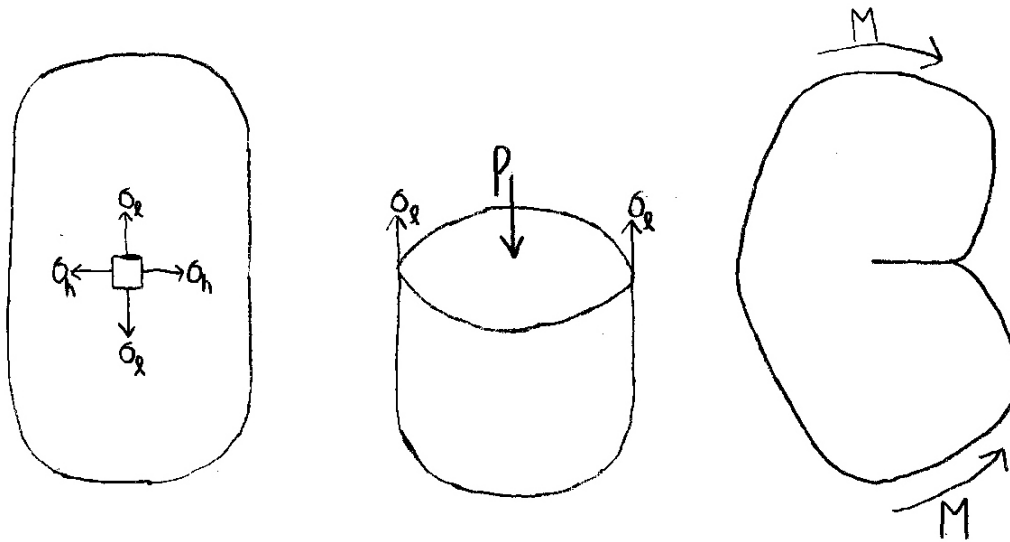


Figure 4.8. Diagram explaining the balloon hypothesis. On the far left a fluid filled cylinder, representing the abdomen, is shown. A stress coordinate system is established representing longitudinal (σ_l) and hoop (σ_h) stresses on the abdominal wall. The middle figure displays a free body diagram of the cylinder cut across its longitudinal axis. As the abdominal muscles contract, the pressure (P) within the cylinder increases, causing a subsequent increase in the longitudinal and hoop (not shown based on this cut) stresses acting on the wall. As moments (M) are applied to bend the cylinder, pressure builds within. Eventually, the cylinder will kink and buckle, creating a “yielding” (ie. a reduced resistance to bend). The greater the pressure within the cylinder, the greater its resistance to bend and consequently the greater the likelihood of the kink and yield occurring.

A number of factors contributed to the trunk stiffness examined in the current study. During rapid length changes, muscles display a “short-range” stiffness that is proportional to the number of strongly attached cross-bridges to produce contraction (Joyce & Rack, 1969; Ford et al., 1981; Ettema & Huijing, 1990). This stiffness lasts only for very small length changes, until cross-bridge bonds break, and is most pronounced at high velocities (Rack & Westbury, 1984; Mutungi & Ranatunga, 1996). Due to the slow velocity, long-range nature of the stretches in the current study, it is unlikely that the muscles displayed the full potential stiffness residing in the cross-bridges. Some additional stiffness inherent to the muscle may

reside in the reorganizing of the intramuscular and extramuscular connective tissues that occurs with contraction (Monti et al., 1999; Meijer et al., 2006).

Tissues directly unrelated to muscle activation provide additional stiffness to the trunk, especially as end ROM is approached. Ligaments and intervertebral discs (Adams et al., 1980), buckled abdominal contents, and bony contact all provide varying amounts of stiffness towards end ROM in each of the three motion directions. Because these factors are a function of spine posture and tissue length, their stiffness contributions would be the same for each level of muscle activation. Furthermore, an increase in intra-abdominal pressure coincides with increased abdominal muscle activation (Cholewicki et al., 1999; Essendrop et al., 2002), which also results in increased spine stiffness (Cholewicki et al., 1999; Essendrop et al., 2002; Hodges et al., 2005).

A limitation of this study that may have additionally confounded the end ROM data is the structure and shape of the passive motion jig itself. Care was taken when securing participants on the lower and upper body cradles to allow freedom of movement through as much of the ROM as possible. However, towards the very end of movement in flexion and lateral bend, participants occasionally became partially obstructed by contact between the two cradles; this was then considered the end point so as not to affect the stiffness estimates. Individuals for whom this was the case all stated that they felt like they were at or very near their true end ROM when the movement ended. A second limitation is that no separation was made between viscous and elastic resistive forces; credit for all resistance to the applied moment was given to the stiffness of the system. Thus, the stiffness curves in the current study represent a simplified effective stiffness of the trunk. Finally, nine healthy males participated in the current study. A larger and more diverse sample population might help to

shed light onto the cause of the relatively unexpected findings regarding the potential degradation of trunk stiffness at the highest activation levels towards the end ROM.

It was thus concluded that the ability of increasing torso, and in particular abdominal, muscle activation to increase trunk stiffness is partially dependent upon trunk posture. In extension, spine stiffness increased with successive increases in muscle activation throughout the ROM. Similarly, in trunk postures most commonly adopted by individuals through daily activities (neutral to approximately 40% of maximum ROM) spine stiffness increased in the flexion and lateral bend directions as muscle activation increased. However, towards the end ROM in both flexion and lateral bend, individuals became less stiff at the maximum abdominal muscle co-activation levels. The source or mechanism of this apparent yielding phenomenon is not yet clear; future work will be directed to uncover the cause.

Chapter 5:

The Intrinsic Stiffness of the in-vivo Human Trunk in Response to Quick Releases: Implications for Reflexive Requirements

Chapter Synopsis

Torso muscles contribute both intrinsic and reflexive stiffness to the spine; recent modeling studies indicate that intrinsic stiffness alone is sometimes insufficient to maintain stability in dynamic situations. The purpose of this study was to experimentally test this idea by limiting muscular reflexive responses to sudden trunk perturbations. Nine healthy males lay on a near-frictionless apparatus and were subjected to quick trunk releases from the neutral position into flexion or right-side lateral bend. Different magnitudes of moment release were accomplished by having participants contract their musculature to create a range of moment levels. EMG was recorded from 12 torso muscles and 3-dimensional lumbar spine rotations were monitored. A second-order linear model of the trunk was employed to estimate trunk stiffness and damping during each quick release. Participants displayed very limited reflex responses to the quick load release paradigm, and consequently underwent substantial trunk displacements (>50% flexion range of motion and >70% lateral bend range of motion in the maximum moment trials). Trunk stiffness increased significantly with significant increases in muscle activation, but was still unable to prevent the largest trunk displacements in the absence of reflexes. Thus, it was concluded that the intrinsic stiffness of the trunk was insufficient to adequately prevent the spine from undergoing potentially harmful rotational displacements. Voluntary muscular responses were more apparent than reflexive responses, but occurred too late and of too low magnitude to sufficiently make up for the absent reflexes.

5.1 Introduction

The study of spine stability has advanced from limitations of static analyses of the instantaneous potential energy state of the muscularly supported vertebral column, to more thoughtful and probing analyses of the continually changing trade-off between loading states and stored energy, or compliancy and stiffness. A stiff system will usually be quite stable, with the trade-off of high joint compressive loads, whereas a compliant system will present an inherently greater opportunity for instability but experience less load. Performing dynamic activities requires consideration of both mobility and stability, and often requires individuals to adopt muscular patterns that may not, in themselves, lend much of a margin of safety in terms of preventing spine buckling type injuries. In these instances, the ability for reflexes to respond appropriately appears essential to adapt to unexpected changes in the environment.

Muscular reflexes are thought to be modulated or gained to pre-existing levels of activation, so as activation increases, the reflexive response increases to maintain a fairly consistent relation (Matthews, 1986). This can be confounded, however, by the current state of the system, presumably to optimally select the strategy to best serve the needs of the system. For example, reflexes can be either inhibited (Gottlieb and Agarwal, 1979; Stein et al., 2007) or facilitated (Nielsen et al., 1994; Akazawa et al., 1983) by the presence of activity in antagonist muscle groups (Gottlieb and Agarwal, 1979; Stein et al., 2007). In addition, reflex contribution to joint stiffness has been documented by different research groups to either increase (Carter et al., 1990; Zhang and Rymer, 1997) or decrease (Toft et al., 1991; Mirbagheri et al., 2000) with increasing moment demands on the system. The contradictory findings of these studies highlight the potential dependence of reflexes on the

ability of the intrinsic stiffness alone to adequately respond to situational perturbations, as well as limiting large reflex gains from preventing oscillations in the system. Further, research has demonstrated situations in which torso muscles, opposing the recovery from a perturbation, actually reflexively increase activation in response to the perturbation (Krajcarski et al., 1999; Gregory et al., in press; Thomas et al., 1998; Stokes et al., 2000), presumably to rapidly increase stiffness of the spine. It has also been recently hypothesized that the motor control system will sometimes reflexively respond to exacerbate a perturbation, providing that it assists an already planned voluntary movement response (Hasan, 2005). All of this research suggests that muscular reflexes play a role in stabilizing and stiffening the spine, but to what extent these are essential, or potentially complimentary, to limiting trunk displacements, and how an inhibition to isolate inherent stiffness can affect system stability, still requires further experimental research.

Properly functioning reflexes play a fundamental role in maintaining the integrity of spinal tissues in a dynamically changing environment. Repeated links have been made to delayed reflexes in numerous muscles in individuals experiencing back pain or disorders (eg. Hodges and Richardson, 1998; Radebold et al., 2000; Reeves et al., 2005; Thomas et al., 2007), or, potentially more importantly, those at an increased risk of developing back injury (Cholewicki et al., 2005). More recently, muscular reflexes were suggested to account for approximately 42 percent of trunk stiffness necessary to stabilize the spine in a dynamically loaded state (Moorhouse and Granata, 2007), and it has been predicted that the spine, even supported by substantial levels of muscular activation and corresponding stiffness, could not adequately stiffen the spine to resist externally applied perturbations in the absence of reflex responses (Franklin and Granata, 2007). Therefore, based on modeling analyses, it appears

that intrinsic trunk stiffness cannot adequately stiffen the spine to prevent substantial trunk displacements in response to dynamic perturbations; however, this needs to be further tested experimentally. Thus, the current study was designed to examine the effect of increasing co-activation of the trunk on its dynamic stiffness response to perturbation, while limiting both reflexive responses of the musculature and the inherent passive stiffness of the spinal joints. This was accomplished by applying trunk perturbations to participants lying both on their backs and right sides; pilot work indicated that participants would be much less likely to reflexively respond to the perturbations in these positions. Further, the removal of the gravity vector acted to minimize the inherent spinal joint compressive stiffness. By generating trunk perturbations similar to those in the previously mentioned studies, with the added effects of inhibiting reflexive responses and innate joint passive stiffness, the role of both intrinsic and reflex muscular stiffness components on overall trunk stiffness was elucidated.

5.2 Methods

5.2.1 Participants

Nine healthy male individuals volunteered from the University population (mean/SD: age 23.9/2.8 years; height 1.81/0.05 m; 79.0/7.1 kg). All signed consent forms approved by the University Office of Research Ethics.

5.2.2 Data Collection

Participants were secured at the hips, knees and ankles on a solid lower body platform. Each participant's upper body was secured to a cradle with a plexi-glass bottom surface, about their upper arms, torso and shoulders. The upper body cradle was free to glide

overtop of a similar plexi-glass surface with precision nylon balls between the two structures. This jig eliminates measurable friction and allows trunk movement about either the flexion-extension or lateral bend axis, depending upon how the participant is secured. Participants lay on their right side for the flexion trials and on their back for the lateral bend trials. Each participant's torso was supported in both positions to ensure that his adopted and maintained spine posture did not deviate throughout the testing.

Participants began each trial in their position of neutral elastic equilibrium (no applied moments acting on them). They were then instructed to generate either a flexor or right-side lateral bend moment to one of three distinct target activation levels as monitored from biofeedback of their right external oblique muscle site. The target levels were set at 5%, 10%, and 15% of maximum isometric activation (termed Light, Moderate, and Heavy, respectively, for the remainder of the paper). The 15% level corresponded to the maximum activation that they were able to achieve during an isometric abdominal brace contraction (producing no external moment) in the test position. Six of the nine participants also performed a fourth target activation of the maximum flexor or lateral bend moment that they could produce in the test position (termed Maximum). The internally generated moments were resisted (so as to keep the participant in their neutral position) by the experimenter via a cable instrumented with a force transducer. The line of pull of the cable was maintained perpendicular to the upper body cradle at all times, necessary to maintain the consistency of the resistive moment that opposed torso motion. Once the target activation was achieved and held steadily for a period ranging between one to three seconds, the cable was rapidly released via a latch mechanism, thus causing a rotational perturbation of the participants'

trunk in either the flexion or right-side lateral bend direction. Participants were instructed to react in a natural manner to the perturbation.

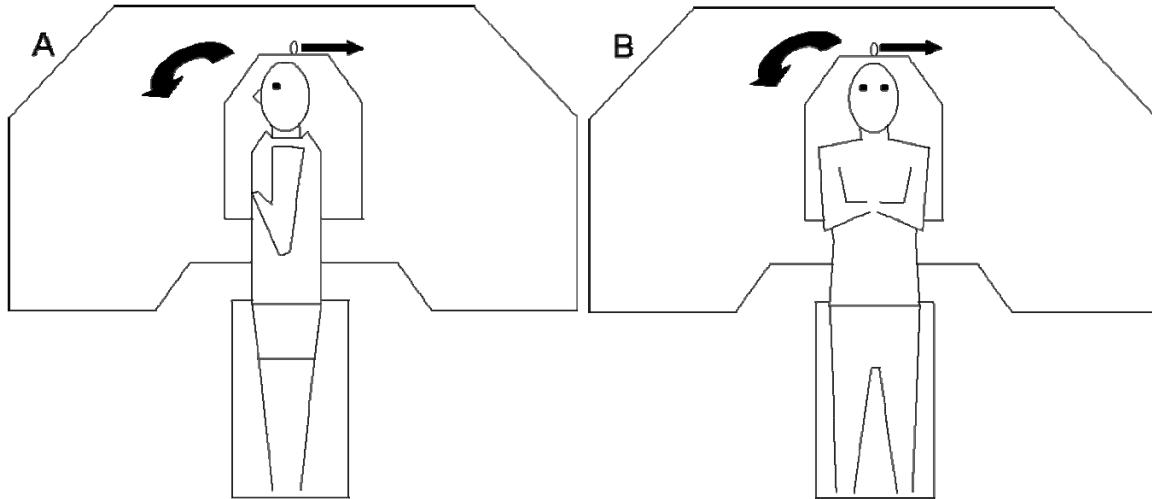


Figure 5.1. Experimental set-up for the quick release in flexion (A) and lateral bend (B). Bold straight arrow indicate the direction of the applied force, bold curved arrows indicated the direction of rotational trunk displacement post-release.

5.2.3 Instrumentation

EMG was recorded and analyzed as reported in Chapter 2, with the exception that the erector spinae at the L5 level were not documented.

An EMG biofeedback device (MyoTrac, Thought Technology Ltd., Montreal, Canada) was placed in line with the right EO electrode site to allow participants to visually monitor muscle activity at this level.

Three-Dimensional trunk motion was recorded using an electromagnetic tracking system (Isotrak, Polhemus, Colchester, VT, USA) with the source secured over the sacrum and the sensor over T12 for the flexion/extension trials, and the source over the lower abdomen at a level slightly below the ASIS and the sensor over the xiphoid process for the

lateral bend trials. The trunk motion data was sampled digitally at 32 Hz and dual-pass filtered (effective 4th order 3 Hz low-pass Butterworth).

The moments applied to the torso were recorded by the product of the force applied perpendicular to the distal end of the upper body cradle and the moment arm from the location of the applied force to the L4/L5 joint. Force was recorded with a force transducer (Transducer Techniques Inc., Temecula, CA, USA) and digitally sampled at 2048 Hz. Force signals were dual-pass filtered (effective 4th order 3 Hz low-pass Butterworth). Both the linear enveloped EMG and force signals were downsampled to 32 Hz to match the trunk motion data.

5.2.4 Second-Order Linear Model of the Trunk

A second-order linear viscoelastic model of the trunk was used to model the rotational motion of the trunk post-perturbation. The form of the model was as follows:

$$I\ddot{\theta} + B\dot{\theta} + K(\theta - \theta_0) = 0 \quad (5.1)$$

where I = moment of inertia of the upper body and cradle (kgm^2)

B = trunk rotational damping (Nm*s/rad)

K = trunk rotational stiffness (Nm/rad)

θ = trunk angle offset (release angle of the trunk in the plane of interest)

θ_0 = trunk rotational displacement

This K is different from that of the previous chapter, as the second-order model employed here allows for the separation of the elastic (stiffness) and viscous (damping) resistive forces, thereby providing an estimate of the true torso stiffness. The length of post-perturbation data analyzed in order to obtain trunk characteristics of K , B , and θ_0 was taken

from the time of quick release to the time of maximum trunk deflection (Cholewicki et al. 2000). In the current study this time averaged 1150 ms.

The upper body moment of inertia was calculated for each participant via anthropometrics (Winter 2004). The moment of inertia of the upper body cradle was calculated via the pendulum method (Dowling et al. 2006). An optimization algorithm was utilized to solve for the three equation unknowns by minimizing the root-mean-square difference between the measured and modeled trunk angular displacements.

5.2.5 EMG Onset and Offset Latencies

Muscle latencies were calculated by rectifying and low-pass filtering (dual-pass effective 4th order 50Hz Butterworth) each individual raw EMG channel (Hodges and Bui 1996; Gregory et al. in press). A muscle was considered to respond with an onset at the time when the signal crossed the threshold of the mean plus three standard deviations of the signal pre-perturbation baseline (calculated over the 50ms prior to the perturbation) and was maintained for at least 20 ms. A muscle offset was determined by analyzing the signal in reverse time order (from time 1second to time zero), and was considered to occur if the signal crossed the threshold of the mean plus three standard deviations of the signal post-perturbation baseline (calculated over the 50ms from 950-1000ms post-perturbation) and maintained for at least 20 ms.

Muscle latencies were analyzed between 20 and 1000ms post-release. If a latency occurred between 20 and 150ms it was considered reflexive in nature (Cholewicki et al. 2005) and between 150 and 1000ms voluntary in nature.

Probability of onset was calculated as the percentage of muscles acting in opposition to the originally generated internal moment that turned on in response to the perturbation; probability of offset was calculated as the percentage of muscles acting to generate the original internal moment that turned off in response to the perturbation. For example, in the flexor moment trials, the six back muscles opposed the generated internal moment and thus would be expected to turn on in response to the trunk flexion displacement while the six abdominal muscles generated the original internal moment and thus would be expected to turn off in response to the perturbation.

5.2.6 Statistical Analysis

Repeated Measures 2-way (movement direction and contraction level) ANOVAs were performed on both the rotational trunk stiffness and damping. Repeated Measures 1-way (contraction level) ANOVAs were performed on the applied moments, as well as the pre-perturbation activation levels and EMG latency probabilities for all muscles in each movement direction. Participants who did not perform the maximum moment contraction trials were not considered for this condition in the statistical analyses; thus, in comparing the maximum contraction condition to each of the other contraction levels, only the six relevant participants were analyzed statistically. Finally, Repeated Measures 1-way (on versus off) ANOVAs were run on the likelihood of muscle onset and offset for time periods of 150ms and 1000ms post-perturbation for each movement direction. Tukey's HSD post-hoc analyses were utilized to test for differences when alpha levels were determined significant ($p < 0.05$).

5.3 Results

5.3.1 Stiffness and Damping

Table 5.1 displays the average and standard deviations of the root-mean-square differences between the model predicted and experimentally determined trunk rotational displacements, calculated as a percentage of the actual experimental displacements. The modeling analysis fit the experimental data quite well, with average model predicted trunk rotational displacements never exceeding an error of 4.2 % of the true experimentally calculated displacements (Table 5.1; Figure 5.2).

Table 5.1. Mean and standard deviation (S.D.) of the percent root-mean-square error between the model predicted and the experimentally calculated trunk rotational displacements for each moment magnitude.

	Flexion				Lateral Bend			
	Light	Moderate	Heavy	Maximum	Light	Moderate	Heavy	Maximum
mean (%)	2.91	2.67	3.08	3.76	3.06	3.49	3.49	4.24
S.D.	1.59	0.95	2.24	1.36	1.40	1.25	1.43	1.31

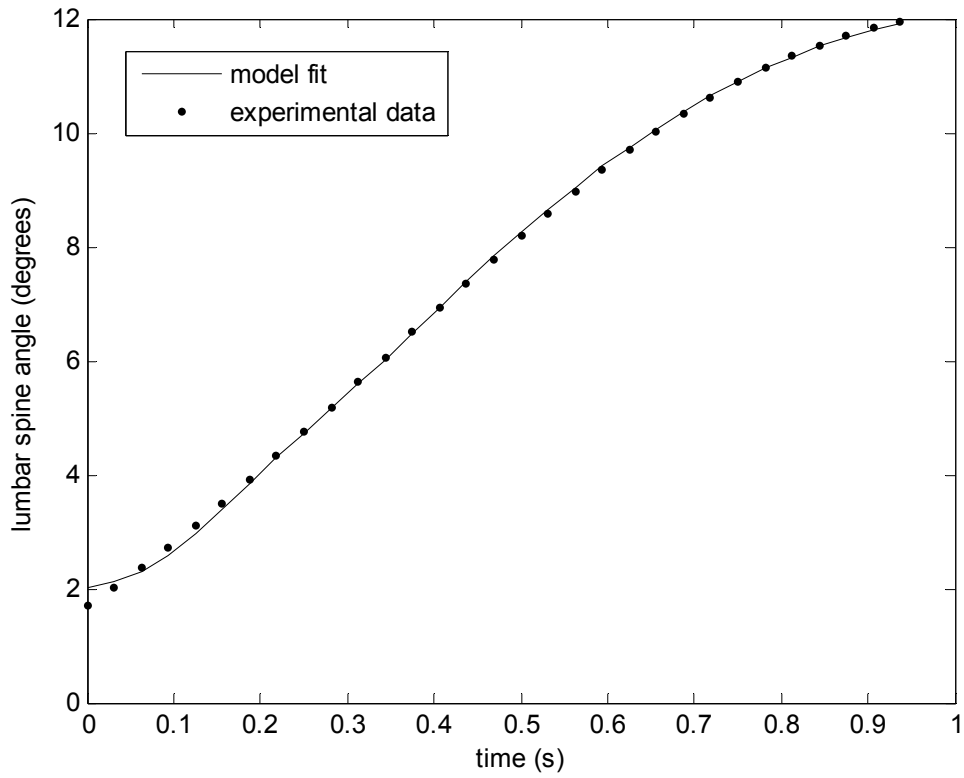


Figure 5.2. Example of the model predicted and experimentally determined lumbar spine rotational displacement for a heavy flexor moment contraction trial. Model parameters for this trial: stiffness = 141 Nm/rad; damping = 11 Nm*s/rad; percent RMS error = 0.78 %.

There was a significant effect of movement direction on rotational trunk stiffness ($p < 0.0001$; LB > Flex) (Figure 5.3). Also, collapsed across flexion and lateral bend trials, stiffness was higher in the maximum contraction condition as compared to each of the light, moderate and heavy contraction conditions ($p < 0.0001$).

There was also a significant effect of movement direction on rotational trunk damping ($p < 0.0019$; Flex > LB) (Figure 5.4).

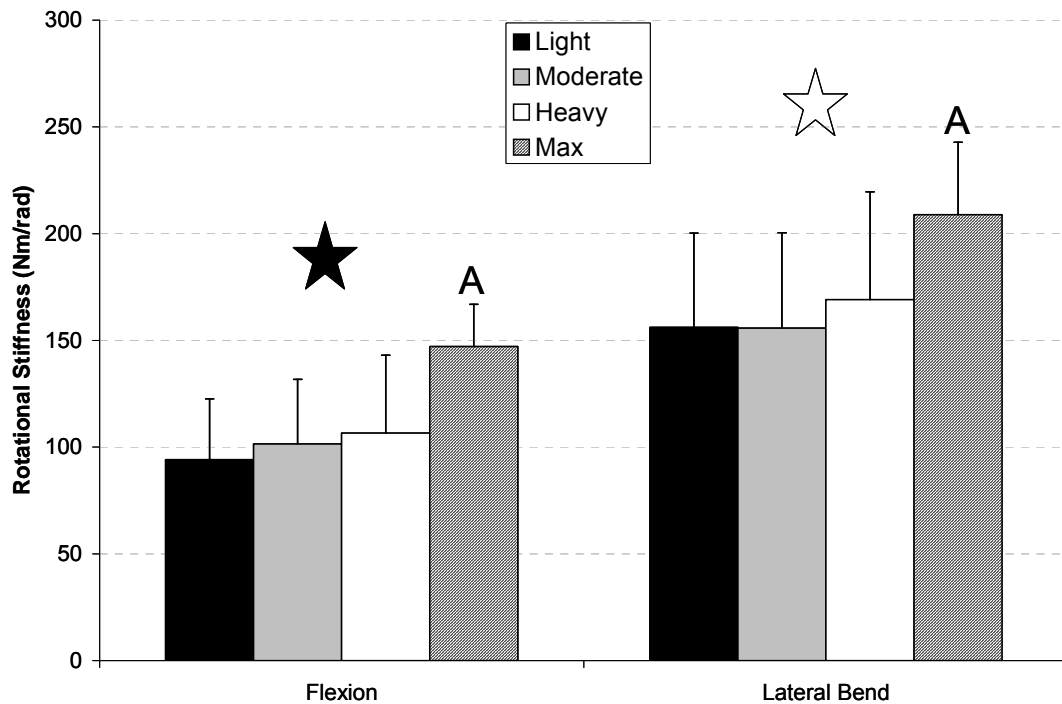


Figure 5.3. Average rotational stiffness values calculated for each of the four muscle activation levels in the flexion and lateral bend directions. Directions highlighted by stars of different colour indicate significant differences between one another ($p < 0.05$). A = heavy contraction level significantly different from each of relaxed, light and moderate contraction levels ($p < 0.05$). Error bars denote standard deviations.

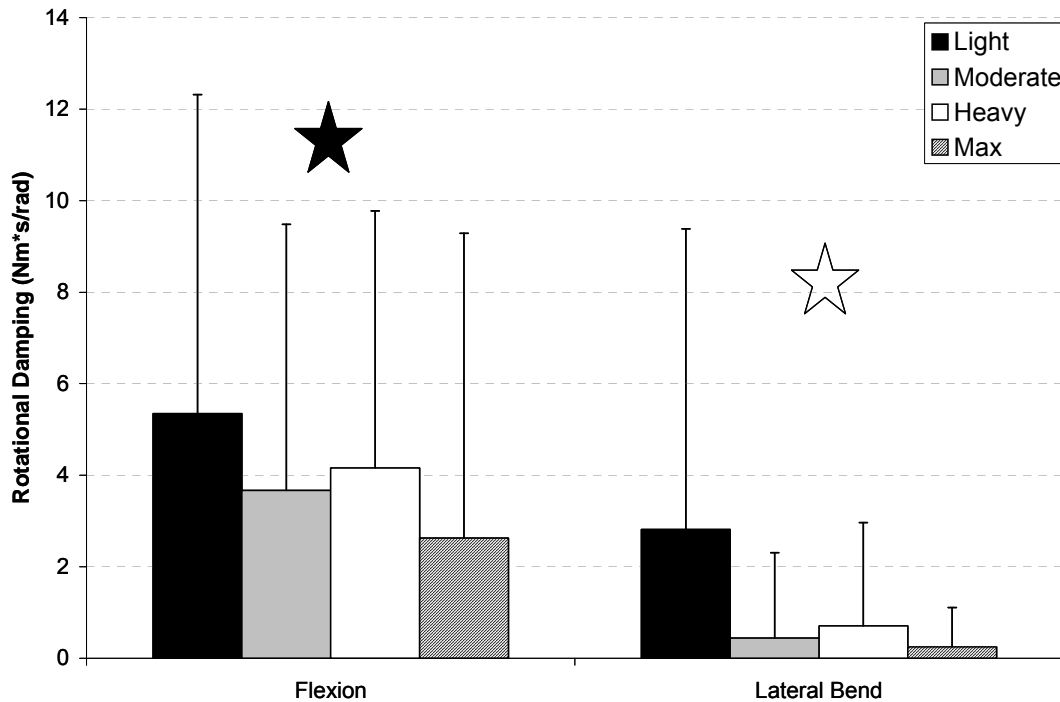


Figure 5.4. Average rotational damping values calculated for each of the four muscle activation levels in the flexion and lateral bend directions. Directions highlighted by stars of different colour indicate significant differences between one another ($p < 0.05$). Error bars denote standard deviations.

5.3.2 Applied Moment and EMG Pre-Perturbation Activation

In flexion, the applied moments were significantly different ($p < 0.0001$) between the maximum (mean/sd = 46.9/21.1 Nm) and each of the light (14.4/11.3 Nm), moderate (19.6/16.1) and heavy (22.5/19.5 Nm) contraction levels. Similarly, the pre-perturbation activation level was significantly different in the maximum as compared to each of the light, moderate, and heavy contractions for all muscles except the L3 erector spinae where the maximum was different from only each of the light and moderate contractions. In addition, the IO was significantly different in the light as compared to the heavy contraction condition (Figure 5.5).

In lateral bend, the applied moments were significantly different ($p < 0.0001$) between the maximum (mean/sd = 53.0/10.7 Nm) and each of the light (19.0/13.6 Nm), moderate (22.2/13.8) and heavy (27.9/18.7 Nm) contraction levels. Again similarly, pre-perturbation activation level was significantly different in the maximum as compared to each of the light, moderate, and heavy contractions for all left side muscles, as well as for the right RA, right EO and right IO muscles (Figure 5.5).

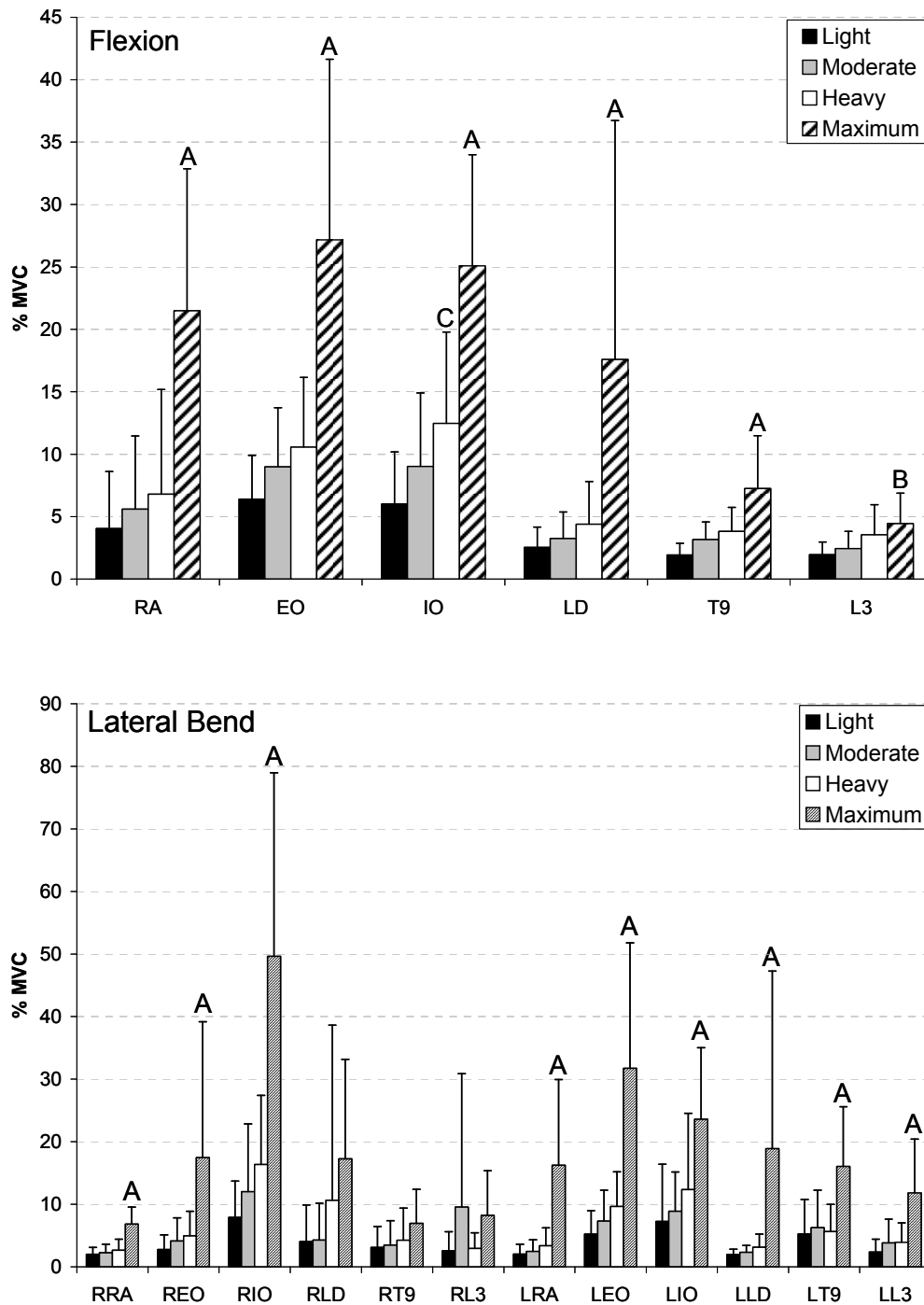


Figure 5.5. EMG averages for the 50ms prior to quick release, across all trials for flexion (averaged bilaterally) and lateral bend (both right and left-side muscles) directions. Significance ($p < 0.05$): A = different from all other levels; B = different from light and moderate levels; C = different from moderate level. Error bars denote standard deviations.

5.3.3 EMG Latency Probabilities

In the flexion trials, the only muscle to display differences in the probability of post-perturbation onset was the right T9 muscle ($p=0.0388$), which displayed an increased likelihood of onset in the light (27.8%) as compared to the heavy (0%) contraction conditions. EMG traces for two muscles (one shutting off and one turning on) in an example flexion trial are shown in Figure 5.6.

Also in the flexion trials, there was a significant difference ($p<0.0001$) in the likelihood of muscle reflex (within 150ms post-perturbation) onset (11.4%) as compared to offset (1.5%). However, when allowing for voluntary reactions within 1-second post-perturbation, the significant difference ($p<0.0001$) became opposite (offset 79.8% as compared to onset 42.4%).

In the lateral bend trials, no differences in muscle contraction level were detected for individual muscle latency probabilities. The same trend existed, however, in the lateral bend as in the flexion trials for the likelihood of muscle reflex ($p=0.0172$; onset 5.6% versus offset 2.3%) and voluntary reaction ($p<0.0001$; offset 70.5% versus onset 35.6%).

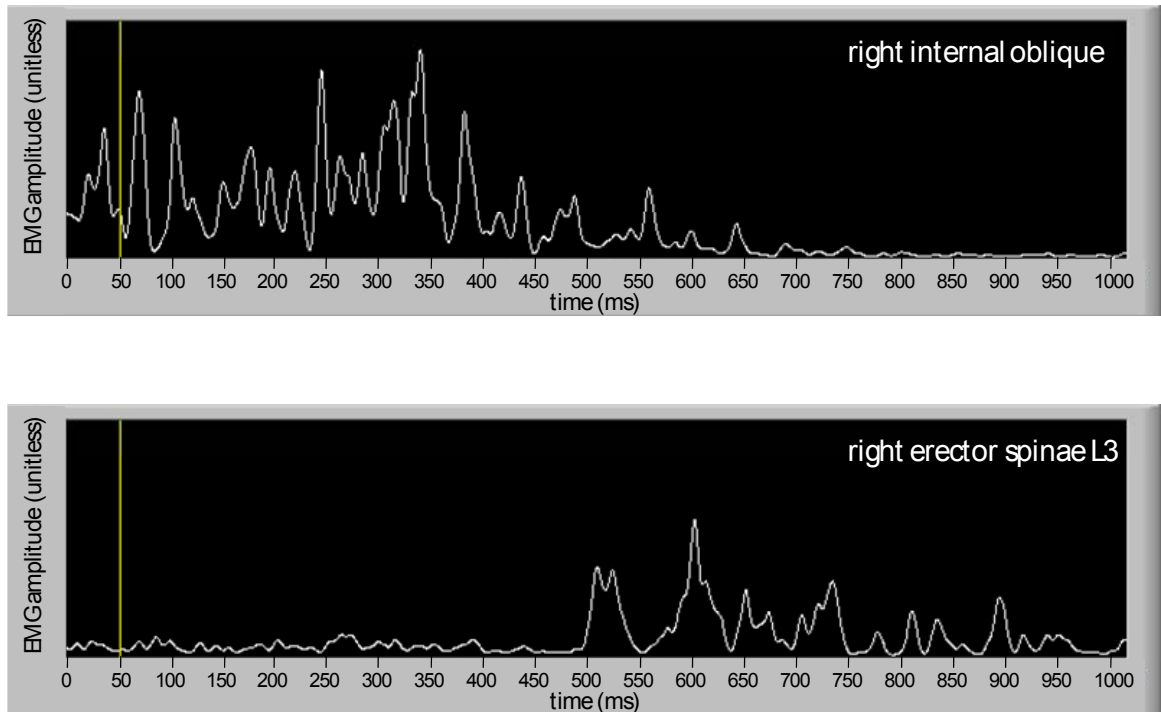


Figure 5.6. EMG traces from an example maximum flexion trial. Top: right internal oblique (RIO); Bottom: right erector spinae at the level of L3 (RES-L3). Vertical line on each plot indicates the time of perturbation. EMG signals have been rectified and dual low-passed filtered at 50Hz (4th order Butterworth). Note that the RIO responded by turning off and the RES-L3 responded by turning on; however, both responses were voluntary in nature, as evidenced by their relatively long latencies.

5.4 Discussion

The primary result of this study is that despite voluntary muscular responses that acted to influence the quantified trunk motion, rotational joint stiffness was much lower than would be expected in the presence of reflexive responses. Average trunk deflections during maximum moment trials exceeded 50% of the trunk's passive limit in flexion and 70% in lateral bend, far greater than what has been shown to occur when reflex responses are fully active (eg. Krajcarski et al. 1999; Cholewicki et al. 2000; Chiang and Potvin 2001; Vera-Garcia et al. 2007). This indicates that reflexes play an essential role in stiffening the trunk

to dynamic perturbations, and that voluntary responses are unable to make up for any neural deficits in reflexive ability within these shortened time periods. In addition, it was found that rotational trunk stiffness increased significantly in conjunction with significant increases in trunk activation that were generated to produce external trunk moments. Smaller, non-significant increases in trunk muscle activation did not result in significant increases in trunk stiffness in these trials.

It has previously been estimated that reflexes can account for levels approaching 50% of the rotational stiffness about a joint during dynamic motions (Sinkjaer et al. 1988; Bennett et al. 1994; Kearney and Stein 1997; Moorhouse and Granata 2007; Mirbagheri et al. 2000). The total rotational stiffness is a combination of intrinsic passive tissue, intrinsic muscle, and reflexive muscle contributions. The current study confirms that, of the total muscular contribution to spine rotational joint stiffness, reflexive components contribute a major portion of the stiffness. In the current protocol, the effects of intrinsic stiffness due to passive joint structures were somewhat minimized, in particular in the conditions with relaxed musculature, due to the removal of the gravity vector acting to compress the spinal joints. A great deal of stiffening of the intervertebral joints occurs as a result of compressive loading (eg. Edwards et al. 1987; Janevic et al. 1991; Gardner-Morse and Stokes 2003). The average rotational joint stiffness values calculated here were 109 Nm/rad for the flexion perturbations, which corresponds to approximately 9-11% of the average values calculated by Cholewicki et al. (2000) in the presence of full reflexes using similar modeling approaches. Assuming, based on documented research, that approximately 40% of trunk stiffness in the Cholewicki et al. study resulted from reflex responses, yields reflexive stiffness values nearly four to five times greater than our intrinsic muscle stiffness values.

This is slightly higher than Hoffer and Andreassen (1981) who showed a nearly 3-fold increase in the stiffness of cat muscle when allowing for reflexes at moderate force levels; the higher stiffness theoretically created by the reflexes in Cholewicki et al. (2000) is most likely due to the additional intrinsic compressive effects of muscular responses on the human trunk.

As participants increased moment levels through the flexor contraction of their abdominal muscles, the only significant differences in EMG level occurred in the maximum as compared to each of the light, moderate and heavy contractions. Fittingly, rotational joint stiffness was significantly higher in the maximum as compared each of the other conditions, but not between any of the other conditions. Despite the increase in EMG activity and stiffness, the likelihood or latency of reflexes did not change, thereby indicating that stiffness was due primarily to changes in the intrinsic stiffness of the muscle. Previous work has shown that reflexes are gained to match background muscle activation levels (Neilson and McCaughey 1981; Matthews 1986; Slot and Sinkjaer 1994), at least from low to mid-range activation levels; however, the current work has detailed a situation whereby reflexes were inhibited by the experimental protocol, thereby nullifying this normal gain adjustment.

A number of factors potentially contributed to the lack of reflexive responses during the perturbation trials in the current study. First, the mechanical set-up of the experimental protocol acted to remove the force of gravity that would serve to carry the trunk away from its position post-release were an upright posture initially adopted. Participants lay either on their right-side or back on a near-frictionless apparatus, and were perturbed only by their own internal moment generation. Thus, the peak rotational trunk velocities in response to the perturbations were relatively low (avg/sd 26.3/16.7 deg/s), thus resulting in longer times to

maximum trunk deflection than in previous studies (1150/200 ms, as compared to 250/112 ms in Cholewicki et al. 2000). Furthermore, maximum trunk deflections were likely not limited by muscle responses, as in the maximum moment generation trials, maximum deflections approached the trunk's elastic limit (54.3/13.3 % or 29.0/7.8 degrees of flexion; 74.0/14.0% or 24.7/6.8 degrees lateral bend). These rotational displacements are far greater than those documented previously in our laboratory for quick releases from upright positions (average 4.9 degrees; Brown et al. 2006 unpublished portion of study) despite similar ranges of EMG activity. Further, the large displacements combined with the relatively slow velocities may not be conducive to eliciting muscle spindle responses (Hunt and Ottoson 1976; Houk et al. 1981; Proske et al. 2000). Finally, in the lying down position, the threat to trunk stability was most likely perceived by the participants as relatively low, which may have influenced the reflexive responses. It has previously been shown that reflex magnitudes are reduced when threat is minimized in postural control and gait (Cordo and Nasher 1982; Rietdyk and Patla 1998), and also when muscles no longer act in their normal postural sense (Marsden et al. 1981; van der Fits et al. 1998), indicating that reflexes likely have a cortical pre-setting of gain and therefore may be context dependent (Matthews 1991).

In conclusion, it has been demonstrated that intrinsic muscle stiffness does not provide adequate stiffening of the spinal joints to prevent excessive rotations upon rapid perturbation. Torso muscle activation levels were similar in the current report as in previous quick release studies, yet spine displacements, and thus the potential for injury, were far greater in the current work, thereby highlighting the lack of adequate stiffening present due to intrinsic muscle properties. This experimental finding substantiates previous model based predictions (Moorhouse and Granata 2007; Franklin and Granata 2007) that intrinsic stiffness

alone is inadequate to stabilize the human spine. It is clear that reflexive pathways serve to provide a bulk of the muscular contribution to torso stiffness, and thus continues to shed light on mechanisms necessary for the optimal maintenance of spine control and stability during dynamic activities.

Chapter 6:

An Ultrasound Investigation into the Morphology of the Human Abdominal Wall Uncovers Complex Deformation Patterns During Contraction

Chapter Synopsis

The abdominal wall components, specifically muscle and connective tissue, must meet and accommodate a wide range of force demands used for torso movement, spine stabilization, and respiration. The composite laminate nature of the abdominal wall is quite unique in its structure within the human body, and may lend itself to facilitating the required tissue responses. Despite the great deal of attention paid to the importance of the control of abdominal muscles in the maintenance of back health, little consideration has been given to the actual mechanical workings of these muscles. The purpose of this study was to examine the deformations of the abdominal wall, with a special focus on both the internal oblique aponeurosis and the tendinous intersections of the rectus abdominis, using ultrasound imaging, during relatively simple contractions of the abdominal musculature. The main finding of this study was that the connective tissues of the abdominal wall do not behave in any simple manner in response to the forces generated within and acting upon the wall during contraction. Deformations occurred in nearly 50 percent of contractions that would be characterized by a negative Poisson's ratio. Further, the laterally generated forces of the oblique and transverse muscles transfer a great deal of force across the rectus abdominis muscle and sheath, leading to a lateral movement of the rectus muscle during abdominal contraction. It would appear that the mechanisms regulating these deformations, including the unique, angle-plied nature of the abdominal muscles and their investing connective tissues may enable simultaneous expansions in multiple planes to accommodate the competing forces acting in these planes.

6.0 Introduction

Very little research has been dedicated to the examination of the morphology of the abdominal muscles and connective tissues during contraction, and even less on the means of force sharing among these components. The muscles within the abdominal wall, the internal oblique (IO), external oblique (EO), and transverse abdominis (TrA), along with the rectus abdominis (RA) are responsible for producing movements of the torso (McGill, 1991), ensuring a stable spinal column (Granata & Marras, 2000), regulating intra-abdominal pressure (Cholewicki et al., 2002), and assisting with respiration (Campbell & Green, 1953). Many of these abdominal demands occur simultaneously, thus producing an array of forces acting within and upon the abdominal wall. A lack of knowledge concerning the mechanisms integrating the muscles with the various tissues encompassing and investing the abdominal wall motivated this investigation.

A limited number of biomechanical studies have been conducted on the abdominal wall. Nilsson (1982 a & b), Rath et al. (1997), Junge et al., (2001), and Hwang et al., (2005a) all performed fine investigations into the mechanical properties of abdominal wall structures, but all did so with harvested dead tissues, which limits the applicability of the results to live contracting muscle.

Ultrasound imaging enables views of contracting muscle and connective tissues, and has recently begun to be utilized to study the mechanical properties of tendon (eg. Maganaris & Paul, 2002; Bojsen-Moller et al., 2005; Ishikawa et al., 2005), as well as the contraction of the abdominal muscles (eg. Misuri et al., 1997; Hodges et al., 2003). The majority of work on the abdominal muscles using ultrasound imaging has focused on thickness changes during

contraction, but has not examined the complex deformation interactions of the connective tissues investing the musculature.

Connective tissues serve a complex and demanding role within the abdominal wall. Unlike the majority of muscles found in the human body, the abdominal wall muscles do not necessarily transmit force through tendinous attachments directly to bone. Many of the fibres of the EO, IO and TrA terminate into anterior aponeuroses that attach into and make up the sheath surrounding the RA, continuing to the midline region of the linea alba and even crossing over the midline to fuse into the contra-lateral rectus sheath (Rizk, 1980).

Connective tissues in the human body are arranged in a variety of manners and compositions, necessary to meet the demands placed upon the tissue. In general, these tissues can be thought as a matrix of protein fibres, primarily collagen, at varying degrees of parallel or random arrangement, encompassed within a gel-like ground substance. The assortment of compositions of these structures in different connective tissues allows for many unique properties that have been recorded in tissues such as skin (Lees et al., 1991), artery (L'Italien et al., 1994) and diaphragm central tendon (Hwang et al., 2005b), suitable to the demands placed on these tissues. With the range of demands placed on the abdominal wall muscles and tissues, it is reasonable to expect quite distinctive deformations during contraction.

The purpose of this exploratory study was to document the deformations of the abdominal wall muscles and connective tissues, with a specific focus on the aponeurosis of the internal oblique muscle and the tendinous intersections (referred to from now on as tendon) of the rectus abdominis muscle during relatively simple abdominal contractions. Ultrasound imaging was utilized to record and view the contractions, and electromyography

(EMG) based modeling was employed to estimate the forces exerted by the muscles during contraction.

2.0 Methods

2.1 Participants

Eight healthy males (average/standard deviation: age = 25.1/3.2 years; height = 1.78/0.06 m; mass = 75.5/4.6 kg) volunteered from the University population. None had a history of any chronic or acute episodes of back pain or abdominal pathology/injury. Informed consent, approved by the University Office of Research Ethics was obtained from each participant.

2.2 Data Collection

EMG was recorded and analyzed as reported in Chapter 2, with the exception that only right-side muscles were examined.

An EMG biofeedback (MyoTrac, Thought Technology Ltd., Montreal, Canada) electrode was also secured over the right EO muscle, to allow participants to visually monitor the activation level of this muscle during contraction.

Three-dimensional lumbar spine angles, using an electromagnetic tracking system (Isotrak, Polhemus, Colchester, VT, USA) with the source secured over the sacrum and the sensor over T12, were recorded (32 Hz) to ensure minimal movement during contractions.

Ultrasound images were obtained in B-Mode (MicroMaxx, Sonosite Inc., Bothell, WA) with a 38-mm linear transducer (6-13 MHz).

2.3 Procedures

Participants performed a series of static abdominal brace contractions in a modified sit-kneel position, designed to keep the spine in a neutral posture (Figure 6.1).

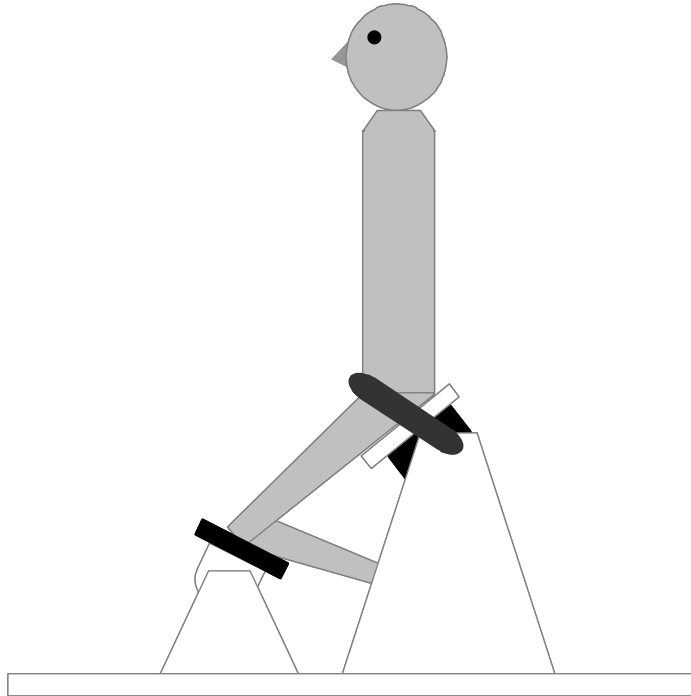


Figure 6.1. Participant posture in which ultrasound images were obtained.

Target contraction levels were set to 25%, 50% and 100% of the maximum activation capability of the right EO in the testing position. Two trials of each activation level were performed in randomly assigned order. To view the aponeurosis of the IO muscle, ultrasound images were taken with the probe at the level of the umbilicus on the left side of the body, with the lateral position adjusted to ensure a view of the IO aponeurosis between the medial edge of the IO muscle and the lateral edge of the RA muscle (Figure 6.2a). The standard orientation of the probe was horizontal along the transverse plane of the torso. For a sub-set of four participants another series of the identical contractions were performed with

the probe at two additional orientations: 1) angled 35 degrees inferior-laterally (along the approximate line of the IO fibres, Urquhart et al., 2005); 2) angled 60 degrees superior-laterally (along the approximate line of the EO fibres, Urquhart et al., 2005) (Figure 6.2b&c). The mid point of the probe was positioned in the same location for each of the three orientations. For the RA tendon, the ultrasound probe was positioned over the intersection lying most closely superior to the umbilicus, oriented in the inferior-superior direction along the anterior of the RA muscle, and positioned approximately mid-way between the linea alba and linea semilunaris (Figure 6.2d). For every ultrasound image, care was taken to secure the probe perpendicularly to the body at all times and to maintain the same position of the probe throughout and between each contraction. Two still ultrasound images were captured on a video cassette for each trial, the first when the muscles were relaxed and the second when the target activation level had been reached at a steady state.

Each participant also performed two ramped torso contractions producing a net flexor muscle moment (as per Chapter 3). Participants were seated, and secured around the hips. A trunk harness was fit snugly over the shoulders and attached through a cable in-series with a force transducer to a weight stack loaded so as to prevent any torso movement. Participants used their torso to slowly pull against the weight stack, ramping the moment from zero up to maximum and back down to zero.

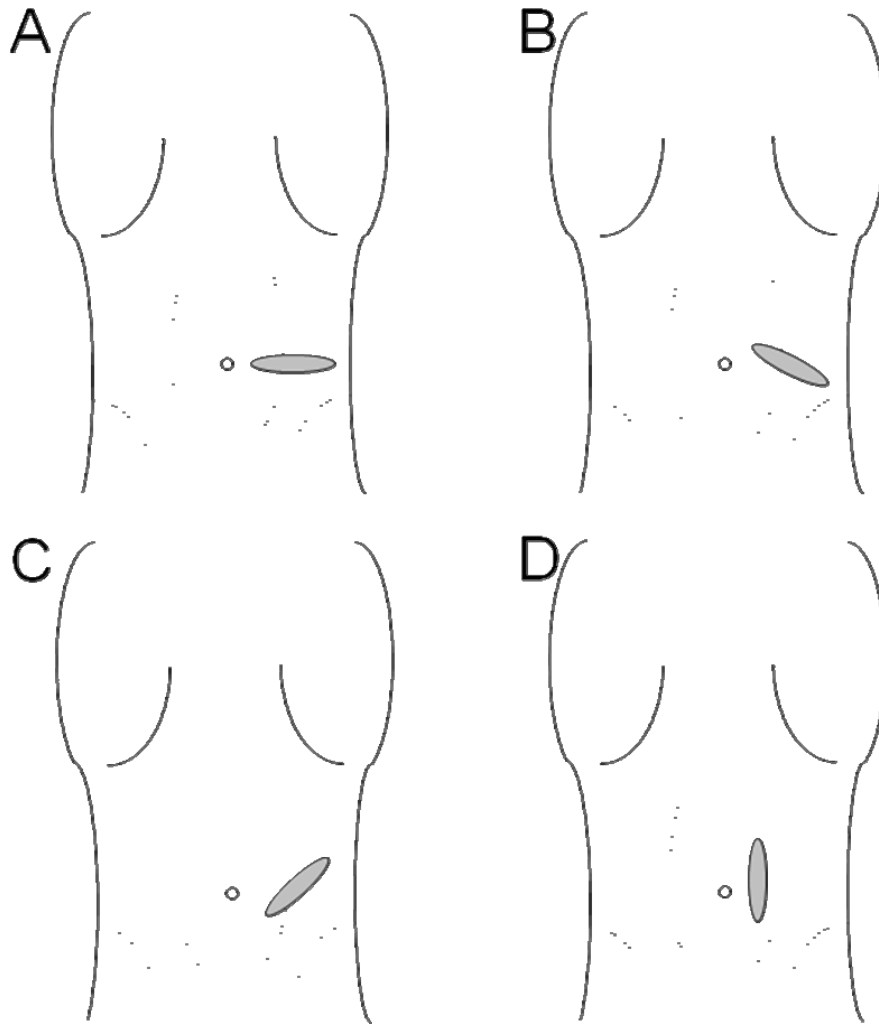


Figure 6.2. Locations of the three probe orientations to view the IO aponeurosis: A) horizontal along the transverse plane; B) oriented 35 degrees inferior-laterally (along the approximate line of the IO fibres); C) oriented 60 degrees superior-laterally (along the approximate line of the EO fibres). D) Location of the probe to view the RA tendinous intersection.

6.2.4 Ultrasound Image Analysis

For the IO aponeurosis images, the length and thickness of the aponeurosis were measured in both the relaxed and contracted image (Figure 6.3). The same measures were taken for the RA tendon (Figure 6.4). All measures were performed visually. Specifically, the IO aponeurosis was digitized at the inner edge of both its deep and superficial fascial borders, mid-way between its medial and lateral edges; a straight line was drawn between the two points as a measure of the aponeurosis thickness. The length of the aponeurosis was measured by digitizing a point on both its medial and lateral borders, mid-way between its superficial and deep edges; a straight line was drawn between the two points as a measure of the aponeurosis length. For the RA tendinous intersection, a point was digitized on inner edge of both the superficial and deep fascial borders, mid-way between its superior and inferior edges; a straight line was drawn between the two points as a measure of the tendon thickness. Tendon length was measured by drawing a straight line connecting a digitized point on each of the superior and inferior borders, mid-way between its superficial and deep edges. The changes in length and thickness were recorded as both an absolute magnitude (in mm), as well as a percent change from the resting measure. The lateral most position of the RA muscle was also measured from the IO aponeurosis trials, to assess any lateral movement of this muscle during contraction.

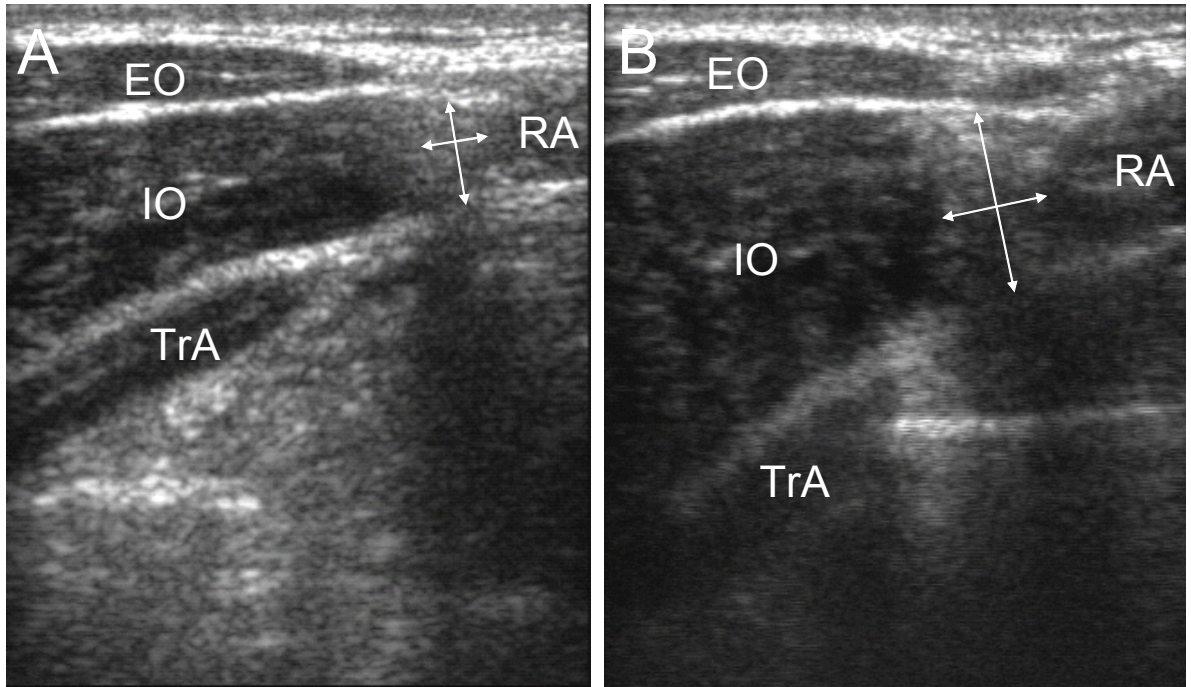


Figure 6.3. Example of an ultrasound image, taken transverse through the abdomen, of the IO aponeurosis captured at relaxation (A) and 100% of maximum contraction (B). The more vertically oriented arrows indicate the measure of aponeurosis thickness; the more horizontally oriented arrows indicate the measure of aponeurosis length.

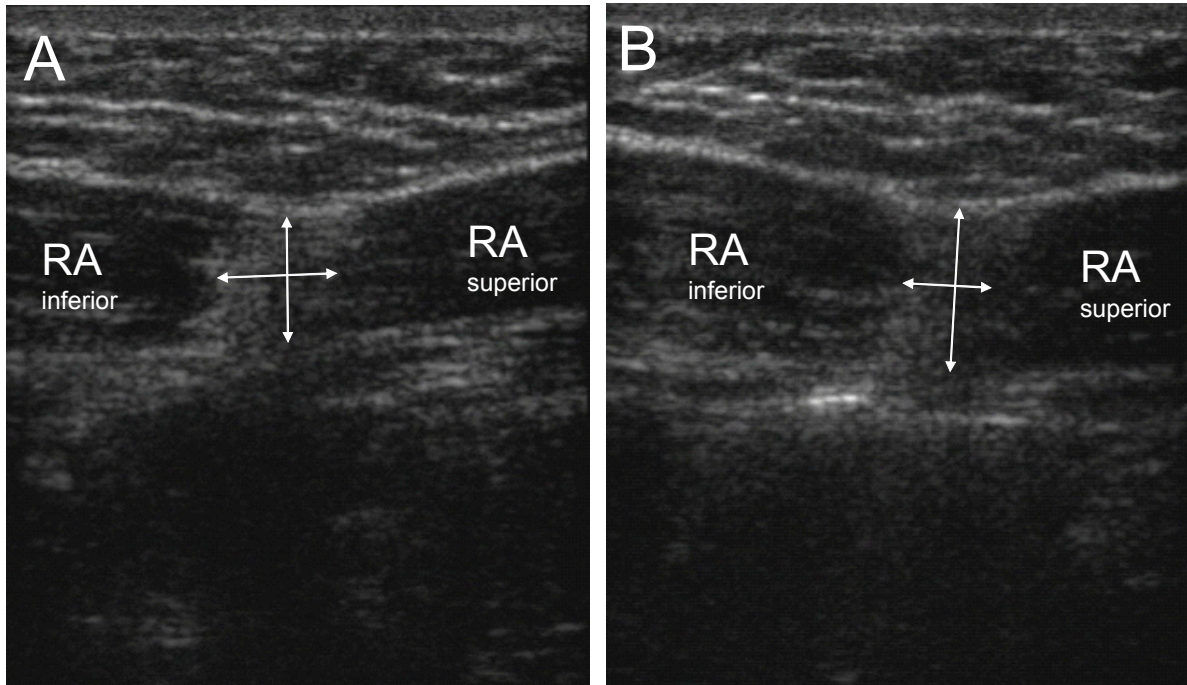


Figure 6.4. Example of an ultrasound image, taken sagittally through the abdomen, of the RA tendinous intersection captured at relaxation (A) and 50% of maximum contraction (B). The portion of the image above the RA is subcutaneous tissue and skin, while below the RA is visceral content. The more vertically oriented arrows indicate the measure of tendon thickness; the more horizontally oriented arrows indicate the measure of tendon length.

6.2.5 Reliability

To assess the intra-rater reliability in determining the change in aponeurosis/tendon length and thickness from rest to contraction, visual measures of the images were repeated (on a day separated by one week), by the same experimenter, on thirty randomly chosen trials. Each of a Pearson correlation and a paired t-test were computed to test the relationship and mean difference, respectively, between the days.

6.2.6 Muscle Force Estimates

The forces produced by the RA, EO, IO, and TrA muscles were estimated using the following equation:

$$F_m = NEMG_m * PCSA_m * \sigma_m * l_m * G \quad (6.1)$$

where F_m = force in muscle m (N)

$NEMG_m$ = normalized EMG signal for muscle m (% MVC)

$PCSA_m$ = physiological cross-sectional area of muscle m (cm²)

σ_m = maximum stress generated by the muscle m (set at 35 N/cm²)

l_m = length coefficient of the muscle m (unitless)

G = participant specific gain factor (unitless)

The participant specific gain factor was determined from the ramped force contraction trials. In these trials the combined moment generated by the abdominal muscles was estimated and compared to the estimated net resistive moment (measured externally as the sum of the moment produced by the upper body weight and the moment measured as the product of the force in the force transducer and the moment arm to the L4/L5 joint, and combined with the moment produced by the trunk extensor muscles). A gain factor was obtained as the value that produced the least-squares best fit between the abdominal muscle and resistive moments.

The increase in force generated by each of the muscles, with respect to the relaxed state, was recorded for each ultrasound trial.

Activation recorded by the IO electrode site was used to estimate the force produced by the TrA muscle. McGill et al., (1996) demonstrated a moderately good relationship

between the activations of these two muscles, such that this produced an estimate at the force produced by the TrA.

6.2.7 Statistical Analysis

Two-way Repeated Measures ANOVAs were utilized to assess the effect of contraction level and probe orientation on the absolute and relative length and thickness changes of the IO aponeurosis. One-way Repeated Measures ANOVAs were performed to assess the effect of contraction level on the absolute and relative length and thickness change of the RA tendon, the lateral movement of the RA muscle, and the estimated force produced by each of the RA, EO, IO and TrA muscles.

A Tukey HSD test was performed to examine post-hoc differences where appropriate. The alpha level was set at 0.05 for all analyses.

6.3 Results

All eight participants followed the classical basic anatomical form of the abdominal wall (Monkhouse & Khalique, 1986); external oblique aponeurosis anterior to rectus, internal oblique aponeurosis splitting anterior and posterior to rectus, and transverse abdominis posterior to rectus.

6.3.1 Muscle Force Production

There was a significant effect of the level of abdominal contraction on the estimated muscle force produced by each of the abdominal muscle groups ($p < 0.0001$ for RA, EO, IO, TrA) (Figure 6.5). Specifically, each of the EO, IO and TrA increased their force output for

each successive increase in contraction level; for the RA the force output for the 25 and 50% contraction levels were not significantly different from each other, but were from the 100% contraction level.

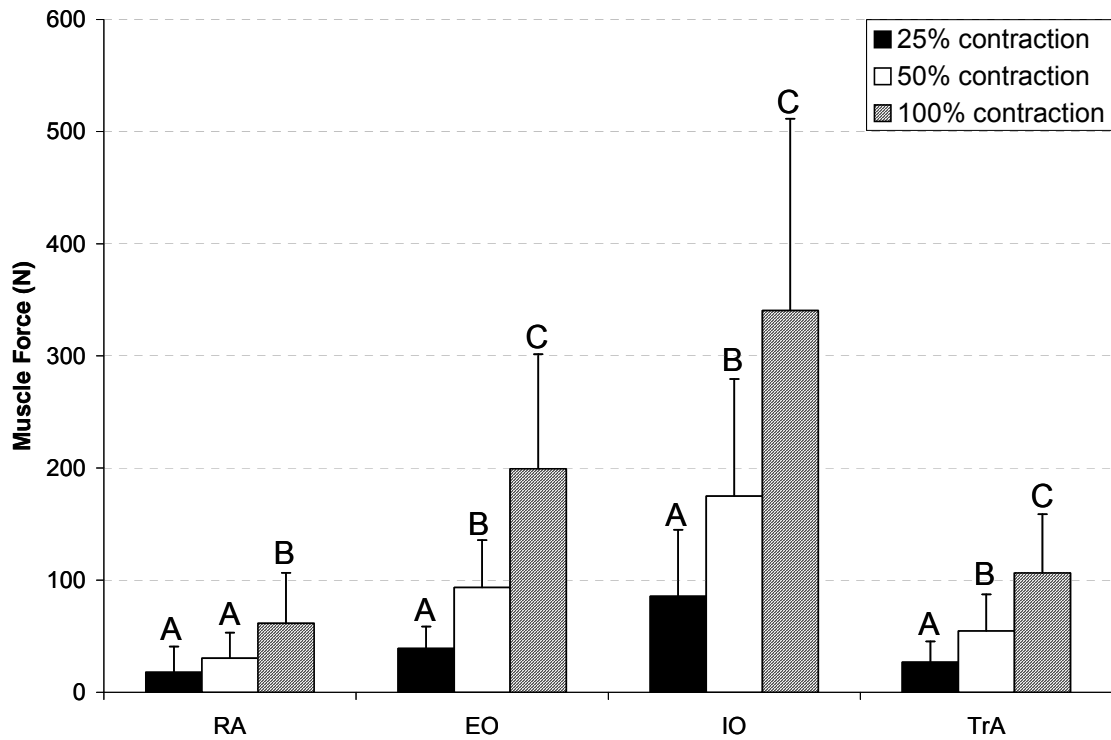


Figure 6.5. Averages and standard deviations, taken across all trials and participants, of the estimated increase in force, with respect to the relaxed state, generated by each of the RA, EO, IO and TrA muscles during abdominal contractions. Different letters indicate contraction levels which are significantly different from one another within a given muscle.

6.3.2 Reliability of Ultrasound Image Digitization

A high correlation ($r = 0.89$) was found between the measures made on the two separate days, while the paired t-test showed no significant difference ($p = 0.609$) between days.

6.3.3 *Rectus Abdominis Tendon and Muscle*

During contraction the RA transverse tendon lengthened (along the fibre direction of the RA) in 26 of the 48 trials examined. The level of abdominal brace did not affect the absolute or relative magnitude of RA tendon length change ($p = 0.1395$ absolute; $p = 0.2768$ relative), and no apparent trends existed. The tendon appeared to thicken (depth-wise) in 47 of 48 trials. This again was not statistically affected by the level of abdominal brace ($p = 0.3678$ absolute; $p = 0.2967$ relative) although there was a trend of increasing thickness change with brace level (1.5 mm or 18.3% increase at 25% contraction; 1.6 mm or 19.6% increase at 50% contraction; 1.9 mm or 23.9% increase at 100% contraction). The one trial in which the tendon thinned it also lengthened. Therefore, in 25 of the 48 trials, the RA tendon lengthened and thickened simultaneously.

Across all probe orientations, the lateral border of the RA muscle was pulled more laterally upon contraction in 64 of 94 trials (68%). This was not affected by contraction level ($p=0.6519$) but was by the orientation of the ultrasound probe ($p=0.0496$), with the horizontal orientation displaying a greater movement as compared to each of the 35 and 60 degree orientations. The ratio of summed oblique muscle (EO, IO, TrA) force to RA muscle force was used to assess a relationship with the lateral displacement of the RA muscle, with an exponential R-squared fit of 0.54 (Figure 6.6). This indicates that the lateral forces produced by the oblique and transverse muscles dominate over the longitudinal force of the RA muscle, causing the RA to be pulled laterally.

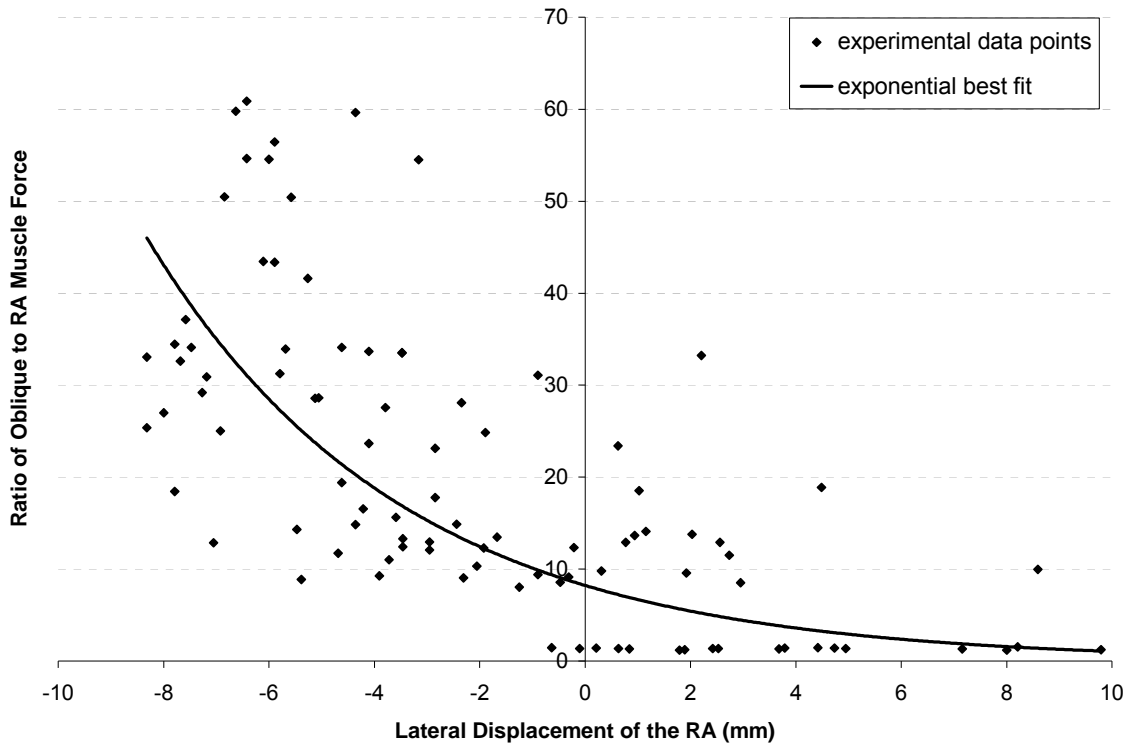


Figure 6.6. Relationship between the ratio of summed oblique (IO, EO, TrA) muscle force to RA muscle force and the lateral displacement (mm) of the RA muscle. Each data point represents an individual trial (all trials and participants are shown). A negative displacement indicates lateral movement of the RA. The exponential best fit produced an $R^2 = 0.54$.

6.3.4 Oblique Aponeurosis

The aponeurosis of the IO lengthened (in the medio-lateral direction) upon contraction in 77 of the 94 trials examined. The level of abdominal contraction did not significantly affect the magnitude of length change of the IO aponeurosis ($p = 0.3645$ absolute; $p = 0.1620$ relative). Probe orientation did have an effect on the absolute magnitude of length change ($p=0.0428$) with the 35 and 60 degrees views being significantly different from each other (mean/S.D. 35 degree 0.9/1.6 mm; horizontal 1.6/1.7 mm; 60 degree 3.2/5.5 mm). When normalizing to rest length, probe orientation was no longer significant ($p = 0.0792$) but showed the same trend as the absolute measure.

The IO aponeurosis became thicker depth-wise in 51 of the 94 trials examined. In this case neither the level of abdominal contraction ($p = 0.9213$ absolute; $p = 0.9539$ relative) nor probe orientation ($p = 0.1750$ absolute; $p = 0.9646$ relative) significantly affected the magnitude of thickness change. In 38 of the 94 trials the IO aponeurosis appeared to lengthen and become thicker. In 5 of the 94 trials the IO aponeurosis appeared to shorten and become thinner. Comparing probe orientations for the sub-set of four participants shows potential differences in the number of trials in which the aponeurosis simultaneously lengthened and thickened or shortened and thinned (10 of 24 trials horizontal orientation (8 lengthened and thickened; 2 shortened and thinned); 5 of 24 35 degree orientation (4 lengthened and thickened; 1 shortened and thinned); 10 of 24 60 degree orientation (8 lengthened and thickened; 2 shortened and thinned)).

6.4 Discussion

This study was designed as exploratory in nature in order to provide insight into the interactions between muscle and connective tissue in the abdominal wall during relatively simple contractions. The neural control of the abdominal muscles has garnered a great deal of attention and claims have been made as to the importance of these muscles in the stabilizing of the spine, yet little attention has been paid to the actual mechanical workings of these muscles. The primary finding of this study is that the connective tissues supporting the various attachments to the muscles of the anterior abdominal wall take on a composite arrangement that allow them to deform in complex manners to conform to the different forces acting throughout the system. Further, the laterally produced forces of the oblique and transverse muscles appear to dominate the longitudinally produced force of the RA muscle,

such that the connective tissues intervening these muscles (specifically the transverse RA tendons and linea alba) must function to accommodate such force distribution.

The major complexity uncovered in the current investigation was that in approximately half of the recorded abdominal contractions, each of the tendinous intersection of the RA and the IO aponeurosis deformed in a manner that takes on the appearance of a negative Poisson's ratio. The sagittal view of the RA tendon showed it simultaneously lengthening longitudinally and thickening depth-wise in approximately 52% of the trials. Likewise, the transverse view of the IO aponeurosis displayed it simultaneously either lengthening and thickening or shortening and thinning in approximately 46% of trials. Two general explanations can be posed for this phenomenon. The first is simply a function of the methodology. The ultrasound image is a two-dimensional representation of a three-dimensional structure. Therefore it is possible that out of plane deformation was occurring that negates the apparent volume expansion of the tissue. An attempt was made to account for this possibility by imaging the IO aponeurosis at three different orientations, two of which were nearly orthogonal to each other (35 degrees superior-medial and 60 degrees infero-medial). The apparent negative Poisson's ratio was documented at all three views within a given participant, albeit in fewer instances when the probe was oriented along the direction of the IO fibres. Further, for this possibility to hold true, the RA tendon would have to shorten along its approximate medio-lateral direction, which seems unlikely considering the large forces exerted laterally upon it by the oblique musculature. Thus, the finding most likely cannot be completely explained by this methodological limitation.

A second explanation relates to the composite laminate nature of the abdominal wall. Composite laminate structures can display negative Poisson's ratios (Tsai & Hahn, 1980), the

more anisotropic the plies, the more readily (Yeh et al., 1999) negative Poisson's ratios are observed. The abdominal wall is composed of three sheet-like muscles and their corresponding aponeuroses overlying each other, each with what has been anecdotally described as loose connective tissue intervening (Bendavid & Howarth, 2000). Also, other authors have noted that each aponeurosis is made up of two layers (Rizk, 1980; Askar, 1977); the IO in particular separates into an anterior and posterior portion to encompass the rectus sheath. Further, Axer et al. (2001a) described an intermingling of oblique fibres throughout neighboring layers of the aponeuroses and hypothesized that the mesh-work nature of the collagen fibres of the rectus sheath and linea alba allow for unique deformations, or adaptability, to the different demands of the tissue. The abdominal wall produces and resists forces in a number of competing directions; stress along the direction of the fibres in each of the angle-ply muscle layers; the hydrostatic force created within the abdomen and acting outwardly on the wall of the musculature, the force of which is related to the level of muscular contraction. Also, stress is exerted along the plane of thickening at the muscle-aponeurosis junction. The abdominal wall muscles have been shown repeatedly with ultrasound to thicken depth-wise during contraction (Misuri et al., 1997; Hodges et al., 2003; Hides et al., 2006). It was noted here that the muscles, in particular the IO, did not show a great deal of tapering at the muscle-aponeurosis junction; both the RA and IO muscles demonstrated thickening right up to the aponeurosis border. It would thus be beneficial for the aponeurosis to deform (thicken) along with the muscle to avoid potentially detrimental stress concentrations from developing at the muscle-aponeurosis junction. Perhaps the layered nature of the abdominal wall and aponeurotic or fascial structures allows for such expanding deformations by accommodating a slight separating between the layers in

response to the diverse forces acting on the various tissues, while still providing the shear connections that allow for the binding and toughening of tissues.

Connective tissues, while not having the capability of actively contracting, do possess the potential for passive contraction dependent upon the stiffness of the tissue at a given time. Connective tissues resisting a force at a given length will effectively contract as the stiffness within the tissue increases. This increase in stiffness may effectively occur due to a rearrangement of fibres as the tissue deforms in response to other applied forces.

Alternatively, tissue with an apparent pre-stress to give the fibres an initial orientation prior to contraction may relax during contraction as the fibres rearrange to resist other forces.

Challenged breathing recruits the abdominal muscles, and deformation of the connective tissues probably occurs cyclically during respiration, both due to muscular contraction and also simply due to changes in the IAP and the distention of the abdomen (Campbell & Green, 1953). In the current study, participants were told not to alter their breathing during contractions; however, it is possible that in some instances a slightly exaggerated inspiration may have occurred prior to the target contraction which may have pre-stressed the tissue. This may explain the connective tissue structures seemingly contracting (becoming shorter) during a high number of trials.

The lateral border of the RA moved laterally during contraction in approximately 68% of trials. The documented lateralization of the muscle could be movement of the whole RA muscle by stretching of the linea alba, or alternatively transverse stretching the RA (by separating parallel fibres). The tendinous intersections are thought to function, at least in part, to provide transverse strength to the RA by giving it anchor points along its length (McGill, 2002). For this to function as hypothesized, the transverse stiffness of the tendinous

region must be greater than the muscle region, which has been shown to be true for the diaphragm muscle (Hwang et al., 2005b). The lateral movement of the RA muscle should be dictated by the competing forces generated by the RA muscle, which will stiffen its fibres both along and transverse to its fibre direction, and the forces generated in the abdominal wall muscles (EO, IO, TrA), which will act to pull the RA muscle transversely across its fibres. An interesting relationship was found to partially support this idea, where the amount of lateral movement of the RA was related (exponential $R^2 = 0.54$) to the ratio of oblique muscle to RA muscle force (Figure 6.6).

The magnitude of abdominal contraction did not affect the deformation of any of the connective tissue structures examined. In other words, the deformations could not be statistically separated for any of the abdominal contraction levels. This is despite the fact that the estimated magnitude of force generated by the abdominal muscles was significantly different between the contraction levels. This again points to connective tissues being a highly non-linear network, with great deformations occurring at low contraction levels, most likely as fibres rearrange in response to the applied forces, and then leveling off with higher levels of contraction as the fibres have reached their most organized arrangement. This effective toe region of lower stiffness followed by a more linear region of high stiffness has been reported and reviewed at length for connective tissue (Viidik, 1973; Jeronimidis & Vincent, 1984).

Orientation of the ultrasound probe had a significant effect on the measure of the length change of the IO aponeurosis, as well as the lateral movement of the RA muscle during contraction. The smallest IO aponeurosis lengthening was recorded when the probe was oriented along the fibre direction of the IO muscle, which would most likely produce the

most accurate measure of this variable. The largest lengthening was recorded when the probe was oriented 95 degrees away from this orientation, along the line of the EO fibre direction. This may be partially explained by a difference in the rest length of the aponeurosis in the two orientations, as when the length changes were normalized as a percent of rest length, the measure was no longer statistically affected, although the same trend still existed and may have again reached statistical significance with a larger sample population. The lateral movement of the RA muscle could not be normalized to a rest position, as the entire muscle was not able to be captured completely in a single image. In this case, the largest movement of the RA was found with the probe oriented horizontally, statistically greater than either of the angled orientations. The horizontal position should capture the image nearly perpendicular to the fibre direction of the RA muscle, and thus may provide the most accurate measure of its lateral or transverse movement.

No forces were directly measured within the abdomen. Surface EMG was recorded and used to estimate the force generated by the individual muscles. This requires a number of assumptions, including the form of the relationship between EMG and muscle force (Chapter 3), and the scaled magnitude of the relationship. Calibration trials were used here to attempt to generate inter-individual scaling to obtain the most accurate estimates of muscle force as possible. Still, assumptions were made as to the partitioning of muscle force based on assumed sizes and lengths of muscles relative to one another. Intra-abdominal pressure was not measured. Previous work has established a link between the activation of the abdominal musculature and intra-abdominal pressure (Cresswell, 1993; Cholewicki et al., 2002), so that it can be safely assumed that internal abdominal pressure increased along with

contraction levels; future work should however attempt to measure the IAP while imaging muscular contractions within the abdomen.

The most important conclusion of this work is that the connective tissues supporting and intervening the muscles of the abdominal wall function to allow these muscles to operate within the context of the array competing forces and demands acting on the system. The deformations of the connective tissues cannot be explained by simple mechanical and tissue properties; a complex network of fibres and matrix interact to accommodate the deformations necessary for varying demands. In addition, the high laterally produced forces of the oblique and transverse muscles appear to dominate over the longitudinal force of the RA, thereby creating lateral movement of the RA during abdominal contraction. Future work should be dedicated to testing the morphology and mechanics of the abdominal wall muscles and tissues, in order to better understand how these structures function to produce movements of the torso, stabilize the spine, and regulate intra-abdominal pressure and respiration under a wide array of demands.

Chapter 7:

Transmission of Muscularly Generated Force and Stiffness between Layers of the Rat Abdominal Wall

Chapter Synopsis

The abdominal wall is comprised of three obliquely-oriented sheet-like muscles bound together through a connective tissue network. This anatomical arrangement would seem ideal to facilitate myofascial force transmission, which if present would indicate shear connections between the muscle layers that could have important mechanical consequences. In ten Sprague-Dawley rats, the three layers of the abdominal wall were isolated together and attached to a servomotor force/displacement system. The abdominal wall was stimulated via electrodes over the surface of the transverse abdominis, and measures of force and stiffness were obtained. The aponeurosis attaching the transverse abdominis to the rectus sheath was then cut and the wall was re-stimulated and the same measures were again obtained. Active force and stiffness were both reduced in the cut aponeurosis state, with the drop in stiffness being statistically significant ($p < 0.0346$). These drops (10.6 and 10.7 %, respectively) were much lower than would be expected if the transverse abdominis were completely removed (39 %). Furthermore, a control group (five rats), in which the aponeurosis was not cut, but a similar amount of time to that necessary to perform the aponeurosis surgery was allowed to elapse, showed reductions in active force and stiffness (7.9 and 8.2 %, respectively) nearing that seen in the cut state. This indicates that at least a portion of the drop in these variables was due to the passage of time in the compromised surgical state. Thus, it was concluded that the majority (at least 72 %) of the force and stiffness generated by the transverse abdominis was transferred through alternate means, most likely through the connective tissue network adhering to the internal oblique muscle. This has implications for the mechanical function of the abdominal wall muscles, as strong shear connections between the muscular layers probably facilitate the synergistic interactions necessary to meet their array of roles.

7.1 Introduction

The abdominal wall musculature is highly unique in its architectural arrangement. It is composed of three sheet-like muscle layers, transverse abdominis (TrA), internal oblique (IO), and external oblique (EO), that are tightly bound together by a connective tissue network that exists between each consecutive layer. The abdominal wall muscles have a number of important mechanical roles, ranging from the generation of twist, lateral bend and flexion moments and motions (McGill, 1991), maintenance and control of a stable spinal column (Cholewicki & McGill, 1996; Granata & Marras, 2000) and intra-abdominal pressure (Cholewicki et al., 2002), and assistance with respiration (Campbell & Green, 1953). The diversity and highly demanding nature of these roles has inevitably produced an anatomical/geometrical arrangement of the muscles and connective tissues that are most suitable to meeting these demands. However, very little is known about the exact mechanisms by which the anatomical structures suit and optimize the function of the abdominal muscles. Thus, the purpose of this study was to examine a specific mechanical function, the ability to directly transmit force and stiffness between the muscle layers, related to the composite nature of the abdominal wall.

Recent work has demonstrated that muscles linked through their bellies to connective tissue networks adjoining adjacent muscles should not be considered completely independent generators of force and stiffness (Huijing and Baan, 2003). The position and length of each muscle affect the output of the other muscles through what has been termed myofascial force transmission. Briefly, the force generated by sarcomeres in a given muscle need not be transferred entirely to the tendinous collagen fibres with which they are in series. Some of the force can be transmitted through adjacent fibres in parallel, and subsequently, through a shear

linkage mechanism, outwards through fascial or connective tissue attachments between muscles.

The tightly bound layered formation of the abdominal wall musculature would seem to be an ideal anatomical scenario for myofascial force transmission. This has been hypothesized as the mechanism underlying the documented enhanced passive stiffness of the combined IO and TrA muscles in comparison to the stiffness of these individual muscle layers in isolation (Hwang et al., 2005a), but has not been tested during active contraction. Demonstrating that direct active force transmission is possible through the connective tissue networks between the muscle layers would provide a proof of principle for important shear connections binding the muscles to one another. Such shear connections can establish a mechanical link that can significantly affect the function and ability of the muscles to perform their needed roles. This is specifically important to the abdominal wall muscles, as enhancement in function to meet the vast mechanical demands can be achieved via shear connections through potential avenues such as the regulation of muscle lengths around optimal, the strengthening and toughening of the wall as a composite structure, and the direct transmission of force and stiffness in the case of potential neural deficits in a particular muscle layer. Thus, the current study was designed to test the ability of the force generated by the TrA muscle to be transferred, in the absence of its normal avenue of transmission, through its connective tissue attachments to the IO muscle, ultimately reaching its originally intended location on the rectus sheath.

7.2 Methods

7.2.1 Pilot Work

Before describing the methodology of the study, it is first necessary to describe the initial efforts that were made with regards to the animal model. The original goal of this study was to test the force and stiffness characteristics of the intact abdominal wall, and then compare to the force and stiffness characteristics of each individual (isolated) muscular layer of the wall. Pilot work was conducted with anaesthetized rats to determine the feasibility of separating the muscular layers from one another. It was determined that this could not be accomplished within a reasonable time frame (even dissections of up to 45 minutes did not even allow the separation of the entire wall) without tearing or damaging the muscles. The thin nature of the muscles appeared to be the limiting factor; thus, a second pilot study was conducted with a single anaesthetized piglet (approximately 8 weeks old and 10 kg). The muscle layers were much thicker in the piglet; however, bleeding could not be adequately controlled during the invasive surgery and this animal model was thus considered unfeasible.

The lack of success of this pilot work lead to the re-addressing of the problem and the development of the study described here.

7.2.2 Experimental Procedures

All procedures were approved by the University Office of Animal Research Ethics. Fifteen male Sprague-Dawley rats (mean/sd mass 501.5/38.2 grams; age 29.5/1.8 weeks) were used in this study. Ten rats served as part of the experimental group and the remaining five served as controls. Rats were initially anaesthetized using 5 % isoflurane gas, which was then reduced to a maintenance level for the remainder of the experiment. The rats were

placed on a heated water pad (39°C) for all surgical and experimental procedures. Skin was removed from the abdomen and a cranial (just below the sternum) to caudal (inguinal level) incision was made just lateral to the right of the linea alba. Two transverse cuts were then made, the first caudal to the ribcage, the second cranial to the inguinal region. This isolated a region of the left side of the abdominal wall muscle and aponeurosis spanning the linea alba to the approximate beginning of the thoraco-lumbar fascia. The average (standard deviation) cranial to caudal width of the isolated wall was 26.5 (3.3) mm. The muscle wall remained attached dorsally to a portion of its blood and nervous supply. Throughout all procedures, the muscle unit was consistently wetted with an isotonic saline solution to prevent drying. Light wooden rods were glued to both the superficial and deep sides of the wall along the linea alba, and a 24-gauge copper wire was sutured just medial to the rods through the abdominal aponeurosis/rectus abdominis complex and attached, in line with the TrA fibres, to a servomotor force/displacement system (S300, Cambridge Technologies) (Figure 7.1). The spinal column was immobilized by inserting a pin, secured from above, into an intervertebral disc at a spinal level corresponding to the middle of the isolated muscle wall.

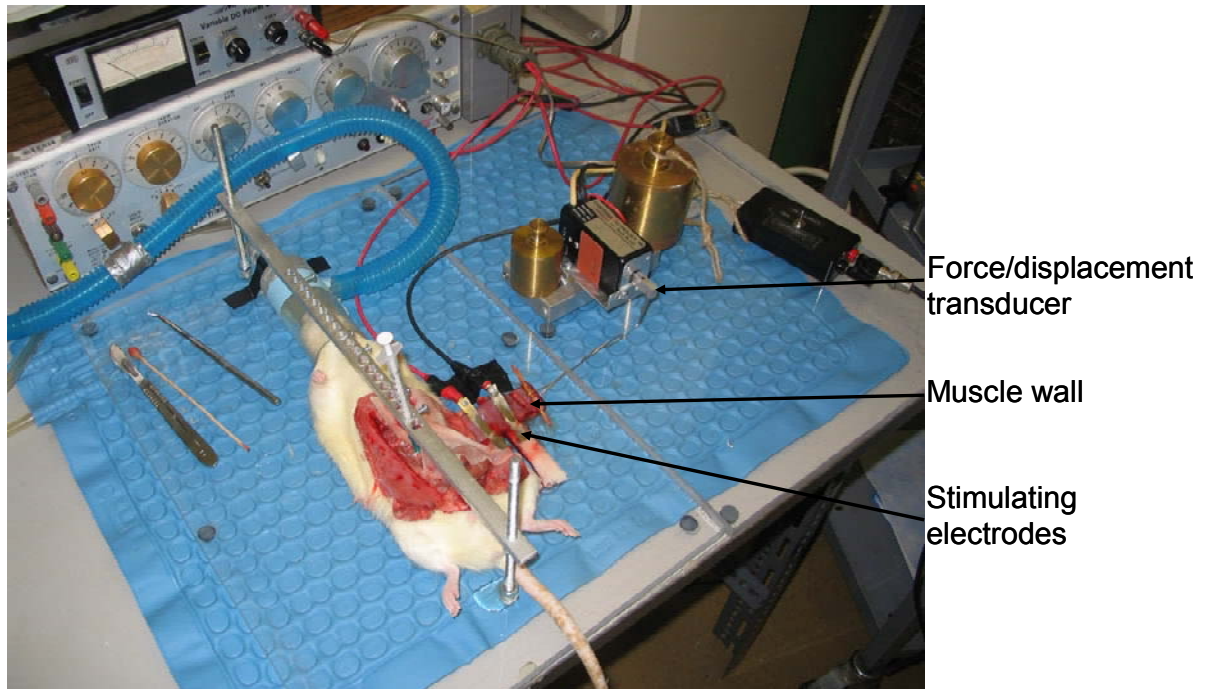


Figure 7.1. Picture of the experimental set-up.

The muscle wall was placed at its optimal length for active force production, and all tests were performed at this length. Two platinum plate electrodes were used to stimulate the abdominal wall. These plates were placed across the line of fibres of the transverse abdominis muscle, at an average (s.d.) distance of 27.5 (5.0) mm apart from one another. Electrode conductivity gel (Conmed, Utica, NY) was used to increase the conductance of the stimulus. A constant voltage stimulus ranging between 20 and 40 V (S48, Grass Medical Instruments, Quincy, Mass.), depending on the specimen, was used for all tests; voltages higher than this were found to occasionally saturate the range of the force transducer. Initial tests (400 ms duration pulse trains; 100 Hz stimulation) were conducted to pre-condition the muscle and to ensure that electrodes had settled into a consistent location on the muscle. Once a consistent force reading was obtained the experimental testing was begun. The

experimental protocol consisted of a 100Hz (0.1 ms/pulse) pulse train stimulation for 800 ms with a quick length change (muscle shortened by 0.35 mm) applied 400ms into the train.

Force and position were digitally recorded at 1000Hz.

Force was measured over a 100 ms period at the plateau of the initial force recording, and the active contribution was obtained by subtracting this value from the initial passive force prior to the onset of stimulus. Stiffness was measured as the change in force over the change in position (g/mm) resulting from the quick release. Approximately one minute rest was given between all trials to allow for recovery.

In the ten experimental rats the TrA was then cut along its aponeurosis (posterior aponeurosis of the abdominal wall; Figure 7.2) so that it no longer attached in series to the force/displacement transducer. The aforementioned force and stiffness tests were repeated in this new “cut” state. In the remaining five rats an amount of time approximately equal to the amount of time required to perform the cutting of the aponeurosis (average of three minutes) was allowed to elapse and the force and stiffness tests were repeated. In these five rats the aponeurosis was never cut. This control group served to test the hypothesis that an elapse of time, in the compromised surgical state, caused a decrease in the force and stiffness generating capabilities of the abdominal wall muscle group.

Finally, in eleven of the rats, the thickness of each of the abdominal wall muscles was measured, and in seven of these rats the fibre angle of the IO and EO muscles, with respect to the fibre line of action of the TrA, was measured.

A one-way repeated measures ANOVA was conducted to test for differences between the intact and cut aponeurosis states for each of abdominal wall passive force, active force and stiffness ($\alpha = 0.05$).

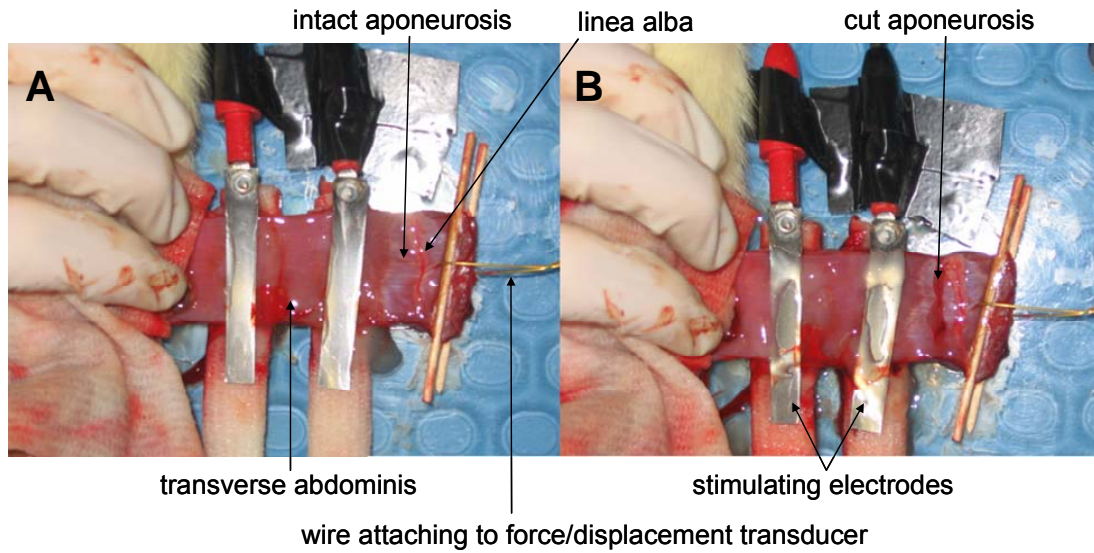


Figure 7.2. Picture of the abdominal wall in the intact state (A) and with the TrA aponeurosis cut (B). Note that both the IO and EO muscles are intact and attached beneath to the TrA muscle.

7.3 Results

7.3.1 Muscle Measurements

The TrA, IO and EO were measured to make up an average (S.D.) of 30 (4.0), 39 (3.1) and 31 (3.6) percent of the total thickness of the abdominal wall, respectively. The EO fibres were measured to act at an average (S.D.) angle of 46 (3.7) degrees from the line of pull of the TrA fibres, in an inferior-medial orientation, while the IO fibres were measured to act at an average (S.D.) angle of 50 (3.0) degrees from the line of pull of the TrA fibres, in a superior-medial orientation.

As the fibres of the EO and IO would transmit a proportion of their active force equal to the cosine of their angle of pull, it was estimated that the force transducer would record approximately 69 and 64 percent of the force of these muscles, respectively. Considering these proportions in conjunction with the relative thickness of the muscle layers to determine

the total force recorded at the transducer, the TrA should produce approximately 39 percent of the total active force recorded in the current experiment. Thus, if the force from the TrA was completely eliminated by the cutting of the aponeurosis, a force drop of 39 percent would be expected.

7.3.2 The Effect of Cutting the Aponeurosis

There was no significant difference in the passive abdominal wall force between the intact and cut aponeurosis conditions ($p=0.6195$; mean/sd (grams) = 15.2/11.8 intact; 13.4/10.9 cut). Thus, there was no statistically significant change in the passive state of the abdominal wall, most likely indicating that no significant length change occurred as a result of the cutting of the aponeurosis.

The active force produced by the abdominal wall did not change in a statistically significant manner ($p=0.0998$), although there was a definite trend of a reduced active force production when the aponeurosis was cut (mean/sd (grams) = 235.7/46.2 intact; 210.8/47.4 cut) (Figure 7.3). When calculated as a percent drop for each rat and averaged, this amounted to a reduction of 11.0 percent.

The stiffness of the abdominal wall significantly reduced ($p=0.0346$) as a result of the cutting of the posterior aponeurosis (mean/sd (grams/mm) = 104.3/16.1 intact; 93.1/16.2 cut) (Figure 7.4). When calculated as a percent drop for each rat and averaged, this amounted to a reduction of 10.8 percent.

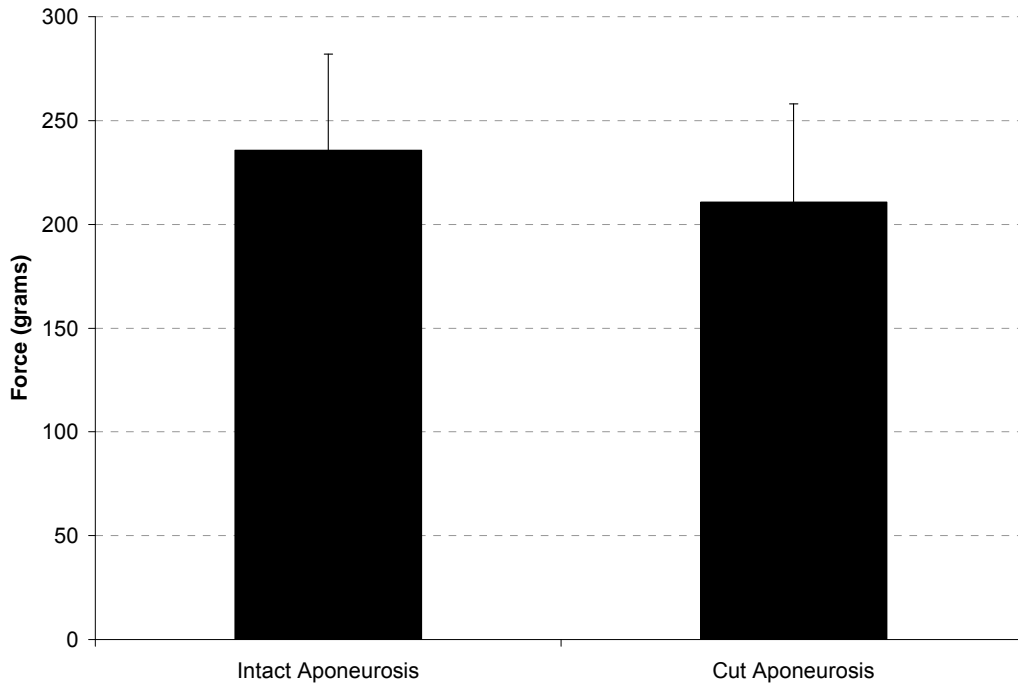


Figure 7.3. Average active force generated by the abdominal wall in the intact and cut aponeurosis states. Standard deviation bars are shown.

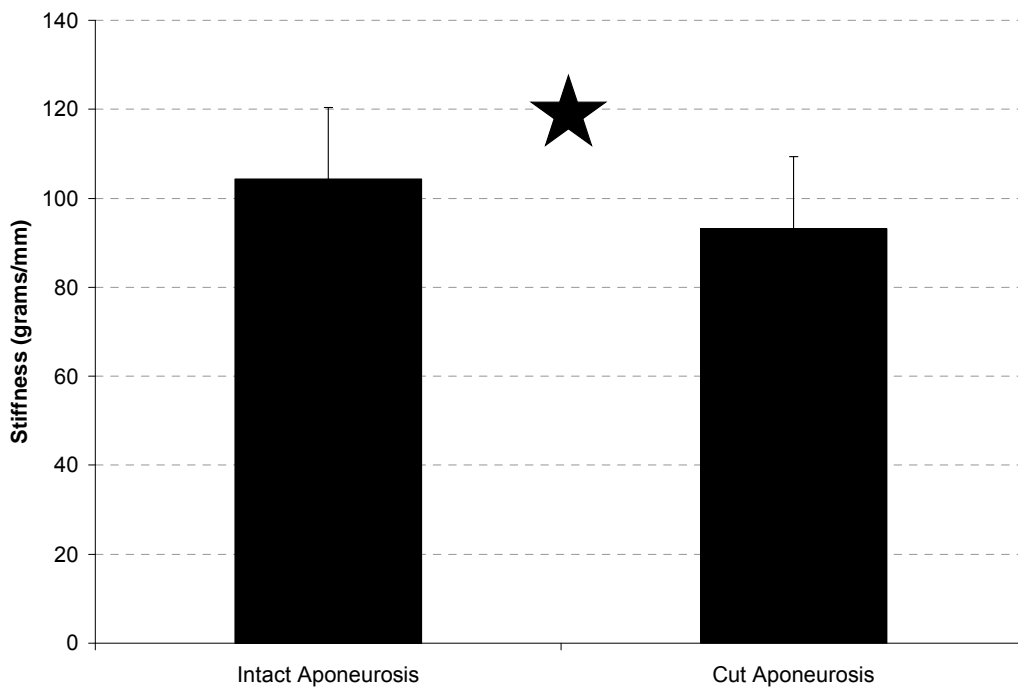


Figure 7.4. Average abdominal wall stiffness in the intact and cut aponeurosis states. The star indicates a statistically significant difference between the two states ($p < 0.0346$). Standard deviation bars are shown.

7.3.3 The Effect of Time

Five rats served as controls to determine if the reductions in active force and stiffness were influenced by the amount of elapsed time between the measurements pre and post the cutting of the aponeurosis. The average amount of time that was required to cut the aponeurosis and begin re-testing was approximately three minutes, thus this amount of time was allowed to elapse in the control group while the aponeurosis remained intact. Percent drops of 8.6 and 8.2 were found for active force and stiffness, respectively. These reductions are below, but approaching, the reductions determined for the cut aponeurosis state (Figure 7.5), thus indicating that at least a portion of the drop in these parameters was a result of the passage of time in a compromised muscular state.

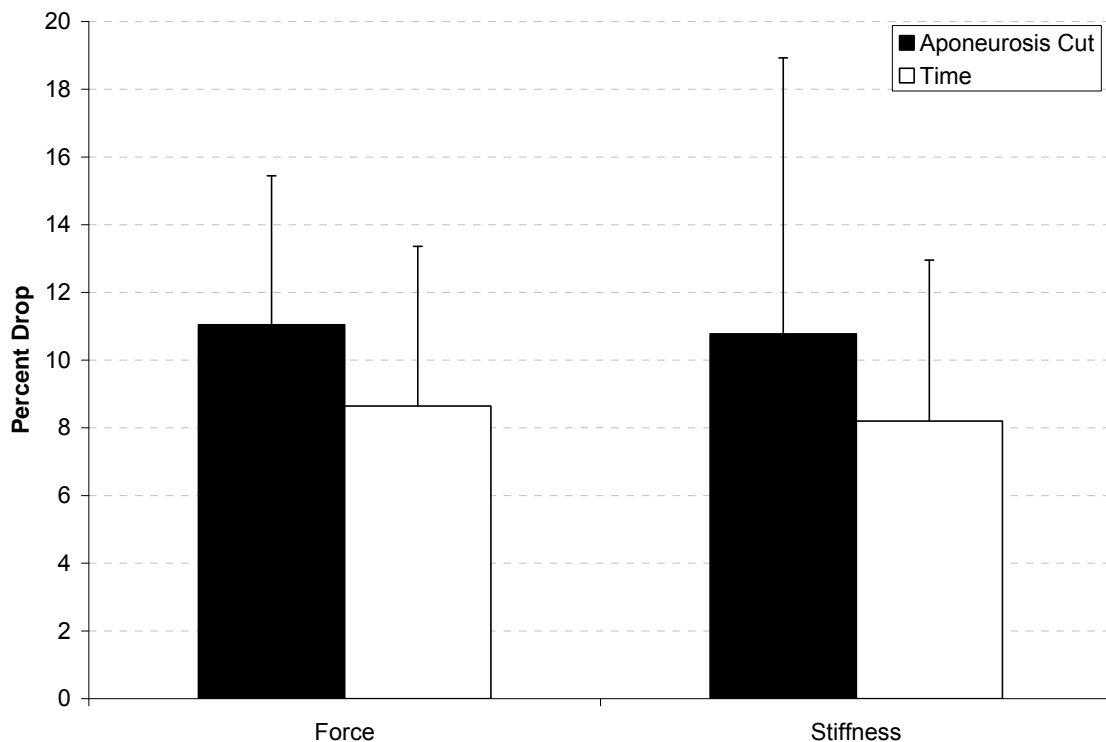


Figure 7.5. Percent drops, relative to the initial state, in each of abdominal wall active force and stiffness in the cut aponeurosis and time elapsed conditions. Percent drops were calculated for each rat and then averaged. Standard deviation bars are shown.

7.4 Discussion

Cutting of the posterior aponeurosis of the abdominal wall, thereby eliminating the direct path of force transmission of the TrA muscle, did not reduce the force and stiffness production of the abdominal wall to a level that would be expected had the TrA been completely eliminated. Thus, force and stiffness generated by the active contraction of this muscle was transmitted in another manner, most likely through the connective tissue attachments binding it to the IO muscle, and still resulted in a highly significant portion of its force and stiffness reaching its originally intended point of application.

It was estimated, based on measurements of the sizes and orientations of the three abdominal wall muscles, that the TrA should be responsible for producing approximately 39 percent of the active force and stiffness recorded horizontally (in line with the TrA fibres) at the linea alba. The average percent drops in these two variables measured in the current study when the TrA aponeurosis was cut were 10.6 and 10.7, respectively, or approximately 28 percent of the reduction that would be expected had the TrA been completely eliminated. Therefore, in a best case experimental scenario, where the only variable affecting the force and stiffness recorded was the status of the aponeurosis, 72 percent of the force and stiffness generated by the TrA was transferred through alternate means to the linea alba.

Due to the highly invasive nature of the surgery required to isolate a portion of the abdominal wall, it was suspected that the blood supply to the muscle group may have been disrupted to the point that the function of the muscles may have degraded over time. Indeed, in the control group comprised of five rats, an elapsed amount of time approximately equal to the time required to perform the cutting of the aponeurosis, resulted in a reduction in both active force and stiffness, despite the aponeurosis remaining intact (Figure 7.5). This further

strengthens the argument that the force and stiffness actively generated by the contraction of the TrA was transferred through alternate connective tissue attachments in the situation in which the aponeurosis was cut. Considering that the passage of time may have had a significant influence on force and stiffness generation, it appears possible that nearly the complete force and stiffness production reached its intended destination through alternate transfer means.

Numerous research studies have in recent years demonstrated the ability for muscle force to be transferred through non-tendinous means (eg. Huijing et al., 1998; Huijing & Baan, 2003; Maas et al., 2003). Connective tissue networks are able to transmit force in a fairly efficient manner, highlighted when the normal route of transmission is disrupted, and the force maintains a substantial proportion of its original output (Huijing, 1999; Huijing & Baan, 2001). The unique anatomical design of the abdominal wall seems especially capable of this type of force transfer. The three sheet-like abdominal wall muscles (TrA, IO, EO) are tightly bound to one another through complex connective tissue attachments. The current study has demonstrated that these connective tissues appear capable of transferring the vast majority (at least 72 percent) of the force and stiffness generated by a single muscle in the situation where the traditionally held “normal” route of transmission has been removed. It would normally be expected for some force generating capability to be lost due to the cutting of the aponeurosis, as the muscle to which it was attached would shorten, thereby inhibiting its force producing ability, until a point is reached at which the shear strain of the inter-connective tissues has reached a level of sufficient stiffness to allow the requisite force transmission. That the force drop measured in the current study is, at most, relatively low suggests an inherently high shear modulus between the muscle layers. It is not possible from

the current study to determine the degree to which, if at all, this inter-muscle connective tissue transmission route is utilized in the healthy or undamaged state; however, it can be stated that the force produced by the muscles will be transferred in the majority through the stiffest path. The suspected high shear modulus may suggest that force would be readily transferred between the muscle layers during in vivo situations. It has already been suspected that shear transmission of contractile force occurs readily between fibres within individual canine abdominal muscles, necessitated due to the high prevalence of fibres that do not span the entire muscle length (Boriek et al., 2002). However, future work will need to isolate the stiffness of the connective tissues intervening the musculature and comprising the aponeuroses to definitively ascertain the most likely routes of force transmission between muscle layers.

The importance of this work lies in the establishment of the probable functional necessity of the anatomical arrangement of the abdominal wall musculature. The abdominal muscles, and their connective tissue networks, produce, respond to, and are acted upon by a variety of complex forces and demands. The improper functioning of the abdominal muscles, in particular, has been shown to be highly linked to low back pain and injury (Ferreira et al., 2004; Cholewicki et al., 2005). The connective tissue attachments binding the muscles to one another may promote a more synergistic and unified mechanical function, thereby enhancing the stabilizing and stiffening effect of the muscle group while still enabling the generation of multifaceted movement patterns. Recent work has documented that individual abdominal wall muscles and regions within muscles can be neurally activated in a relatively independent manner (Mirka et al., 1997; Urquhart and Hodges, 2005; Urquhart et al., 2005). Mechanical links between the muscles may allow for this independent neural activation to enable

complex function while still ensuring that force and stiffness generated by these muscles is well distributed around the torso. Further, neural deficits in a single or small group of muscles, while clearly detrimental, may be somewhat protected against by the ability of the activation of the other muscles to transfer their capabilities to produce similar mechanical effects.

Due to the constraints of the testing system, sub-maximal stimuli were utilized to activate the abdominal wall. This level of activation was most likely beneficial to test the hypotheses posed in the current study. Meijer et al. (2006) recently demonstrated that transmission of muscle force through non-tendinous connective tissues was more relevant and important to the in-vivo situation at lower levels of force generation. Further, these lower levels of activation are much more representative of the levels that would be seen in the human abdominals during every day tasks (Essendrop et al., 2002; Butler et al., 2007). Indeed, maximal abdominal activation levels are rarely accomplished, even during near maximal torque generation situations (McGill, 1991; Marras et al., 1998), and levels of approximately one quarter of maximal are considered very difficult to achieve during isometric contractions that are generally associated with a stabilizing function (Brown et al., 2006; Hall et al., in press). Although the rat model used in the current study may not be directly replicable to the human condition, previous work has established precise similarities in terms of morphology and architecture of the muscles, intervening connective tissues and aponeuroses (Rizk 1980; Rizk and Adieb, 1982).

From the results of the current study, it can be concluded that the vast majority of the force and stiffness generated by the abdominal wall muscles, particularly the TrA tested here, can be transferred around the abdomen through the linea alba, even when the normal route of

transmission (aponeurosis) is eliminated. The most likely alternative path of transmission is through the connective tissue network that intervenes the three muscular layers. This may highlight the ability of these muscles to work in a mechanically synergistic fashion, thought to be necessary to effectively stabilize the spinal column, through the linking of force and stiffness during contraction. Thus, the muscles of the abdominal wall should not be considered as totally independent from one another in terms of their mechanical function. Their activation and corresponding force and stiffness output will highly influence each of the other muscle layers, making the intact wall a synergistically functioning muscle unit. In this way, it appears that the abdominal wall functions as a composite laminate structure; this architecture enhances the ability of the tissues to achieve substantial multi-directional stiffness.

Chapter 8:

Summary

The goal of this thesis was to progress the understanding of the mechanical function of the abdominal musculature, with a special focus on a neuromuscular-mechanical integration, to further our knowledge of spine stiffening mechanisms. A number of advances have been made: 1) The EMG-moment relationship displays a similar form for the abdominal and back musculature, in generating moments about the flexion/extension axis. This relationship is more linear than has been previously reported, with past misgivings the result of the inadequate consideration of antagonist muscle moments; 2) consciously increasing abdominal muscle activation, and consequently torso muscle activation as a whole, creates an increased trunk stiffness over the low to moderate ROMs in flexion, extension, and lateral bend. Towards the end-ROM in flexion and lateral bend, trunk stiffness at activation levels approaching maximum appears to be compromised; 3) the inherent trunk stiffness, in the absence of muscular reflex responses, is not sufficient to limit trunk displacements in response to dynamic physical perturbations; 4) abdominal muscle and connective tissues deform in a highly complex manner that cannot be explained on the basis of simple mechanical models. Most likely it is the composite laminate nature of the abdominal wall that facilitates expansion in multiple simultaneous directions, necessary to meet the competing demands due to contraction of muscle fibres shortening and thickening, along with the maintenance of the distended abdomen created through the rise in IAP; 5) the connective tissues binding the sequential layers of the abdominal wall enable the transfer of muscularly generated force and stiffness. This suggests that strong shear connections exist between these layers, which can have important mechanical consequences regarding the synergistic contraction of the abdominal wall to transfer force and stiffness around the torso.

Combined with the work of which I was a part during the initial stages of my PhD progress, a substantial improvement in our understanding of abdominal muscle function to ensure spine stiffness and stability has been achieved. The early work (Vera-Garcia et al., 2006) demonstrated that conscious increases in abdominal and torso muscle activation improved the muscular response and limited spine displacements in reaction to suddenly applied trunk loads. An important advancement was made, somewhat accidentally, during a separate experiment (Brown et al., 2006), when participants were asked to consciously overdrive naturally selected abdominal activation patterns. Every participant experienced at least some difficulty performing these contractions, and many showed a subsequent loss of stability. The main culprit for this loss of stability was uncovered to be unbalanced abdominal activation patterns, in particular large increases in activation in a single or small group of muscles. Vera-Garcia et al. (2007) further established that robust contractions of the abdominal wall, achieved through abdominal bracing techniques, better served to mechanically stabilize the spine as compared isolationist contraction techniques achieve through abdominal hollowing. A theoretical explanation for the potential detrimental effects of isolationist activation was provided by Brown and McGill (2005). In this paper we proved mathematically that, considering a biologically relevant non-linear force-stiffness relationship of the muscle-tendon unit (with stiffness levelling off at moderate to high force levels), the joint stiffening potential of a muscle may peak well before maximum force is achieved, and may actually become negative (destabilizing) at the highest force potential. This highlighted the importance of ensuring balanced activation patterns amongst all torso muscles in order to reduce the likelihood of any instance of instability.

At the completion of this thesis, a greatly advanced understanding of abdominal muscle function has been realized. However, a number of the studies uncovered new questions that will need to be answered in order to achieve a complete appreciation of the integration of abdominal muscle into the mechanics of the spine and mechanisms for spine function and injury. First, concerning the basic mechanics of the abdominal wall musculature, the shear properties of the connective tissues that intervene the oblique and transverse muscles must be examined. This will enable more definitive explanations for the synergistic workings and transfer of force and stiffness between the abdominal muscles. Next, the form and magnitude of the force-stiffness relationship of the abdominal muscles (as well as the back muscles) need to be established. This relationship can greatly affect our understanding and modeling of the stabilizing potential of the torso musculature (Cholewicki & McGill, 1995; Brown & McGill, 2005). While these questions will need to be first approached using a basic animal model, continued human imaging can be employed in an attempt to establish some stiffness estimates of the muscles and connective tissues surrounding the torso during contraction. Force estimates in the torso muscles, as examined in the current thesis, will need to be bolstered by quantifying and modeling IAP as well as the forces regulating muscle thickening and potential stresses occurring at the muscle-connective tissue interfaces. EMG recording of the abdominal and back musculature will remain a vital tool in the study of low back pain/injury; therefore, further work will need to be done in order to improve our modeling of the EMG-force/moment relationship of these muscles. In particular, studies examining this relationship about the isolated lateral bend and axial twist axes, as well as in combinations of axes, need to be conducted. Finally, the importance of muscle reflex control of spine stiffness cannot be underestimated. How these reflexes can be

facilitated and optimized, the effect that their absence and/or decline can have on injury potential, and the specific mechanisms regarding their regulation are just some of the questions that will need to be addressed in the future.

8.1 Closing

The importance of the abdominal musculature in producing movement of the spine, ensuring a level of stability appropriate to achieve such movement in the absence of injury, regulating IAP, and assisting with respiration, are well established. Despite such readily apparent consequences and the focus over the last ten years on the speculative link between abdominal muscle neural dysfunction and low back pain, very little research had been done focusing on the mechanical and neuro-mechanical characteristics of the abdominal muscles. Thus, the motivation for this thesis is clear: to further the knowledge regarding the function of the abdominal muscles, specifically in relation to mechanisms for stiffening the human spine. The work of the five studies combined in this thesis succeeded in establishing new insights into the complexities of abdominal muscle and connective tissue deformation, providing definitive resolutions regarding EMG-moment relationships and force/stiffness transfer capabilities, and uncovering an array of avenues of research and questioning that require additional study.

Appendix

Chapter 4 presented some unexpected findings regarding an apparent “yielding” effect of reduced stiffness at the highest abdominal activation levels, towards end ROM in each of flexion and lateral bend. A series of representative time-series EMG data are displayed here to demonstrate some possible activation driven effects.

Figure A.1 displays an example of two abdominal muscles (EO and IO) from two separate trials that maintain a relatively constant activity level throughout the flexion ROM (in the figures the trial time represents the total time required to pull the participant through his ROM; it thus begins at neutral and ends at end ROM). An opposing example is provided in Figure A.2, which shows two abdominal muscles (EO and IO), again from two separate trials, that reduce activation over the course of the flexion ROM. The patterns of reduction in these two muscles, however, are quite different. The EO displays a gradual decrease in activation over the entire ROM, whereas the IO shows a relatively constant activation level over the first 50% of ROM, a subsequent increase in activation between approximately 50% and 70% ROM, followed by a gradual decrease in activation to the end ROM. The varying IO pattern would seem to indicate some difficulty in controlling the activation level beyond 50% ROM, which supports the hypothesis for the “yielding” effect provided in Chapter 4.

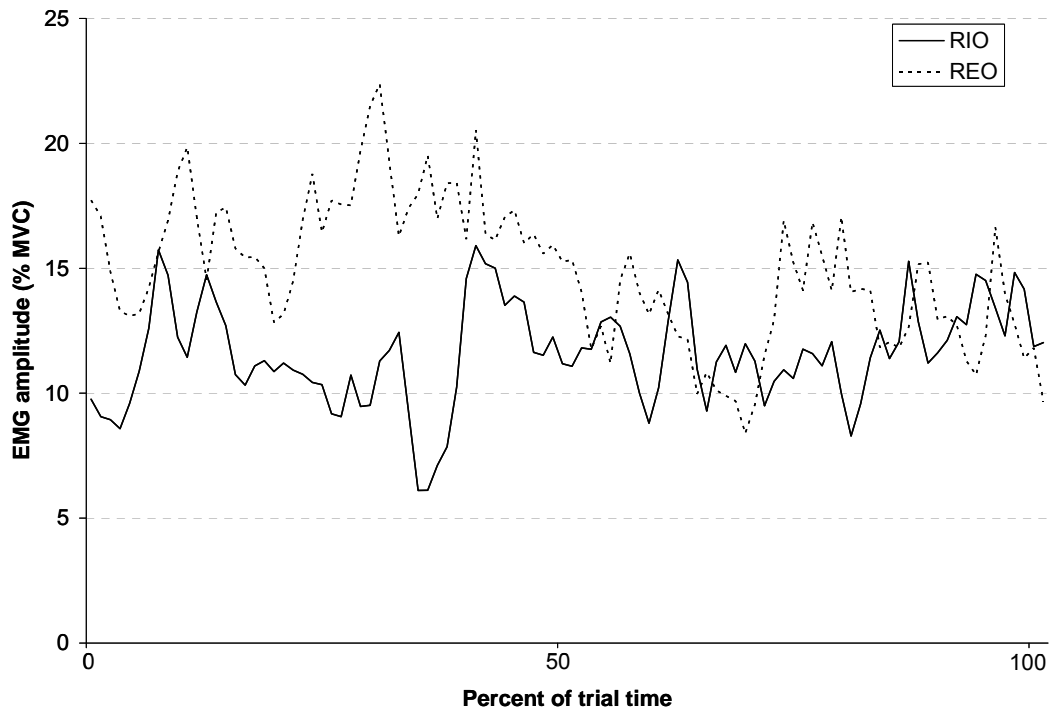


Figure A.1. Example of two muscles, taken from different heavy brace trials, that display a relatively constant level of activation over the course of the flexion ROM (as described in Chapter 4).

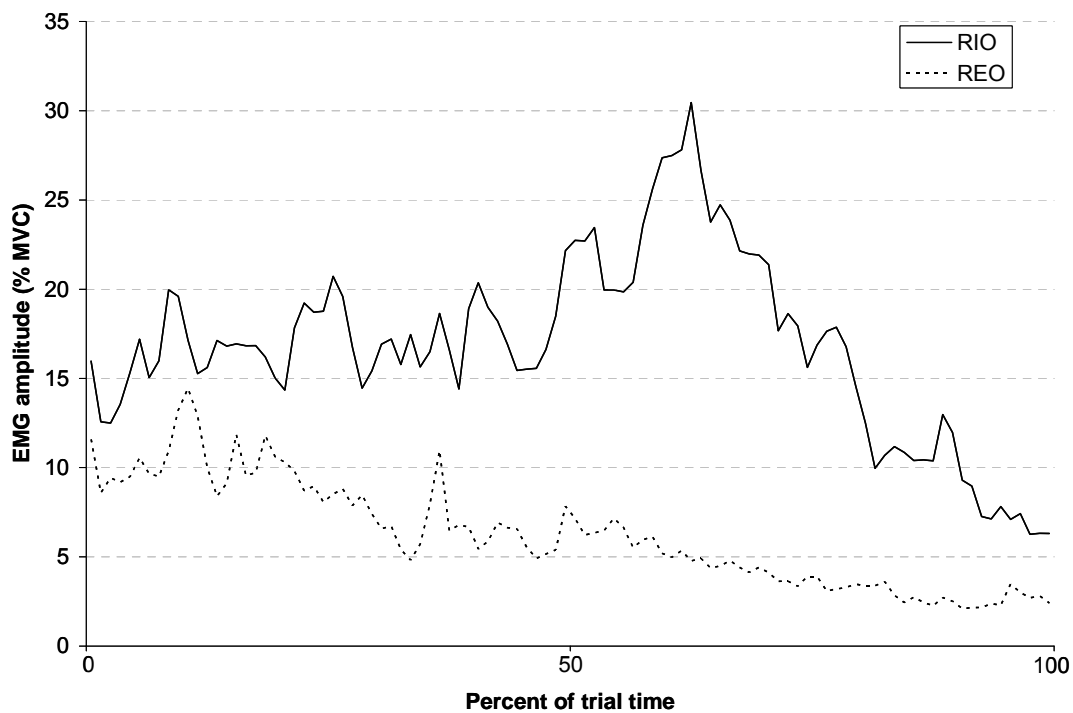


Figure A.2. Example of two muscles, taken from different heavy brace trials, that display a reduced activation level over the course of the flexion ROM (as described in Chapter 4).

It is important to note that as participants were rotated through their ROM, the location of the surface electrodes relative to the underlying muscle most likely changed. This may have affected the energy of the signal picked up by the electrode, consequently creating the amplitude changes that are sometimes apparent. Further, as the muscles changed length over the course of the ROM, the amount of electrical activity necessary to maintain a given force level would change in conjunction with the muscle's force-length relation. A potential example of this may be seen in Figure A.3. Here, in this right-side lateral bend ROM trial (both muscles taken from the same trial), the right IO gradually increases its activation over the course of ROM (as it shortens), while the left IO reduces its activation over the course of ROM (as it lengthens).

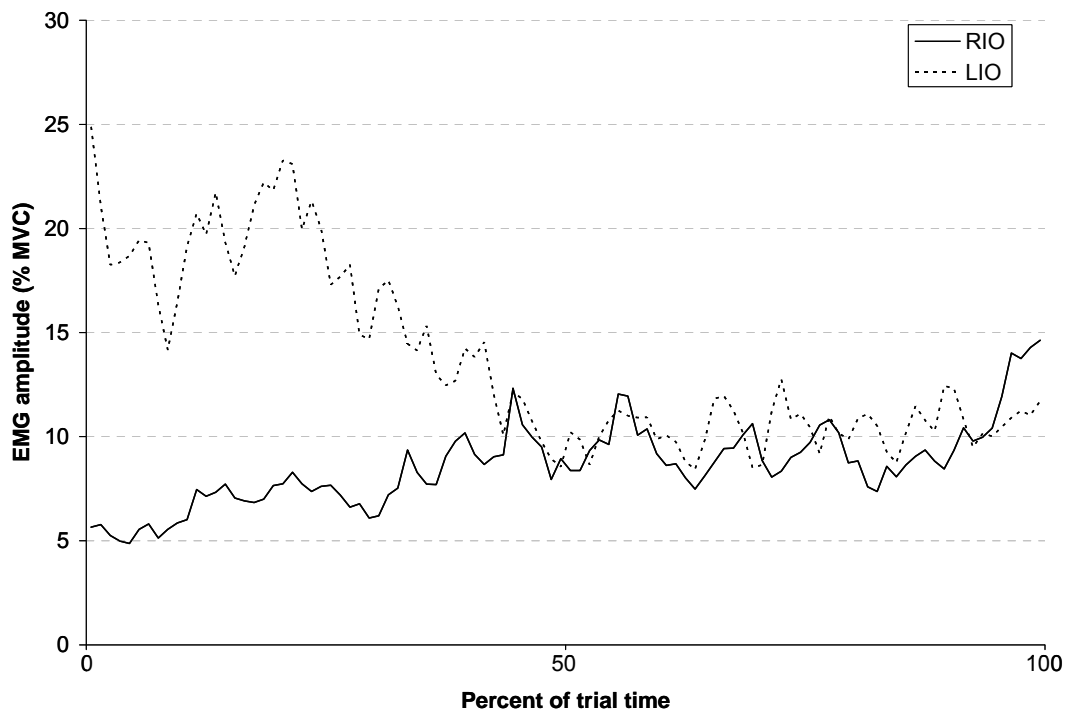


Figure A.3. Example of two muscles, taken from the same heavy brace trial, that display opposing changes over the course of the right-side lateral bend ROM (as described in Chapter 4). As the right IO shortens it increases its activation level; as the left IO lengthens it decreases its activation level.

References

Adams M.A., Hutton W.C., Stott J.R.R. (1980). The resistance to flexion of the lumbar intervertebral joint. *Spine* 5:245-253.

Akazawa K., Milner T.E., Stein R.B. (1983). Modulation of reflex EMG and stiffness in response to stretch of human finger muscle. *J Neurophysiol* 49:16-27.

Andersen T.B., Essendrop M., Schibye B. (2004). Movement of the upper body and muscle activity patterns following a rapidly applied load: the influence of pre-load alterations. *Eur J Appl Physiol* 91:488-492.

Askar O.M. (1977). Surgical anatomy of the aponeurotic expansions of the anterior abdominal wall. *Annals of the Royal College of Surgeons of England* 59:313-321.

Axer H., von Keyserlingk D.G., Prescher A. (2001). Collagen fibers in linea alba and rectus sheaths: I. general scheme and morphological aspects. *J Surg Res* 96:127-134.

Beach T.A.C., Parkinson R.J., Stothart J.P., Callaghan J.P. (2005). Effects of prolonged sitting on the passive flexion stiffness of the in vivo lumbar spine. *Spine J* 5:145-154.

Bendavid R., Howarth D. (2000). Transversalis fascia rediscovered. *Surgical Anatomy and Embryology* 80, 25-33.

Bennett D.J., Gorassini M., Prochazka A. (1994). Catching a ball: contributions of intrinsic muscle stiffness, reflexes, and higher order responses. *Can J Physiol Pharmacol* 72:25-534.

Bergmark A. (1989). Stability of the lumbar spine: a study in mechanical engineering. *Acta Orthopaedica Scandinavica Supplementum* 60:3-52.

Bojsen-Moller J., Magnussen S.P., Raundahl Rasmussen L., Kjaer M., Aagaard P. (2005). Muscle performance during maximal isometric and dynamic contractions is influenced by the stiffness of the tendinous structures. *J Appl Physiol* 99:986-994.

Boriek, A.M., Ortize, J., Zhu, D. (2002). Fiber architecture of canine abdominal muscles. *J Appl Physiol* 92:725-735.

Brown S.H.M., McGill S.M. (2005). Muscle force-stiffness characteristics influence joint stability: a spine example. *Clin Biomech* 20:917-922.

Brown S.H.M., Potvin J.R. (2005). Constraining spine stability levels in an optimization model leads to the prediction of trunk muscle cocontraction and improved spine compression force estimates. *J Biomech* 38:745-754.

Brown S.H.M., Potvin J.R. (2007). Exploring the geometric and mechanical characteristics of the spine musculature to provide rotational stiffness to two spine joints in the neutral posture. *Hum Move Sci* 26:113-123.

Brown S.H.M., Vera-Garcia F.J., McGill S.M. (2006). Effects of abdominal muscle coactivation on the externally pre-loaded trunk: variations in motor control and its effect on spine stability. *Spine* 31:E387-E393.

Butler H.L., Hubley-Kozey C.L., Kozey J.W. (2007). Changes in trunk muscle activation and lumbar-pelvic position associated with abdominal hollowing and reach during a simulated manual material handling task. *Ergonomics* 50:410-425.

Campbell E.J.M., Green J.H. (1953). The variations in intra-abdominal pressure and the activity of the abdominal muscles during breathing; a study in man. *J Physiol* 122:282-290.

Carter R.R., Crago P.E., Keith M.W. (1990). Stiffness regulation by reflex action in the normal human hand. *J Neurophysiol* 64:105-118.

Chiang J., Potvin J.R. (2001). The in vivo dynamic response of the human spine to rapid lateral bend perturbation: effects of preload and step input magnitude. *Spine* 26:1457-1464.

Cholewicki J., Ivancic P.C., Radebold A. (2002). Can increased intra-abdominal pressure in humans be decoupled from trunk muscle co-contraction during steady state isometric exercise. *Eur J Appl Physiol* 87:127-133.

Cholewicki J., Juluru K., Radebold A., Panjabi M.M., McGill S.M. (1999). Lumbar spine stability can be augmented with an abdominal belt and/or increased intra-abdominal pressure. *Eur Spine J* 8:388-395.

Cholewicki J., McGill S.M. (1996). Mechanical stability of the in vivo lumbar spine: implications for injury and chronic low back pain. *Clin Biomech* 11:1-15.

Cholewicki J., Silfies S.P., Shah R.A., Greene H.S., Reeves N.P., Alvi K., Goldberg B. (2005). Delayed trunk muscle reflex responses increase the risk of low back injuries. *Spine* 30:2614-2620.

Cholewicki J., Simons A.P.D., Radebold A. (2000). Effects of external trunk loads on lumbar spine stability. *J Biomech* 33:1377-1385.

Cordo P.J., Nashner L.M. (1982). Properties of postural adjustments associated with rapid arm movements. *J Neurophysiol* 47:287-302.

Cresswell A.G. (1993). Responses of intra-abdominal pressure and abdominal muscle activity during dynamic trunk loading in man. *Eur J Appl Physiol* 66:315-320.

Crisco J.J., Panjabi M.M., Yamamoto I., Oxland R. (1992). Euler stability of the human ligamentous lumbar spine. Part 2: experiment. *Clin Biomech* 7:27-32.

Dolan P., Adams M.A. (1993). The relationship between EMG activity and extensor moment generation in the erector spinae muscles during bending and lifting activities. *J Biomech* 26:513-522.

Dowling J.J., Durkin J.L., Andrews D.M. (2007). The uncertainty of the pendulum method for the determination of the moment of inertia. *Med Eng Phys* 28:837-841.

Edwards W.T., Hayes W.C., Posner I., White A.A., Mann R.W. (1987). Variation of lumbar spine stiffness with load. *J Biomech Eng* 109:35-42.

Essendrop M., Andersen T.B., Schibye B. (2002). Increase in spinal stability obtained at levels of intra-abdominal pressure and back muscle activity realistic to work situations. *Appl Ergonomics* 33:471-476.

Essendrop M., Schibye B. (2004). Intra-abdominal pressure and activation of abdominal muscles in highly trained participants during sudden heavy trunk loadings. *Spine* 29:2445-2451.

Ettema G.J.C., Huijing P.A. (1994). Skeletal muscle stiffness in static and dynamic contractions. *J Biomech* 27:1361-1368.

Farfan H.F. (1973). *Mechanical Disorders of the Low Back*. Lea & Febiger, Philadelphia, PA, USA.

Ferreira P.H., Ferreira M.L., Hodges P.W. (2004). Changes in recruitment of the abdominal muscles in people with low back pain: ultrasound measurement of muscle activity. *Spine* 29:2560-2566.

Ford L.E., Huxley A.F., Simmons R.M. (1981). The relation between stiffness and filament overlap in stimulated frog muscle fibres. *J Physiol* 311:219-249.

Franklin T.C., Granata K.P. (2007). Role of reflex gain and reflex delay in spinal stability: a dynamic simulation. *J Biomech* 40:1762-1767.

Fuglevand A.J., Winter D.A., Patla A.E. (1993). Models of recruitment and rate coding organization in motor-unit pools. *J Neurophysiol* 70:2470-2488.

Gajdosik R.L. (2001). Passive extensibility of skeletal muscle: review of the literature with clinical implications. *Clin Biomech* 16:87-101.

Gardner-Morse M.G., Stokes I.A.F. (1998). The effects of abdominal muscle coactivation on lumbar spine stability. *Spine* 23:86-91.

Gardner-Morse M.G., Stokes I.A.F. (2001). Trunk stiffness increases with steady-state effort. *J Biomech* 34:457-463.

Gardner-Morse M., Stokes I.A.F. (2003). Physiological axial compressive preloads increase motion segment stiffness, linearity and hysteresis in all six degrees of freedom for small displacements about the neutral posture. *J Orthop Res* 21:547-552.

Gottlieb G.L., Agarwal G.C. (1979). Response to sudden torques about ankle in man: myotatic reflex. *J Neurophysiol* 42:91-106.

Granata K.P., Marras, W.S. (2000). Cost-benefit of muscle cocontraction in protecting against spinal instability. *Spine* 25:1398-1404.

Gregory D.E., Brown S.H.M., Callaghan J.P. (in press). Trunk muscle responses to suddenly applied loads: Do individuals who develop discomfort during prolonged standing respond differently? *J Electromyogr Kinesiol* doi:10.1016/j.jelekin.2006.12.005.

Hasan Z. (2005). The human motor control system's response to mechanical perturbation: should it, can it, and does it ensure stability? *J Mot Behav* 37:484-493.

Hides J., Wilson S., Stanton W., McMahon S., Keto H., McMahon K., Bryant M., Richardson C. (2006). An MRI investigation into the function of the transversus abdominis muscle during "drawing-in" of the abdominal wall. *Spine* 31:E175-E178.

Hodges P.W., Bui B.H. (1996). A comparison of computer-based methods for the determination of onset of muscle contraction using electromyography. *Electroencephal Clin Neurophysiol* 101:511-519.

Hodges P.W., Eriksson A.E.M., Shirley D., Gandevia S.C. (2005). Intra-abdominal pressure increases stiffness of the lumbar spine. *J Biomech* 38:1873-1880.

Hodges P.W., Pengel L.H.M., Herbert R.D., Gandevia S.C. (2003). Measurement of muscle contraction with ultrasound imaging. *Muscle & Nerve* 27:682-692.

Hodges P.W., Richardson C.A. (1998). Delayed postural contraction of transversus abdominis in low back pain associated with movement of the lower limb. *J Spinal Disord* 11:46-56.

Hoffer J.A., Andreassen S. (1981). Regulation of soleus muscle stiffness in pre-mammillary cats: intrinsic and reflex components. *J Neurophysiol* 45:267-285.

Houk J.C., Rymer W.Z., Crago P.E. (1981). Dependence of dynamic response of spindle receptors on muscle length and velocity. *J Neurophysiol* 46:143-166.

Hubley-Kozey C.L., Vezina M.J. (2002). Muscle activation during exercises to improve trunk stability in men with low back pain. *Arch Phys Med Rehabil* 83:1100-1108.

Huijing P.A. (1999). Muscle as a collagen fiber reinforced composite: a review of force transmission in muscle and whole limb. *J Biomech* 32:329-345.

Huijing P.A., Baan G.C. (2001). Myofascial force transmission causes interaction between adjacent muscles and connective tissue: effects of blunt dissection and compartmental fasciotomy on length force characteristics of rat extensor digitorum longus muscle. *Arch Physiol Biochem* 109:97-109.

Huijing P.A., Baan G.C. (2003). Myofascial force transmission: muscle relative position and length determine agonist and synergist muscle force. *J Appl Physiol* 94:1092-1107.

Huijing P.A., Baan G.C., Rebel G.T. (1998). Non-myotendinous force transmission in rat extensor digitorum longus muscle. *J Exp Biol* 201:683-691.

Hunt C.C., Ottoson D. (1976). Initial burst of primary endings of isolated mammalian muscle spindles. *J Neurophysiol* 39:324-330.

Hwang W., Carvalho, J.C., Tarlovsky, I., Boriek, A.M. (2005a). Passive mechanics of canine internal abdominal muscles. *J Appl Physiol* 98:1829-1835.

Hwang W., Kelly N.G., Boriek A.M. (2005b). Passive mechanics of muscle tendinous junction of canine diaphragm. *J Appl Physiol* 98:1328-1333.

Ishikawa M., Niemela E., Komi P.V. (2005). Interaction between fascicle and tendinous tissues is short-contact stretch-shortening cycle exercise with varying eccentric intensities. *J Appl Physiol* 99:217-223.

Janevic J., Ashton-Miller J.A., Schultz A.B. (1991). Large compressive preloads decrease lumbar motion segment flexibility. *J Orthop Res* 9:228-236.

Jeronimidis G., Vincent J.F.V. (1984). Composite Materials. In: *Connective Tissue Matrix*. Ed. Hukins, D.W.L., The MacMillan Press Ltd., London, UK.

Joyce G.C., Rack P.M.H. (1969). Isotonic lengthening and shortening movements of cat soleus muscle. *J Physiol* 204:475-491.

Junge K., Klinge U., Prescher A., Giboni P., Niewiera M., Schumpelick V. (2001). Elasticity of the anterior abdominal wall and impact for reparation of incisional hernias using mesh implants. *Hernia* 5:113-118.

Kearney R.E., Stein R.B. (1997). Identification of intrinsic and reflex contributions to human ankle stiffness dynamics. *IEEE Trans Biomed Eng* 44:493-504.

Krajcarski S.R., Potvin J.R., Chiang J. (1999). The in vivo dynamic response of the spine to perturbations causing rapid flexion: effects of pre-load and step input magnitude. *Clin Biomech* 14:54-62.

Lawrence J.H., DeLuca C.J. (1983). Myoelectric signal versus force relationship in different human muscles. *J Appl Physiol* 54:1653-1659.

Lee P.J., Rogers E.L., Granata K.P. (2006). Active trunk stiffness increases with co-contraction. *J Electromyogr Kinesiol* 16:51-57.

Lee P.J., Granata K.P., Moorhouse K.M. (2007). Active trunk stiffness during voluntary isometric flexion and extension exertions. *Human Factors* 49:100-109.

Lees C., Vincent J.F.V., Hillerton J.E. (1991). Poisson's ratio in skin. *Bio-Medical Materials and Engineering* 1:19-23.

Lieber R.L., Brown C.G., Trestik C.L. (1992). Model of muscle-tendon interaction during frog semitendinosus fixed-end contractions. *J Biomech* 25:421:428.

L'Italien G.J., Chandrasekar N.R., Lamuraglia G.M., Pevec W.C., Dhara S., Warnock D.F., Abbott W.M. (1994). Biaxial elastic properties of rat arteries in vivo: influence of vascular wall cells on anisotropy. *Am J Physiol* 267:H574-H579.

Lucas D.B., Bresler, B. (1961). Stability of the ligamentous spine. Technical Report 40. Biomechanics Laboratory, University of California, San Francisco, CA, USA.

Maas H., Yucesoy C.A., Baan G.C., Huijing P.A. (2003). Implications of muscle relative position as a co-determinant of isometric muscle force: a review and some experimental results. *J Mech Med Biol* 3:145-168.

Maganaris C.N., Paul J.P. (2002). Tensile properties of the in vivo human gastrocnemius tendon. *J Biomech* 35:1639-1646.

Marras W.S., Davis K.G., Granata K.P. (1998). Trunk muscle activities during asymmetric twisting motions. *J Electromyogr Kinesiol* 8:247-256.

Marsden C.D., Merton P.A., Morton H.B. (1981). Human postural responses. *Brain* 104:513-534.

Matthews P.B.C. (1986). Observations on the automatic compensation of reflex gain on varying the pre-existing level of motor discharge in man. *J Physiol* 374:73-90.

Matthews P.B.C. (1991). The human stretch reflex and the motor cortex. *Trends Neurosci* 14:87-91.

McGill S.M. (1991). Electromyographic activity of the abdominal and low back musculature during the generation of isometric and dynamic axial trunk torque: implications for lumbar mechanics. *J Orthopaed Res* 9:91-103.

McGill S.M. (1992). Kinetic potential of the lumbar trunk musculature about three orthogonal orthopaedic axes in extreme postures. *Spine* 16:809-825.

McGill S.M. (2002). *Low Back Disorders: Evidence Based Prevention and Rehabilitation*. Human Kinetics, Champaign, IL, USA.

McGill S.M., Norman R.W. (1986). Partitioning of the L4-L5 dynamic moment into disc, ligamentous, and muscular components during lifting. *Spine* 11:666-678.

McGill S.M., Norman R.W. (1993). Low back biomechanics in industry: the prevention of injury through safer lifting. In: Grabiner, M.D. (Ed.), *Current Issues in Biomechanics*. Human Kinetics Publishers, Champaign, Il, pp. 69-120.

McGill S.M., Juker D., Kropf P. (1996). Appropriately placed surface EMG electrodes reflect deep muscle activity (psoas, quadratus lumborum, abdominal wall) in the lumbar spine. *J Biomech* 29:1503-1507.

McGill S., Seguin J., Bennett G. (1994). Passive stiffness of the lumbar torso in flexion, extension, lateral bending, and axial rotation: effect of belt wearing and breath holding. *Spine* 19:696-704.

Meijer H.J.M., Baan G.C., Huijing P.A. (2006). Myofascial force transmission is increasingly important at lower forces: firing frequency-related length-force characteristics or rat extensor digitorum longus. *Acta Physiologica* 186:185-195.

Milner-Brown H.S., Stein R.B. (1975). The relation between the surface electromyogram and muscular force. *J Physiol* 246:549-569.

Mirbagheri M.M., Barbeau H., Kearney R.E. (2000). Intrinsic and reflex contributions to human ankle stiffness: variation with activation level and position *Exp Brain Res* 135:423-436.

Mirka G., Kelaher D., Baker A., Harrison A., Davis J. (1997). Selective activation of the external oblique musculature during axial torque production. *Clin Biomech* 12:172-180.

Misuri G., Colagrande S., Gorini M., Iandelli I., Mancini M., Duranti R., Scano G. (1997). In vivo ultrasound assessment of respiratory function of abdominal muscles in normal subjects. *Eur Respiratory J* 10:2861-2867.

Monkhouse W.S., Khalique A. (1986). Variations in the composition of the human rectus sheath: a study of the anterior abdominal wall. *J Anatomy* 145: 61-66.

Monti R.J., Roy R.R., Hodgson J.A., Edgerton V.R. (1999). Transmission of forces within mammalian skeletal muscles. *J Biomech* 32:371-380.

Moorhouse K.M., Granata K.P. (2005). Trunk stiffness and dynamics during active extension exertions. *J Biomech* 38:2000-2007.

Moorhouse K.M., Granata K.P. (2007). Role of reflex dynamics in spinal stability: intrinsic muscle stiffness alone is insufficient for stability. *J Biomech* 40:1058-1065.

Mutungu G., Ranatunga K.W. (1996). The viscous, viscoelastic and elastic characteristics of resting fast and slow mammalian (rat) muscle fibres. *J Physiol* 496:827-836.

Nichols T.R., Houk J.C. (1976). Improvement in linearity and regulation of stiffness that results from actions of stretch reflex. *J Neurophysiol* 39:119-132.

Neilson P.D., McCaughey J. (1981). Effect of contraction level and magnitude of stretch on tonic stretch reflex transmission characteristics. *J Neurol Neurosurg Psychiatry* 44:1007-1012.

Nielsen J., Sinkjaer T., Toft E., Kagamihara Y. (1994). Segmental reflexes and ankle joint stiffness during co-contraction of antagonistic ankle muscles in man. *Exp Brain Res* 102:350-358.

Nilsson T. (1982a). Biomechanical studies of the rabbit abdominal wall. Part 1 - the mechanical properties of specimens from different anatomical positions. *J Biomech* 15:123-129.

Nilsson T. (1982b). Biomechanical studies of rabbit abdominal wall. Part 2 - the mechanical properties of specimens in relation to length, width, and fibre orientation. *J Biomech* 15:131-135.

O'Sullivan P.B., Grahamslaw K.M., Kendell M., Lapenskie S.C., Moller N.E., Richards K.V. (2002). The effect of different standing and sitting postures on trunk muscle activity in a pain-free population. *Spine* 27: 1238-1244.

Parkinson R.J., Beach T.A.C., Callaghan J.P. (2004). The time-varying response of the in vivo lumbar spine to dynamic repetitive flexion. *Clin Biomech* 19:330-336.

Potvin J.R., Norman R.W., McGill S.M. (1996). Mechanically corrected EMG for the continuous estimation of erector spinae muscle loading during repetitive lifting. *Eur J Appl Physiol* 74:119-132.

Proske U., Wise A.K., Gregory J.E. (2000). The role of muscle receptors in the detection of movements. *Prog Neurobiol* 60:85-96.

Rack P.M.H., Westbury D.R. (1984). Elastic properties of the cat soleus tendon and their functional importance. *J Physiol* 347:479-495.

Rath A.M., Zhang J., Chevrel J.P. (1997). The sheath of the rectus abdominis muscle: an anatomical and biomechanical study. *Hernia* 1:139-142.

Reeves N.P., Cholewicki J., Milner T.E. (2005). Muscle reflex classification of low-back pain. *J Electromyogr Kinesiol* 15:53-60.

Reeves N.P., Everding V.Q., Cholewicki J., Morrisette D.C. (2006). The effects of trunk stiffness on postural control during unstable seated balance. *Exp Brain Res* 174:694-700.

Rietdyk S., Patla A.E. (1998) Context-dependent reflex control: some insights into the role of balance. *Exp Brain Res* 119:251-259.

Rizk N.N. (1980). A new description of the anterior abdominal wall in man and mammals. *J Anat* 131:373-385.

Rizk N.N., Adieb N. (1982). The development of the anterior abdominal wall in the rat in the light of a new anatomical description. *J Anat* 134:237-242.

Ross E.C., Parnianpour M., Martin D. (1993). The effects of resistance level on muscle coordination patterns and movement profile during trunk extension. *Spine* 18:1829-1838.

Seroussi R.E., Pope M.H. (1987). The relationship between trunk muscle electromyography and lifting moments in the sagittal and frontal planes. *J Biomech* 20:135-146.

Shirazi-Adl A., El-Rich M., Pop D.G., Parnianpour M. (2005). Spinal muscle forces, internal loads and stability in standing under various postures and loads--application of kinematics-based algorithm. *Eur Spine J* 14:381-392.

Sinkjaer T., Toft E., Andreassen S., Hornemann B.C. (1988). Muscle stiffness in human ankle dorsiflexors: intrinsic and reflex components. *J Neurophysiol* 60:1110-1121.

Slot P.J., Sinkjaer T. (1994). Simulations of the alpha motoneuron pool electromyogram reflex at different preactivation levels in man. *Biol Cybern* 70:351-358.

Sparto P.J., Parnianpour M., Marras W.S., Granata K.P., Reinsel T.E., Simon S. (1998). Effect of electromyogram-force relationships and method of gain estimation on the predictions of an electromyogram-driven model of spinal loading. *Spine* 23:423-429.

Staudenmann D., Potvin J.R., Kingma I., Stegeman D.F., van Dieen J.H. (2007). Effects of EMG processing on biomechanical models of muscle joint systems: sensitivity of trunk muscle moments, spinal forces, and stability. *J Biomech* 40:900-909.

Stein R.B., Estabrooks K.L., McGie S., Roth M.J., Jones K.E. (2007). Quantifying the effects of voluntary contraction and inter-stimulus interval on the human soleus H-reflex. *Exp Brain Res* 182:309-319.

Stokes I.A.F., Moffroid M., Rush S., Haugh L.D. (1989). EMG to torque relationship in rectus abdominis muscle: results with repeated testing. *Spine* 14:857-861.

Stokes I.A.F., Rush S., Moffroid M., Johnson G.B., Haugh L.D. (1987). Trunk extensor EMG-torque relationship. *Spine* 12:770-776.

Stokes I.A.F., Gardner-Morse M. (2001). Lumbar spinal muscle activation synergies predicted by multi-criteria cost function. *J Biomechanics* 34:733-740.

Tesh M.K., Shaw Dunn J., Evans J.H. (1987). The abdominal muscles and vertebral stability. *Spine* 12:501-508.

Thelen D.G., Schultz A.B., Fassois S.D., Ashton-Miller J.A. (1994). Identification of dynamic myoelectric signal-to-force models during isometric lumbar muscle contractions. *J Biomech* 27:907-919.

Thelen D.G., Schultz A.B., Ashton-Miller J.A. (1995). Co-contraction of lumbar muscles during the development of time-varying triaxial moments. *J Orthopaed Res* 13:390-398.

Thomas J.S., Lavender S.A., Corcos D.M., Andersson G.B.J. (1998). Trunk kinematics and trunk muscle activity during a rapidly applied load. *J Electromyogr Kinesiol* 8:215-225.

Thomas J.S., France C.R., Sha D., Vander Wiele N., Moenter S., Swank K. (2007). The effect of chronic low back pain on trunk muscle activations in target reaching movements with various loads. *Spine* 32:E801-E808.

Toft E., Sinkjaer T., Andreassen S., Larsen K. (1991). Mechanical and electromyographic responses to stretch of the human ankle extensors. *J Neurophysiol* 65:1402-1410.

Urquhart D.M., Hodges P.W., Allen T.J., Story I.H. (2005). Abdominal muscle recruitment during a range of voluntary exercises. *Manual Therapy* 10:144-153.

Tsai S.W., Hahn H.T. (1980). *Introduction to Composite Materials*. Technomic Publishing Co., Inc., Westport, CT, USA.

Urquhart D.M., Hodges P.W. (2005). Differential activity of regions of transversus abdominis during trunk rotation. *Eur Spine J* 14:393-400.

Urquhart D.M., Hodges P.W., Allen T.J., Story, I.H. (2005). Abdominal muscle recruitment during a range of voluntary exercises. *Man Ther* 10:144-153.

van der Fits I.B.M., Klip A.W.J., van Eykern L.A., Hadders-Algra M. (1998). Postural adjustments accompanying fast pointing movements in standing, sitting and lying adults. *Exp Brain Res* 120:202-216.

van Dieen J.H., Cholewicki J., Radebold A. (2003). Trunk muscle recruitment patterns in patients with low back pain enhance the stability of the lumbar spine. *Spine* 28:834-841.

Vera-Garcia F.J., Brown S.H.M., Gray J.R, McGill S.M. (2006). Effects of different levels of torso coactivation on trunk muscular and kinematic responses to posteriorly applied sudden loads. *Clin Biomech* 21:443-454.

Vera-Garcia F.J., Elvira J.L.L., Brown S.H.M., McGill S.M. (2007). Effects of abdominal stabilization maneuvers on the control of spine motion and stability against sudden trunk perturbations. *J Electromyogr Kinesiol* 17:556-567.

Viidik, A. (1973). Functional properties of collagenous tissues. In: *International Review of Connective Tissue Research*, Vol. 6. Eds., Hall, D.A., Jackson, D.S. Academic Press Inc., New York, New York.

Watanabe K., Eguchi A., Kobara K., Ishida H. (2007). Influence of trunk muscle co-contraction on spinal curvature during sitting for desk work. *Electromyogr Clin Neurophysiol* 47:273-278.

Winter D.A. (2005). *Biomechanics and Motor Control of Human Movement*. John Wiley & Sons Inc., Hoboken, NJ.

Woods J.J., Bigland-Ritchie B. (1983). Linear and non-linear surface EMG/force relationships in human muscles. An anatomical/functional argument for the existence of both. *Am J Phys Med* 62:287-299.

Yeh H-L., Yeh H-Y., Zhang R. (1999). A study of negative poisson's ratio in randomly oriented quasi-isotropic composite laminates. *J Composite Materials* 33, 1843-1857.

Zhang L.Q., Rymer W.Z. (1997). Simultaneous and nonlinear identification of mechanical and reflex properties of human elbow joint muscles. *IEEE Trans Biomed Eng* 44:1192-1209.